Electronic Thesis and Dissertation Repository

6-14-2024 11:00 AM

Quantifying Resting-State Functional Connectivity in Critically Brain-Injured Patients: A Graph-Theoretical Approach with fNIRS

Ira Gupta, *Western University*

Supervisor: Owen, Adrian M., *The University of Western Ontario*
Co-Supervisor: Debicki, Derek B., *The University of Western Ontario*
A thesis submitted in partial fulfillment of the requirements for the Master of Science degree in Neuroscience
© Ira Gupta 2024

Recommended Citation

Abstract

Assessment of consciousness in behaviourally unresponsive patients with critical brain injuries continues to be a challenge. There remains a need for robust tools that can accurately characterize preserved cortical function and predict patient outcomes. In the present study, functional near-infrared spectroscopy is employed in conjunction with graph theory and machine learning to quantify resting-state functional connectivity in 16 acutely brain-injured patients and 23 healthy controls. Results revealed significant channel-level differences between the groups for three graph metrics, including degree, clustering coefficient, and local efficiency. Further investigation using machine learning algorithms revealed that these metrics can be used to distinguish between patients and healthy controls with 76% accuracy, and between good and poor patient outcomes with 83% accuracy. Overall, findings from this study provide valuable insights into alterations in brain connectivity following acute brain injury, along with a robust statistical approach for determining patient diagnosis and prognosis.

Summary for Lay Audience

Assessing consciousness in unresponsive patients with critical brain injuries in the intensive care unit poses a significant challenge for medical professionals. Accurately detecting preserved brain function and predicting patient outcomes is crucial for making informed decisions regarding patient care and management. To tackle these challenges, researchers are exploring the use of advanced functional neuroimaging techniques.

In this study, we employed a mathematical approach called graph theory to analyze patterns of brain connectivity in 16 patients with critical brain injuries and 23 healthy controls. We used a non-invasive brain imaging technique called functional near-infrared spectroscopy to measure brain activity in both groups. Our analyses revealed significant connectivity differences between the patient and healthy control participants. We then used these connectivity measures to develop machine learning algorithms capable of distinguishing between patients and healthy controls with a 76% accuracy rate. Furthermore, the algorithms were able to predict good or poor patient outcomes with an 83% accuracy rate.

The findings of our study contribute to the understanding of how critical brain injuries impact brain connectivity. The results demonstrate the potential for combining advanced brain imaging techniques and mathematical analyses to enhance diagnostic and prognostic precision in this patient population. By developing more accurate and reliable tools to assess brain function in unresponsive patients, we aim to support medical teams and families in making well-informed decisions regarding patient care.

Acknowledgments

I would like to express my gratitude to my supervisors, Dr. Adrian Owen and Dr. Derek Debicki. Thank you for granting me the opportunity to pursue this research. Your guidance, expertise, and kindness have been instrumental in shaping my academic journey and making this thesis possible.

My gratitude extends to my advisory committee, Dr. Emma Duerden, Dr. Paul Gribble, and Dr. Lyle Muller. Your insightful mentorship and thoughtful contributions have greatly enriched this project, and I am truly grateful for your support.

Thank you to the wonderful members of the Owen Lab for creating a warm and friendly environment filled with kind encouragement and support. Special thanks to Matthew Kolisnyk for his invaluable assistance and guidance throughout this project, and to Garima Gupta for her unwavering friendship and support. Dawn Pavich, thank you for taking care of this lab! Your presence has made my time in the lab truly memorable.

To the incredible friends I have made throughout this journey, words cannot express how much your friendship has meant to me. You have made this experience so much more meaningful, and I will always cherish the time we spent together.

Above all, I would like to express my deepest appreciation to my family. Your unconditional love, limitless support, and endless encouragement have been the driving force behind my success throughout this academic endeavour. Prabh, thank you for being there every step of the way.

Finally, I extend my sincere thanks to all the patients and families who have generously volunteered their time and efforts. Your participation has made this scientific exploration possible, and I will forever be grateful for your contributions.

Table of Contents

List of Tables

List of Figures

List of Appendices

Chapter 1: Introduction

1.1 Disorders of Consciousness

Clinically, consciousness is generally considered as awareness of oneself and one's environment (Posner et al., 2019). Consciousness is composed of two fundamental components: wakefulness (appearing to be awake, e.g., periods of eye-opening) and awareness (the ability to respond to stimuli, e.g., tactile, auditory, visual, noxious; Porcaro et al., 2022). In patients with brain injuries, impairment in either wakefulness or awareness can result in the onset of a disorder of consciousness (DoC; Edlow et al., 2021).

DoC can be distinguished into acute, subacute, and chronic phases. These phases are premised on a temporal continuum, beginning with the onset of the brain injury (Edlow et al., 2021). The acute phase is defined as the first 28 days post-injury, and includes the time spent at the location of the injury, the emergency department, and the intensive care unit (ICU; Edlow et al., 2021; Giacino et al., 2018). Following the acute phase are the subacute (> 28 days and ≤ 3 months) and chronic stages (> 3 months, prolonged DoC). These phases take into consideration the time spent in rehabilitation, nursing facilities, or the home (Edlow et al., 2021; Song et al., 2018).

Besides different phases, DoC diagnoses can be characterized based on the severity of impairments in consciousness (Berlingeri et al., 2019; Owen, 2008, 2019). First, the Minimally Conscious State (MCS) represents the least severe type of DoC. Patients diagnosed with MCS exhibit wakefulness (i.e., preserved sleep-wake cycles), and reproducible yet minimal and inconsistent behavioural signs of awareness, such as simple command following (Giacino et al., 2018; Mat et al., 2022). Second, Unresponsive Wakefulness Syndrome (UWS), commonly referred to as the vegetative state, includes individuals who do not show signs of awareness but have preserved sleep-wake cycles and autonomic functions such as respiration, digestion, or thermoregulation (Laureys et al., 2010; Multi-Society Task Force on PVS, 1994). The third and most severe form of DoC is the coma, which includes individuals who do not show signs of wakefulness or

awareness. Typically, comatose patients remain immobile with their eyes closed and cannot be aroused with any form of stimulation (Posner et al., 2019).

Coma can occur from a diverse range of brain damage. These causes can be classified as structural lesions (e.g., physical damage to brain tissue) or metabolic encephalopathies (e.g., unrelated to physical wounds; Posner et al., 2019). Structural lesions entail traumatic brain injuries (TBI) that physically damage or compress brain tissue. There are different types of TBIs that can result in structural damage in the brain, such as hematomas (i.e., pools of clotted blood), hemorrhages (i.e., ruptured blood vessels), abscesses (i.e., collection of pus due to infection), and infarcts (i.e., obstruction of blood supply; Posner et al., 2019). In contrast to structural lesions, metabolic encephalopathies result from chemical alterations in the brain. Metabolic encephalopathies can be triggered by medical conditions, including but not limited to cardiac arrest, liver disease, toxicity, and renal failure (Butterworth, 1999). Despite their categorization as distinct forms of brain damage, both structural lesions and metabolic encephalopathies result in hypoxic-ischemic brain injury, characterized by inadequate blood flow. Insufficient blood flow to the brain subsequently curtails the delivery of glucose and oxygen to brain tissue, which are sources of energy crucial for maintaining normal brain function (Lacerte et al., 2024; Messina et al., 2024). Deficient energy supply to the brain due to hypoxic-ischemic brain injury can result in neuronal cell dysfunction and even cell death, causing neurological impairment (Huff & Tadi, 2024).

1.1.1 Clinical Assessment of DoC

When admitted to the ICU, behaviourally unresponsive patients with critical brain injuries frequently present medical teams with the challenge of evaluating impairments in consciousness. Presently, the primary assessment methods used by clinicians to assess acute consciousness levels and patient outcomes in DoC include behavioural measures, such as the Glasgow Coma Scale (GCS) and the Glasgow Outcome Scale Extended (GOSE; Berlingeri et al., 2019; Gomez et al., 2023; Teasdale & Jennett, 1974). With these behavioural measures, clinicians observe and evaluate the intentional behaviour of the patient, specifically motor and verbal ability, eye movement, brainstem reflexes, and respiratory patterns (Demertzi et al., 2015; Rohaut et al., 2019).

The GCS, one of the most widely used assessments for impairments in consciousness, evaluates three core components: eye, verbal, and motor response (*Figure 1*). Each component is scored on a range from 1 to 4, 1 to 5, and 1 to 6, respectively. *Figure 1* illustrates how patients are scored on the three components. The total GCS score, obtained by summing the scores of each component, spans from 3 to 15. A GCS score between 3 to 8 indicates severe impairments in consciousness, a score between 9 to 12 denotes moderate impairments, and a score between 13 to 15 signifies mild impairments (S. Jain & Iverson, 2024). Typically, patients with a score of 8 or below on the GCS can be classified as comatose.

Glasgow Coma Score	
Eye Opening	
Spontaneous	4
Open to verbal command	3
Open to pain	2
No eye opening	1
Verbal Response	
Oriented	5
Confused	4
Inappropriate words	3
Incomprehensible sounds	2
No verbal response	1
Motor Response	
Follows commands	6
Localizes to pain	5
Withdrawals from pain	4
Flexes to pain	3
Extends to pain	2
No Movement	1
Total score	3-15

Figure 1. Glasgow Coma Scale focused on eye-opening, verbal response, and motor response. [Interpreted from Kostiuk & Burns, 2023].

Another commonly used assessment is the GOSE, a structured interview that measures global functional outcomes in patients who have experienced a brain injury (Wilson et al., 1998). The GOSE score is based on a patient's functionality in routine life, such as their ability to obey commands, need for assistance at home, and engagement in social and leisurely activities (Wilson et al., 2021). The scores on the GOSE can be classified into eight states: (1) dead, (2) vegetative state, (3) lower severe disability, (4) upper severe disability, (5) lower moderate disability, (6) upper moderate disability, (7) lower good recovery, and (8) upper good recovery. Although the GCS and GOSE are currently the

primary methods for evaluating impairments in consciousness and post-injury outcomes in acute DoC, they have certain limitations, specifically the inability to detect covert awareness and capture subtle cognitive and neurological changes, which reduce their diagnostic and prognostic precision.

1.1.2 Issues with Behavioral Assessments

Assessments that are primarily reliant on behaviour, such as the GCS, can exhibit significant variability based on the patient's condition (e.g., physical brain injury, sensory impairments, medications, sedation) and are prone to high examiner subjectivity, resulting in misdiagnoses (Edlow et al., 2017; Gill-Thwaites, 2006). Indeed, numerous studies have indicated that behavioural measures have high misdiagnosis rates in patients with critical brain injuries, reaching up to 27% for those in the acute stages and 48% for those in the chronic stages (Monti et al., 2010; Owen, 2019; Rohaut et al., 2019; Schnakers et al., 2009; Vanhaudenhuyse et al., 2010). Despite their widespread use and current gold standard status, behavioural measures have repeatedly exhibited unreliable diagnostic efficacy. These measures continue to be used primarily due to the lack of alternatives that can be easily administered at the patient bedside and the need for standardizing implementation of and interpretations from novel assessment techniques.

The continued utilization of unreliable behavioural measures is problematic since precise assessment is critical for informing neuroprognostication and withdrawal of life support decisions during the acute phase of DoC (Edlow et al., 2017; Kazazian et al., 2021; Owen, 2019; Rohaut et al., 2019; Turgeon et al., 2011). Turgeon and colleagues (2011) showed that approximately 65% of deaths in the ICU for patients with TBI are due to the withdrawal of life-sustaining measures (WLSM; Turgeon et al., 2011). This study further reported that patients in the acute phase of DoC underwent WLSM because medical teams prognosticated either a poor chance of survival or poor long-term neurological outcome. While determining whether a patient has the capacity for recovery is difficult, studies have shown that predictions of poor survival or outcome can lead to the self-fulfilling prophecy, such that they can influence the care and attention patients are provided and lead to WLSM (Becker et al., 2001; Izzy et al., 2013).

The importance of precise assessments was further highlighted by a recent study investigating the potential for recovery in 40 patients with an ischemic or hemorrhagic stroke. According to clinical predictions post-injury, none of the 40 patients had a chance of meaningful recovery. At the 6 month mark, while many of these patients had indeed passed away or were diagnosed with UWS, approximately half were still alive and one patient was even able to make a good functional recovery (Egawa et al., 2023). Overall, misdiagnosis or inaccurate neuroprognostication in the acute phase can contribute to withdrawal of life support decisions, highlighting the need for more reliable assessment tools to minimize the risk of withdrawing life support from patients who may have had the potential for recovery.

In light of these limitations of behavioural measures, a promising avenue for objectively and accurately assessing residual brain activity in patients with DoC are anatomical and advanced functional neuroimaging techniques. Anatomical magnetic resonance imaging (MRI) and electroencephalogram are neuroimaging techniques routinely used in clinical settings to evaluate brain structure and electrical activity, respectively. In contrast, functional neuroimaging modalities (e.g., functional magnetic resonance imaging or fMRI) offer a means to measure brain activity in real-time and, therefore, can provide valuable insights into a patient's level of consciousness (Berlingeri et al., 2019; Owen et al., 2006). While neuroimaging techniques have immense potential to improve assessment of consciousness in DoC patients, their adoption in clinical settings has been limited due to factors such as high cost of fMRI and need for specialized analyses to interpret the results. The lack of standardized protocols and the need to further validate neuroimaging techniques with larger patient samples have also contributed to the reliance on behavioural measures. However, these limitations are being continually addressed with the emergence of lower cost neuroimaging techniques and research efforts. Ultimately, by employing robust tools such as functional neuroimaging modalities, clinicians can be better equipped to tackle the challenges surrounding diagnostic and prognostic precision in brain-injured patients.

1.2 Resting-State Functional Connectivity

Functional neuroimaging tasks used to assess brain connectivity can broadly be categorized into active, passive, and resting-state paradigms (Kondziella et al., 2016). Active paradigms evaluate higher-order cognitive functions and require willful execution of tasks, such as command following (e.g., mental imagery or spatial navigation). In contrast, passive paradigms evaluate lower-order cognitive functions and do not require participants to respond. Passive tasks consist of following external stimuli, such as auditory listening, somatosensory evoked potentials, or movie-watching. Lastly, resting-state paradigms examine the brain at rest in the absence of external stimuli or tasks and do not require any intentional response or stimulus following.

Although active task-based paradigms have significantly contributed to the understanding of brain activity in patients with DoC, these paradigms require sustained attention and active participation from the patient (R. Jain & Ramakrishnan, 2020). This can be particularly challenging for acute ICU patients due to fluctuations in awareness (e.g., sleep states, sedation), discomfort (e.g., in pain, delirium), difficulty in understanding the task (e.g., language differences), and/or impaired cognitive function (e.g., working memory, attention; Edlow et al., 2017, 2021; Rohaut et al., 2019). Therefore, in acute ICU patients, active paradigms underestimate the level of consciousness compared to assessments made using passive paradigms (Kondziella et al., 2016). Although a response is not required in passive paradigms, patients are still expected to direct their attention to stimuli. Consequently, active and passive task-based paradigms may not be optimal for evaluating covert brain activity in acutely unresponsive patients.

Resting-State Functional Connectivity (RSFC) is the ideal neuroimaging paradigm for assessing acute ICU patients since it does not require active attention or responses from the patients. The resting-state paradigm entails observation of the intrinsic connections within the brain during periods of rest. When at rest (i.e., not attending to a specific stimuli or performing an explicit task), the brain remains operational and demonstrates spontaneous fluctuations in neural activity (Smitha et al., 2017). The functional connectivity component of RSFC examines the temporal relationship between two anatomically distinct brain regions and provides insight into the communication and

coordination between different brain areas (van den Heuvel & Hulshoff Pol, 2010). In the context of DoC, assessing functional connectivity can help identify alterations in brain network dynamics that may underlie impairments in consciousness that are observed in acute ICU patients. Furthermore, functional connectivity patterns noted in DoC patients during rest can be compared with those found in healthy controls to detect specific network disruptions, which can serve as diagnostic or prognostic markers. On the whole, RSFC can measure spontaneous neural activity and aid in the identification of task-independent brain activity patterns, making it a promising protocol for assessing unresponsive patients (Lv et al., 2018; van den Heuvel & Hulshoff Pol, 2010).

1.2.1 Resting-State Networks

Brain regions that have strong functional connections during rest are referred to as resting-state networks. There are several resting-state networks, including the default mode network (DMN), somatomotor network, dorsal attention network, salience network, frontoparietal control network, visual network, auditory network, and limbic network (Yeo et al., 2011). These networks offer insight into general cognition, attention, sensory and motor systems, memory, and introspective thought processes (Laird et al., 2011). One of the most prominently studied resting-state networks is the DMN (Greicius et al., 2003; Raichle et al., 2001). This network consists of areas of the posterior cingulate cortex/precuneus, medial frontal regions, medial temporal lobe, and inferior parietal regions (van den Heuvel & Hulshoff Pol, 2010). The DMN is notably active during rest and exhibits inactivity when the brain engages with external stimuli.

Resting-state networks have been shown to contribute to human consciousness and describe the inherent functional organization in the brain (Qin et al., 2015; Threlkeld et al., 2018; Vincent et al., 2007). Particularly, investigating the brain at rest in acute patients with DoC can help uncover information about the intrinsic connections crucial for preserving consciousness. Resting-state networks can provide insight into the brain's communication efficiency, specifically information processing and transmission mechanisms (Shu et al., 2023). Overall, examining the resting-state brain in DoC patients could yield valuable insights into functional organization, general cognition and communication, and overall preserved consciousness.

1.2.2 fMRI-based RSFC in DoC

RSFC can be assessed using neuroimaging modalities such as functional MRI (fMRI). Resting-state fMRI has previously been used to evaluate brain connectivity in unresponsive brain-injured patients (Demertzi et al., 2015; Di Perri et al., 2016; Kazazian et al., 2020; Koenig et al., 2014; Kolisnyk et al., 2023; Kondziella et al., 2017; Long et al., 2016; Medina et al., 2022; Norton et al., 2012; Porcaro et al., 2022; Snider & Edlow, 2020; Threlkeld et al., 2018; Vanhaudenhuyse et al., 2010; Wagner et al., 2020; X. Wu et al., 2015). These studies found that patients with brain injuries demonstrate disrupted functional connectivity in resting-state networks, such as the DMN. In addition, resting-state fMRI has been used with machine learning algorithms in critically brain-injured patients to predict functional recovery outcomes with up to 80% accuracy when predicting good outcomes (Kolisnyk et al., 2023). Such robust predictions of good functional outcomes are well above current clinical neuroprognostication methods, indicating the potential for using functional neuroimaging tools in outcome prediction.

Other than their effective implementation in unresponsive patients, available literature indicates that RSFC can provide insight into consciousness levels. Previous studies have shown that DMN RSFC and consciousness levels are positive correlated, such that decreases in DMN connectivity are proportional to decreases in levels of consciousness (Di Perri et al., 2016; Koenig et al., 2014; Snider & Edlow, 2020; Vanhaudenhuyse et al., 2010; X. Wu et al., 2015). Differences in the extent of neural activity during rest can further be used to distinguish between levels of consciousness and types of DoC (Demertzi et al., 2015; Long et al., 2016; Medina et al., 2022; Porcaro et al., 2022). For example, studies suggest that compared to patients in MCS, patients with UWS have a reduced number of identifiable resting-state networks, as well as decreased activity within those networks. These findings indicate that resting-state paradigms can be used to gauge the level of consciousness and severity of DoC.

Furthermore, resting-state paradigms have also been implemented to determine patient outcomes post-injury. Studies have shown that patients who regain consciousness post-injury demonstrate more preserved resting-state network connectivity compared to those who do not recover (Koenig et al., 2014; Kondziella et al., 2017; Norton et al., 2012).

DMN connectivity, especially, may be indicative of recovery of consciousness post-injury. Even during the recovery process, patterns of increased RSFC and normalizations in DMN connectivity have been documented in brain-injured patients (Kazazian et al., 2020; Threlkeld et al., 2018). These findings underscore the significant role of functional and well-connected resting-state networks in the recovery of consciousness among patients with brain injuries.

Resting-state fMRI has been used to assess functional connectivity in patients with DoC with relative success, however, there are merits and limitations to this neuroimaging modality that must be considered. fMRI offers high spatial resolution that allows the detection of localized deep brain activity, which can be used to understand the networks and neural activity associated with consciousness (Wang et al., 2023). However, the costs associated with fMRI act as a barrier to access for hospitals and communities with limited funding. Additionally, fMRI scans include high-noise levels and require participants to lie extremely still in the scanner due to susceptibility to motion artifacts (Wang et al., 2023).

One of the major limitations of fMRI in the context of assessing patients with acute brain-injuries is the need to transport patients from the ICU to the scanner. This process can pose significant risks to patients due to the instability of their medical conditions and the presence of vital monitoring equipment, further resulting in delayed MRI scanning (Kazazian et al., 2020; Koenig et al., 2014; Rohaut et al., 2019). While portable MRI scanners have been developed, their current low field strength limits their ability to perform advanced functional neuroimaging, rendering them insufficient for clinical needs (Sarracanie & Salameh, 2020). Overall, the lack of portability of high-field MRI scanners impedes the utilization of fMRI in clinical settings, such as the ICU.

These limitations indicate that there is a growing need for alternative neuroimaging modalities that can provide insight into brain function and connectivity in acutely brain-injured patients while overcoming the challenges associated with fMRI (i.e., patient transportation, high cost, noise-levels, and motion artifacts). Functional near-infrared spectroscopy (fNIRS) has emerged as a promising neuroimaging alternative that overcomes many of the limitations associated with fMRI in assessing patients in the ICU.

1.3 Functional Near-Infrared Spectroscopy

fNIRS is a non-invasive, optical neuroimaging technique that measures changes in hemoglobin concentration in the cortex and provides an indirect measure of neural activity (Novi et al., 2016; Scholkmann et al., 2014). By measuring the absorption of near-infrared light at different wavelengths, fNIRS detects changes in cerebral blood flow and oxygenation that occur in response to neural activity (Boas et al., 2014). One of the key advantages of fNIRS is its portability, allowing for continuous monitoring of brain activity at the patients' bedside. This advantage can enable clinicians to obtain critical information about brain function and connectivity in real-time without extensive waitlists as common with fMRI (M. Li et al., 2021). In additional to being portable, fNIRS is relatively inexpensive compared to fMRI, making it a more accessible option for hospitals and communities (Rupawala et al., 2018). Unlike fMRI, fNIRS does not offer the advantages of high spatial resolution. However, it does have high temporal resolution, which allows for the detection of rapid changes in brain activity (Pinti et al., 2020). Lastly, fNIRS is less susceptible to motion artifacts than fMRI, making it more suitable to use in populations who may have difficulty remaining still (Pinti et al., 2020).

1.3.1 fNIRS System

The fNIRS system consists of sources (laser diodes) and detectors placed at specific distances on the surface of the head (*Figure 2*). Sources propagate near-infrared light (centered at 785, 808, 830, and 850 nm) through the scalp and cortex (Quaresima & Ferrari, 2019). The propagated light is then received by detectors. The source-detector pairs or (long) channels are placed 3 cm apart, which allows the near-infrared light to reach the cortex of the brain. The amount of light detected measures changes in oxygenated (HbO), deoxygenated (HbR), and total (HbT) hemoglobin concentrations resulting from neural activity in the brain (Liu et al., 2023; Othman et al., 2021).
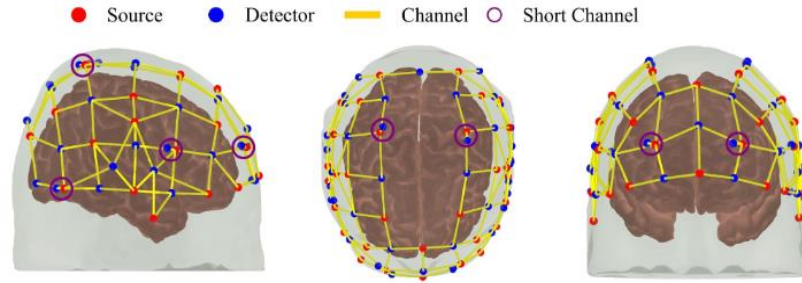
Figure 2. Visual schematic of an fNIRS system, with sources (red dots), detectors (blue dots), channels or source-detector pairs (yellow lines), and short channels (purple circles). [Interpreted from Abdalmalak et al., 2022.]

Short channels, placed 0.8 cm apart, measure scalp activity. Short-channel sources and detectors are placed closer together to ensure that the light is only propagated through the scalp rather than the cortex (*Figure 3*). This information can then be used to eliminate any confounding effects of systemic physiology, such as respiration, heart rate or blood pressure, on the neural signal associated with brain activity. Implementing this approach effectively mitigates the risk of inflating the correlation between fNIRS channels (Abdalmalak et al., 2021).
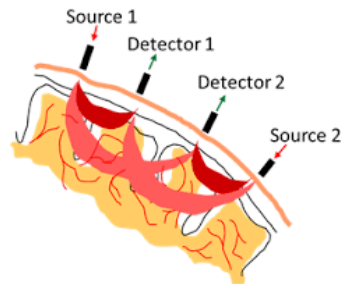
Figure 3. Shows the difference between long-channels (source 1 and detector 2) used to measure changes in local hemodynamic response and short-channels (source 1 and detector 1) used to measure systemic physiology. [Interpreted from https://nirx.net/our-story.]

1.3.2 fNIRS-based RSFC in DoC

Over the past few years, an increasing number of studies have demonstrated that fNIRS is a promising neuroimaging modality with reliable spatial and temporal correlations (Bonilauri et al., 2023; Duan et al., 2012; Huppert et al., 2006). While fNIRS demonstrates potential for assessing acute patients in the ICU, studies using fNIRS to

assess impairments and outcomes of patients with DoC are limited (Abdalmalak et al., 2021; Owen, 2019). Existing literature on fNIRS and DoC patients is focused on chronic DoC. These studies employed task-based paradigms, such as auditory stimuli, to assess whether patients can follow instructions or answer simple yes or no questions (M. Li et al., 2021; Shu et al., 2023). Findings from these studies demonstrate that fNIRS reliably and accurately detected patient responses, thus, emphasizing the feasibility of this modality to assess DoC patients.

Only a handful of studies have employed resting-state fNIRS (rs-fNIRS) to assess DoC patients (Wang et al., 2023). While sparse, these studies suggested that patients with DoC show reduced functional connectivity in the frontal brain regions and altered structural organization of neural networks (Chen et al., 2023; Liu et al., 2023). Indeed, Liu et al. (2023) examined connectivity in MCS and UWS patients using rs-fNIRS. Findings from this study revealed that compared to healthy controls, both patient groups showed significant losses in the topological architecture (i.e., structural and functional organization of brain networks) and impairments in long-distance connectivity within the prefrontal cortex. Similarly, using rs-fNIRS, Chen et al. (2023) showed that MCS patients had highly disrupted functional connectivity in the frontal lobe, specifically the frontopolar area and right dorsolateral prefrontal cortex. It is important to note that both of these studies focused exclusively on the frontal lobe.

This regionally focused approach is common when examining activity in the brain. Most studies use a more directed, seed-based analysis, which involves selecting a region of interest (a "seed") based on *a priori* knowledge. The time series of the seed region is then correlated with all other brain areas, which informs about regions the specific seed is functionally connected with (van den Heuvel & Hulshoff Pol, 2010). Although a seed-based analysis provides direction to study aims, restricting the area of interest to only one brain region can result in losing valuable information regarding functional connectivity patterns in the rest of the brain (Novi et al., 2016). Furthermore, a recent meta-analysis showed that findings on patterns of functional connectivity are typically highly influenced by seed selection, making it challenging to produce reliable results (M.-T. Li et al., 2023). To obtain robust results on functional connectivity, it is optimal to avoid

confining the analysis to a single seed region and instead assess connectivity across the entire brain using a comprehensive approach, such as graph theory.

1.4 Graph Theory

Graph theory studies mathematical structures that model the relationships between objects (Koutrouli et al., 2020). These models are implemented for understanding complex interacting networks by simplifying them to a set of points (i.e., nodes) connected by lines (i.e., edges; Fornito et al., 2016). Common examples of networks that can be quantified and analyzed using graph theory include road maps, the internet, social circles, genomics, and computer science. Graph theory can be extended to neuroscience, such that the brain can be depicted as a graph or network that is composed of nodes and edges (He & Evans, 2010). This mathematical application can quantify the nature of connectivity in the resting brain.

1.4.1 Graphs and Network Metrics

Simplifying the intricate patterns of brain connectivity to a core network of nodes and edges facilitates the computation of mathematical graphs and metrics that can reveal information about the form and function of a system (Newman, 2016). There are various types of graphs and metrics that can be computed. Graphs can be weighted or unweighted (also referred to as binary) and directed or undirected (Fornito et al., 2016). Weighted graphs have edges that represent the strength of connectivity between the nodes, whereas binary graphs have edges that only represent the presence or absence of a connection. Directed graphs have edges that indicate a start and end point between two nodes, whereas undirected graphs only indicate a connection between nodes and do not have direction. In this study, binary, undirected graphs will be the focus.

Graphs can also be simplified into adjacency matrices, A. If two nodes are connected, they are said to be neighbours or adjacent. In other words, the neighbour of a node is the node directly connected to it by an edge. In an adjacency matrix, each row/column (i/j) represents a node, and non-zero elements in the row/column represent the presence of an edge (Fornito et al., 2016). Network metrics (or graph metrics) can be calculated from adjacency matrices to quantify specific properties or characteristics of the network, such

as connectivity, complexity, or efficiency. These metrics can provide insight into the structure and function of the network (Niu et al., 2013). Although there are many network metrics that can be calculated from adjacency matrices, only four will be discussed in this study.

Networks usually consist of multiple components, in which one large component (i.e., the giant component, the most connected component) forms the majority of the network, along with other smaller, disconnected components (*Figure 4*; Newman, 2016). The smaller components may be isolated nodes or consist of only several nodes each. This division into multiple components decreases the values for the network metrics. Hence, network metrics can be recalculated for only the giant component.
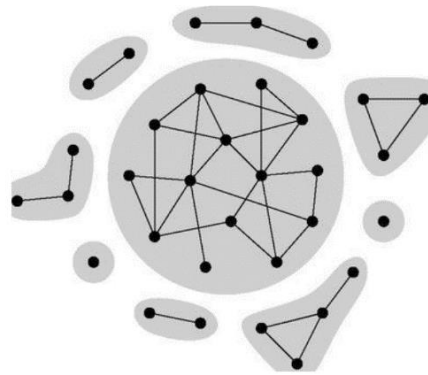
Figure 4. Visual schematic of a giant component (the most connected network, middle) and several smaller components composed of fewer nodes. [Interpreted from Newman, 2016.]

1.4.1a Degree

The degree of a node is the most basic network metric and is defined as the number of edges connected to a node (*Figure 5*). The degree provides information about the connectivity of the node to the rest of the graph and, consequently, the connectivity of the network as a whole (Wang et al., 2010). Values for degree can range from 0 (isolated node) to one less than the total number of nodes (fully connected node), *N*. The degree of a node can be calculated by taking the sum of a row in the adjacency matrix (since the matrix is symmetrical and each row is equivalent to each column). The mean degree of the whole graph can be calculated by taking the average of all nodal degrees.
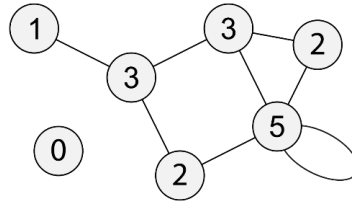
Figure 5. The degree of each node is calculated as the number of edges connected to it. Isolated nodes have a degree of 0 (no edges). The node with 5 edges has a self-loop, where an edge is connected to the same node.

1.4.1b Clustering Coefficient

The clustering coefficient of a node indicates the level of local connectedness within a graph and the tendency of a node to form a tightly connected community (*Figure 6*). This metric assesses the interconnectivity of the nodes that are neighbouring a given node and provides information about the density of connections in the overall network (He & Evans, 2010; Wright et al., 2021). The clustering coefficient is calculated by dividing the number of existing connections (i.e., edges) between the neighbours of a node by the number of possible connections between those neighbours (Koutrouli et al., 2020). The mean clustering coefficient of the whole graph can be calculated by computing the average of all nodal clustering values. Clustering coefficient values can range from 0 to 1, with higher values indicating that the node or graph has a greater inclination to form clusters (Koutrouli et al., 2020).
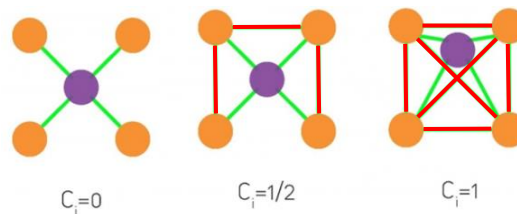
Figure 6. The clustering coefficient of a node (purple). The left image has 0/6 possible connections between the neighbours ($C_i = 0$), the middle image has 3/6 connections ($C_i = 1/2$, red lines), and the image on the right has 6/6 connections ($C_i = 1$, red lines).

1.4.1c Local Efficiency

The local efficiency of a node describes how well information can be transmitted through a network and is closely linked to the clustering coefficient (*Figure 7*; Wang et al., 2010).

Local efficiency provides information about the extent to which the graph is fault-tolerant. In other words, it shows the efficiency of communication between the neighbours of a node, if the node in question was removed (Latora & Marchiori, 2001). This metric is calculated by considering the shortest paths (i.e., the fewest number of edges between two nodes) between neighbouring nodes within a specific node's neighbourhood (Wang et al., 2010). The mean local efficiency of the whole network can be calculated by computing the average across all nodes. Local efficiency values can range from 0 to 1, with 1 suggesting the most effective transmission of information.
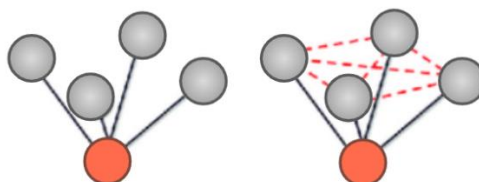
Figure 7. The local efficiency of a node (red). The image on the left has a lower local efficiency since the node's neighbours (grey) are connected by 2 edges each (solid black line, i.e., neighbours are only connected through the node). The image on the right has a higher local efficiency since the node's neighbours (grey) are connected by 1 edge each (dotted red line, i.e., neighbours are not only connected through the node but also connected to each other directly), indicating a shorter path compared to the left.

1.4.1d Betweenness Centrality

The betweenness centrality of a node explains how frequently that node acts as a crucial link or bridge along the shortest path between other pairs of nodes in a network (*Figure 8*; Newman, 2016). Betweenness centrality is calculated as the proportion of shortest paths between two nodes that pass through the node of interest (Koutrouli et al., 2020; Wright et al., 2021). This metric provides information about which nodes are central for connecting two communities. Nodes with higher betweenness centrality values control the flow of information through the system and therefore, play a key role in maintaining efficient communication and connectivity within the network (Fornito et al., 2016; van den Heuvel & Hulshoff Pol, 2010).
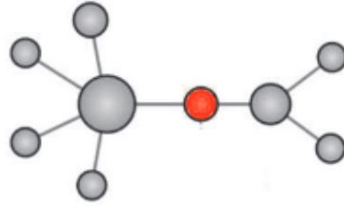
Figure 8. The betweenness centrality of a node. The red node represents the highest betweenness centrality since it acts as a bridge or link between the left (5 nodes) and right (3 nodes) communities of nodes. All paths between the two communities of nodes must pass through the red node.

1.4.2 Graph Theory and fNIRS

Graph theory can easily be applied to fNIRS data. In this case, each channel of the fNIRS system acts as a node, and edges are based on the Pearson's correlations between each possible pair of nodes (*Figure 9*). If these correlation values exceed a given threshold, *r*, the nodes are considered to be functionally linked and have an edge between them (Novi et al., 2016; van den Heuvel & Hulshoff Pol, 2010). This conceptualization of nodes and edges creates a network or graph of the whole brain. Using this graph, network metrics can be calculated to quantify brain activity in different populations, such as acutely brain-injured DoC patients and healthy controls. Only two studies have employed graph theory in rs-fNIRS to assess functional connectivity in the frontal regions of patients with DoC (Chen et al., 2023; Liu et al., 2023). The present study is the first to utilize using graph theory for investigating RSFC across the whole brain in patients with acute brain-injuries.
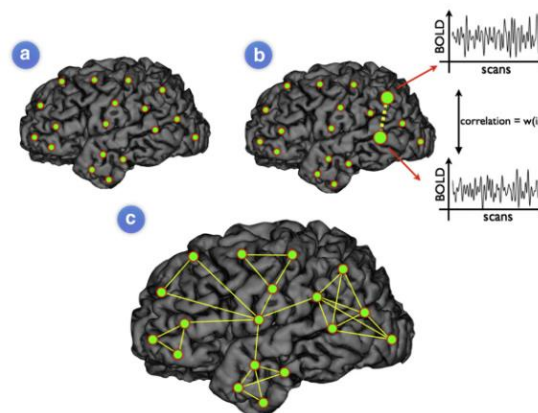
Figure 9. Visual schematic of nodes and edges represented on the brain. (A) Each fNIRS channel acts as one node (green dot). (B) Pearson correlation between each possible pair of nodes acts as edges (green dotted line). (C) Whole-brain functional connectivity of the brain. [Interpreted from van den Heuvel & Hulshoff Pol, 2010.]

1.5 Machine Learning

Machine learning is a branch of artificial intelligence and computer science, where a computer system is trained to identify patterns and make predictions based on a dataset (Shamout et al., 2021). In supervised machine learning, a dataset (X, e.g., graph metrics) is associated with specific labels (Y, e.g., healthy controls versus patients or good versus poor outcomes; Wernick et al., 2010). The dataset and associated labels are then used to generate a predictive model that can classify the labels of new, unseen data (Senders et al., 2018). This type of supervised machine learning is known as classification, which can be used to train a model to identify unique features specific to the labelled data (Nielsen et al., 2020). Machine learning algorithms can identify complex patterns and relationships within large datasets, enabling them to distinguish between groups more accurately and objectively than standard clinical assessments. Indeed, classification models have been previously used to aid patient diagnoses and outcome prediction (Erickson et al., 2017; Kolisnyk et al., 2023).

In the context of this study, classification algorithms were developed and trained on graph theoretical data to differentiate between healthy controls versus patients as well as good versus poor patient outcomes. Classification models can be trained utilizing various algorithms. In this study, three algorithms were used to train the classification models, including the linear support vector classifier (SVC), k-nearest neighbours (KNN) classifier, and radial basis function (rbf) SVC. These classifiers were selected due to their ability to capture complex relationships between features and labels, and their successful application in previous neuroimaging studies (Amiri et al., 2023; Lanka et al., 2020; Magnin et al., 2009; Pereira et al., 2009; Tulay et al., 2019).

1.5.1 Linear Support Vector Classifier

The linear SVC algorithm is the simplest machine learning model, particularly adept for binary classifications. In this model, the algorithm identifies the optimal linear boundary (i.e., line) that separates the data into the different classification groups (*Figure 10*; Bhavsar & Panchal, 2012). The optimal linear boundary is established by maximizing the margin, which represents the space between the linear boundary and the closest data

points from each group. New data points are classified based on their position relative to the boundary line.
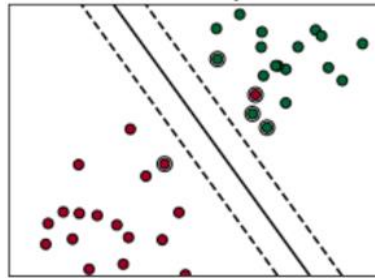
Figure 10. Visual schematic of a linear SVC. A linear boundary is defined that best separates the two data classes. [Interpreted from L. Chen, 2019.]

1.5.2 K-Nearest Neighbors Classifier

The KNN algorithm is a viable option when delineating boundaries between data classes that may be more complex, and therefore, non-binary. This algorithm relies on the premise that similar data points share specific attributes. Hence, the algorithm identifies the data points neighbouring or closest in proximity to the data point of interest based on a given distance metric (*Figure 11*; Laaksonen & Oja, 1996). Once identified, the algorithm assigns the most frequently used label among the closest neighbouring data points to the data point of interest, thus, classifying it into a particular category.
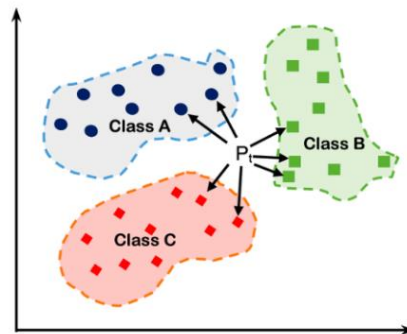
Figure 11. Visual schematic of KNN. The classification of a new data point (P_t) is based on the neighbours nearest to it (the three closest neighbours are from Class B). [Interpreted from Sachinsoni, 2023.]

1.5.3 Radial Basis Function Support Vector Classifier

The rbf SVC is a more complex version of a linear SVC, which is employed when a simple linear boundary may be difficult to define. Unlike the linear SVC model, which defines a linear boundary, the rbf SVC algorithm determines the optimal curved or circular boundary to classify data points into different groups (*Figure 12*; Bhavsar & Panchal, 2012).
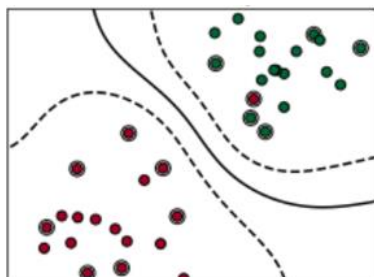
Figure 12. Visual schematic of rbf SVC. A curved or circular boundary is defined between the two classes of data. [Interpreted from L. Chen, 2019.]

1.6 The Present Study

1.6.1 Rationale

To date, no study has employed fNIRS-based RSFC to investigate whole-brain activity in patients with DoC, especially those in the acute phases of injury. Furthermore, no studies have yet applied graph theoretical analyses for fNIRS-based RSFC performed with acutely brain-injured patients in the ICU or integrated machine learning models to classify groups and predict patient outcomes. The present study aimed to bridge this knowledge gap, especially given the promise demonstrated by fNIRS-based RSFC, graph theoretical models, and machine learning classifications in available literature, and the need for objective and precise assessments of consciousness in acutely brain-injured patients.

1.6.2 Objectives

The present study has three objectives premised on the aim to enhance diagnostic and prognostic precision in assessments of acutely brain-injured patients.

1) Quantitatively describe brain functional connectivity using accessible neuroimaging modalities (i.e., fNIRS) and graph theoretical models.

2) To classify healthy controls and patients using machine learning algorithms that can correctly differentiate between network metrics of the study groups.

3) Use machine learning models to predict good and poor patient outcomes using network metrics acquired from acutely brain-injured patients in the ICU.

1.6.3 Hypotheses

Based on the previous literature, this study posits two key hypotheses.

1) Patients will exhibit graphs and graph metrics that differ significantly from those of healthy controls. Particularly, these graph metrics are predicted to be decreased in acutely brain-injured patients, suggesting disruptions in network connectivity and functionality.

2) Machine learning models will successfully distinguish healthy controls from patients and predict patient outcomes using network metrics calculated using graph theory.

1.6.4 Impact

While novel, this research has the potential to profoundly impact the healthcare system and the field of clinical neuroscience. Leveraging rs-fNIRS to evaluate intrinsic connectivity can allow for accurate, non-invasive, and continuous assessment of critically brain-injured patients in the ICU, a setting and population where traditional neuroimaging techniques (i.e., fMRI) and task-based paradigms are challenging to implement. Furthermore, examining the performance of cutting-edge analyses, such as graph theory and machine learning, in this study can facilitate the development of quantitative tools that can improve diagnostic and prognostic precision of acutely brain-injured patients. Ultimately, the present study aims to advance the understanding of functional connectivity in acutely brain-injured patients and empower clinicians and family members to make informed decisions regarding patient care.

Chapter 2: Methods and Materials

2.1 Ethics

The study was approved by the Research Ethics Board at Western University in compliance with the Tri-Council Policy Statement (TCPS): Ethical Conduct for Research Involving Humans guidelines (project identification number: 114967). Written informed consent was obtained for each healthy control participant and from the substitute decision maker for each patient.

2.2 Participants

2.2.1 Patients

This research was part of the larger Multimodal Imaging in the Intensive Care Unit (MIMIC) study. For additional details, please refer to Kazazian et al. (2021).

Patients were screened, recruited, and tested at the London Health Sciences Centre, University Hospital in London, Ontario, Canada from 2021-2023. Patients were tested within the first 10 days after admission to the ICU, with the aim to test at three time points: 2-4 days, 4-6 days, and 7-10 days post-injury, if appropriate. Eligibility included patients aged 18 and older with critical brain injuries that rendered them unresponsive. The severity of brain injury was clinically assessed by medical professionals at the bedside using the GCS (in the absence of sedation), and patients with a score of ≤ 8 prior to neuroimaging were eligible. Patients that were deemed medically unstable, had pre-existing neurological disorders (e.g., Alzheimer's disease, Parkinson's disease), craniotomies, or hemorrhages (resulting in a loss of signal quality which precludes accurate fNIRS measurement) were excluded. Additionally, any patients who had brain injuries that would hinder the placement of the fNIRS cap and probes on their scalp were excluded. Contingent on this criteria, 19 patients (mean age 61.4 years, 7 females) were eligible for testing and proceeded to the data collection phase. I helped collect neuroimaging data for all tasks part of the MIMIC study for 10 of the 19 patients in the acute phase (i.e., in the ICU). From these 19 patients, three were excluded from further data analysis due to unusable short channels or a high count of bad channels (refer to

section 2.4.1). The mean age of the remaining 16 patients was 61.3 years (4 females). Specific patient demographic and clinical information for these 16 patients is provided in *Table 1*.

Patient	Age (years)	Sex	Etiology	GCS (total)	fNIRS Testing Day after ICU admission**	GOSE
1	68	M	Stroke & vertebral artery occlusion	6T	24	1
2	61	M	Return of spontaneous circulation in context of STEMI	6T	5	1*
3	55	M	Ventricular fibrillation arrest in context of STEMI	3T	3	1
4	62	F	Acute sensory-motor axonal neuropathy (GBS)	3T	7	4
5	63	F	PEA arrest	5T	4	1*
6	25	M	OHCA	4T	5	1*
7	67	M	Intraparenchymal hemorrhage	3T	2	1*
8	78	M	Herpes encephalitis	6T	6	1*
9	60	F	OHCA	3T	2	1*
10	78	M	HSV Encephalitis	8T	7	3
11	67	M	Status epilepticus (resolved), metabolic encephalopathy	8T	15	4
12	49	M	Hepatic encephalopathy	6T	16	1
13	54	M	OHCA in context of STEMI	3T	3	1
14	74	M	PEA arrest	3T	3	--
15	61	M	Right middle cerebral artery territory stroke	6T	3	--
16	59	F	Hepatic encephalopathy	5T	6	3

Table 1. Patient clinical and demographic information.

M = male, F = female, GCS = Glasgow Coma Scale, GOSE = Glasgow Outcome Scale Extended (6 months). STEMI: ST elevation myocardial infarction, PEA: Pulseless electrical activity, OHCA: Out-of-hospital cardiac arrest, HSV: Herpes simplex virus.

*Notes: * death was due to Withdrawal of Life Support Measures, -- GOSE score was not recorded, ** determined based on ICU admission and eligibility.*

2.2.2 Healthy Controls Participants

Neuroimaging data was also collected from a group of 25 healthy control participants (mean age 24.9 years, 13 females) prior to my arrival in the lab as a benchmark for typical neural activity during resting-state. From this healthy control group, two participants were removed due to unusable short channels (refer to section 2.4.1). The mean age for the remaining 23 healthy controls was 24.7 years (11 females). These participants had no history of neurological disorders or cognitive impairments.

2.3 Data Acquisition

2.3.1 fNIRS System

Data was collected using the NIRScout system (NIRx Medical Technologies) with an optode design that provided coverage of the frontal, parietal, temporal, and occipital regions. The system consisted of 32 sources and 39 detectors (lasers, centered at 785, 808, 830, and 850 nm), resulting in 121 source-detector pairs at 3 cm (i.e., channels) and 8 source-detector pairs at 0.8 cm (i.e., short channels). In total, there were 129 channels. The optodes were positioned in hemispherically symmetrical grids based on the 10-20 international system of electrode placement and secured on the head using a head cap (Homan et al., 1987). *Figure 13* shows the location of each source and detector.

Figure 13. The fNIRS montage used in this study. Red dots represent sources (32), blue dots represent detectors (31), and blue circles around the sources represent short channels (8). [Interpreted from Kazazian et al., 2021.]

2.3.2 Experimental Procedure

2.3.2a Patient Behavioural Testing Procedure

After consent was acquired from the substitute decision maker for the study, patients underwent behavioural testing prior to neuroimaging procedures. This test was completed by a trained professional and included the GCS.

Patients who survived at the 6-month mark were contacted over the phone to complete behavioural testing to assess patient outcomes (using the GOSE).

2.3.2b Patient fNIRS Testing Procedure

Neuroimaging began after behavioural testing was complete. The patient's bed was adjusted to a low-Fowler's position (30 degrees). The head was supported using a towel behind the neck to ensure proper optode placement on occipital head regions. The patient's head size was measured to find the appropriate cap size; a larger cap size was used for comfort and to prevent any tightness or swelling during testing. The fNIRS cap was fitted on the patient's head and carefully strapped around the chin, if possible. Before each source and detector was individually attached to the cap, hair was gently moved to allow direct contact between the optode and scalp. The sources and detectors were secured using spring-loaded grommets of varying tension. The average setup time was approximately 45 minutes.

The lighting in the patient's room was minimized and the fNIRS system was calibrated to ensure high-quality signal acquisition from each optode. Any optodes that indicated low quality were adjusted (i.e., hair was moved or grommet was replaced) and the system was recalibrated. Once all the sources, detectors, and short channels were attached properly and the calibration was complete, testing began.

It was unclear whether unresponsive patients understood verbal instructions. Nonetheless, standard protocols used in previous resting-state studies were followed. The patient was verbally informed the study was commencing and was provided with verbal instructions to stay relaxed and not focus their thoughts on anything in particular (Abdalmalak et al., 2022). After 6 minutes of data acquisition, the resting-state task was complete.

As this was part of a larger study, several other tasks were performed on each patient, including mental imagery (motor imagery and spatial navigation), auditory processing (movie listening), and somatosensory stimuli (median nerve stimulation). Once all tasks were completed, the lights were turned back on. The patient was verbally informed that the study was complete, and the cap was removed to relieve any tension or discomfort the patient may have felt. The average data acquisition time was approximately 90 minutes.

2.3.2c Healthy Control fNIRS Testing Procedure

Healthy control participants were seated in a dimly lit room. The fNIRS setup was similar to that of patients, except the cap was sized down to ensure a snug fit. The average setup time was approximately 45 minutes. Participants were instructed to close their eyes, stay relaxed, try not to move, and not focus their thoughts on anything in particular. After fNIRS calibration, resting-state data was collected for 6 minutes. To ensure that participants did not fall asleep during the procedure, the research team observed the participant's behaviour. Once the testing was completed, participants were asked if they had fallen asleep at any point and none of the participants reported having done so.

2.4 Data Analysis

Data was analyzed using Matlab R2022b (The Mathworks Inc.) and Python 3.9. First, the data was preprocessed, and graph metrics were calculated on Matlab. Then, the data was assessed using machine learning algorithms in Python.

2.4.1 Preprocessing

Data was preprocessed using scripts adapted from the HomER 2 software package (Huppert et al., 2009).

The data preprocessing pipeline commenced with an evaluation of signal quality. Channels exhibiting a signal-to-noise ratio (SNR) below 8 were identified as poor quality and marked for removal in later analyses (Abdalmalak et al., 2022). Welch power spectral density estimates were plotted for the short channels to confirm the presence of a distinct peak around the heart rate frequency (~1Hz). Short channels that did not display a clear peak were excluded from further analysis. Participants without any usable short channels or excessive bad channels (i.e., the majority of the channels did not have good SNR) were

removed from subsequent analyses. Notably, two healthy controls were excluded due to the absence of usable short channels, and three patients were excluded due to similar issues (two without usable short channels and one with an exceptionally high count of 109 bad channels).

The light intensity measurements for each channel were then converted into changes in optical density. Next, motion artifacts caused by non-perpendicular optode placement and associated movements were corrected. This correction process involved spline interpolation to adjust for baseline shifts ensuring a continuous signal, and wavelet decomposition to mitigate sharp spikes in the data (Abdalmalak et al., 2022). Following this, optical density was converted into changes in hemoglobin concentrations using the modified Beer-Lambert law.

The data was further band-pass filtered between 0.009 and 0.08 Hz to eliminate low- and high-frequency interference noise (Mesquita et al., 2010). Short channel data, derived from good-quality channels only, was regressed using a generalized linear model to remove physiological noise, such as variations in heart rate and respiration. Next, the time series data was pre-whitened to remove temporal autocorrelation and minimize false positives (Abdalmalak et al., 2022; Blanco et al., 2018).

Finally, HbT was calculated as the sum of HbO and HbR concentrations. For further analyses, correlation matrices were then generated for HbO, HbR, and HbT.

2.4.2 Graph Metric Calculation

Once correlation matrices were generated, all diagonals of the matrices were made 0 to remove any self-loops (an edge that is connected to the same node). A threshold ($r = 0.3$) was defined and any channels that needed to be excluded (bad channels and short channels) were replaced with a non-numerical value (nan; Novi et al., 2016). Based on the threshold, binary graphs were then computed using the built-in Matlab *graph* function. These graphs were represented and stored as adjacency matrices, where a non-zero value represents the presence of an edge. Using the adjacency matrices, graph metrics were calculated for degree, clustering coefficient, local efficiency, and betweenness centrality for HbO, HbR, and HbT.

2.4.2a Degree Calculation

The degree of each node was calculated by finding the sum of each row in the adjacency matrix. This value was normalized by dividing each value by the size of the graph to account for the differing number of nodes across participants. The size of the graph was obtained by removing the number of bad channels and short channels from the total number of nodes. The following equation was used to calculate each node's degree, *D*, using the adjacency matrix, *A* (Newman, 2016).

$$D(u) = \frac{\sum_{j=1}^{u} A_{ij}}{N-1}$$

In this equation:

- *u* represents the node of interest,
- *A* represents the adjacency matrix,
- *i* and *j* represent the row and column of the adjacency matrix, and
- *N* represents the size of the graph.

2.4.2b Clustering Coefficient Calculation

The clustering coefficient of each node was calculated by computing the ratio of the number of triangles to the total possible number of triangles that included the node and was only calculated if the degree of the node was ≥ 2. The following equation was used to calculate each node's clustering coefficient, *C*, by finding the number of links between the neighbours of the node, *L*. This value was normalized by dividing *L* with the number of neighbours of the given node (Barabási, 2014; Newman, 2016; Watts & Strogatz, 1998).

$$C(u) = \frac{2L}{k^2 - k}$$

In this equation:

- *u* represents the node of interest,
- *L* represents the number of links between the neighbours of node *u*, and
- *k* represents the number of neighbours of the node.

2.4.2c Local Efficiency Calculation

The local efficiency of each node was calculated by finding the inverse of the shortest path length in the neighbourhood of a node. The following equation was used to calculate each node's local efficiency, E, using the shortest path length, P, between neighbours, j and h. This value was normalized by the number of neighbours of the given node, k (Latora & Marchiori, 2001).

$$E(u) = \frac{1}{k^2 - k} \sum_{j,h \in G} \frac{1}{P_{jh}}$$

In this equation:

- u represents the node of interest,
- G represents the graph,
- P represents the shortest path between two neighbours (j and h), and
- k represents the number of neighbours of the node.

2.4.2d Betweenness Centrality Calculation

The betweenness centrality of each node was calculated using the built-in Matlab *centrality* function, specified with the '*betweenness*' parameter. The following equation was used to calculate each node's betweenness centrality, B, using the number of shortest paths between two nodes, s and t, that pass through the node, l_{st}, and the total number of shortest paths between s and t, L_{st}. This value was normalized by dividing each value by N^2, which represents the total number of nodal pairs (Newman, 2016).

$$B(u) = \frac{\sum_{s,t \neq u} \frac{l_{st}}{L_{st}}}{N^2}$$

In this equation:

- u represents the node of interest,
- l_{st} represents the number of shortest paths between two nodes (s and t) that pass through node u,
- L_{st} represents the total number of shortest paths between two nodes (s and t), and

- *N* represents the total number of nodal pairs.

2.4.2e Giant Component Extraction

The giant component was extracted using the built-in Matlab *conncomp* function. This function finds all the components of the graph and stores the size of the connected components and the number of nodes in the component. The giant component graph was then extracted, and metrics were recalculated using the equations above.

2.4.3 Statistical Analysis

2.4.3a Whole-Brain Differences

The whole-brain differences between patients and healthy controls were investigated for degree, clustering coefficient, and local efficiency for HbO, HbR, and HbT. The mean across all nodes in the brain was calculated to obtain a global brain value for each metric. The distribution of nodes, edges, and degrees was also examined. These whole-brain averages were compared between healthy controls and patients using a two-tailed Wilcoxon rank sum test (positive false discovery rate, PFDR < 0.05).

2.4.3b Giant Component Differences

Since each participant contained one giant network and several disconnected nodes, the giant component was extracted for each participant and metrics were recalculated and compared between groups. The main difference was that isolated nodes (nodes with no edges) were excluded when calculating graph metrics. The degree, clustering coefficient, and local efficiency were compared for HbO, HbR, and HbT using a two-tailed Wilcoxon rank sum test (PFDR < 0.05).

2.4.3c Betweenness Centrality Scores

The betweenness centrality score for each node was examined to find the location of important nodes in the brain. The higher the betweenness centrality, the more often that node acted as a bridge between two other nodes and was a critical connector node in the brain. The top three most important nodes were located for each participant. The proportion of nodes in the frontal, parietal, temporal, or occipital lobe was calculated to determine general regional differences in these nodes between groups. The number of

nodes was then grouped based on higher-order regions (frontal and parietal lobes) and sensory regions (temporal and occipital lobes). This grouping of regions was chosen since nodes in higher-order regions would be more important for higher-order functioning than sensory regions. To observe for differences in higher-order compared to sensory regions, the number of nodes in each of the four lobes was divided by 48 (top 3 nodes x 16 patients) for patients and 69 (top 3 nodes x 23 healthy controls) for healthy controls. By then grouping these proportions into higher-order and sensory regions, a Chi-squared test was run to observe if there was a statistical difference between the number of important nodes in the frontal and parietal regions compared to the temporal and occipital regions.

2.4.3d Local Channel Differences

To observe local channel differences between groups, the distribution of values for each channel was compared between healthy controls and patients using a Wilcoxon rank sum test (PFDR < 0.05) and values were corrected for multiple comparisons (false discovery rate). Bad and short channels were excluded when comparing the distributions, resulting in a comparison of all 121 channels between groups.

2.4.4 Machine Learning Analysis

Graph metrics (degree, clustering coefficient, local efficiency, and betweenness centrality) were used in machine learning algorithms (in Python 3.9 using *scikit-learn* packages) to construct models that would accurately classify groups (Pedregosa et al., 2011). Models were run to assess classification performance between three groups: (1) healthy controls and patients, (2) high and low GOSE scores, and (3) high and low GCS scores. Each model was run first for each individual graph metric (degree, clustering coefficient, local efficiency, betweenness centrality) and then for all metrics combined.

2.4.4a Model Processing

Outliers in the data were removed by calculating the *z*-score for each value and any values beyond 3 standard deviations were omitted from further analyses. This omission removed data points that were unlikely to represent the data and might instead reflect noise. Any values that were missing (i.e., bad channels across all participants; 0.04% for

degree, 1.61% for clustering coefficient, 2.03% for local efficiency, 1.82% for betweenness centrality) were imputed using data from the 3 nearest neighbours (using *KNNImputer*). To standardize the data and prevent any influence by extreme outliers in the dataset, all features were adjusted to have the same scale (using *RobustScaler*). Since combining all four graph metrics produced a dimensionality problem (39 participants x 121 channels x 4 metrics, greatly increasing the complexity of the dataset), a feature selection technique was implemented to reduce the high dimensionality of the data (Zebari et al., 2020). This feature selection technique was only applied when all four metrics (degree, clustering coefficient, local efficiency, and betweenness centrality) were combined and inputted as a feature (not for each individual metric). This technique and other hyperparameter values (which control the model learning process) were optimized using hyperopt, a Bayesian optimization approach (Bergstra et al., 2013).

2.4.4b Models

(i) Linear Support Vector Classifier

A search space for hyperparameters was defined and included (1) *C*, or regularization strength, which controlled the size of the model's coefficients, and (2) *tol*, or tolerance, which determined when the algorithm should stop iterating.

(ii) K-Nearest Neighbours Classifier

A search space for hyperparameters was defined and included (1) the number of neighbours (nearest data points) to use, and (2) the method used to calculate the weights the neighbours would be given based on their distance to the new data point.

(iii) Radial Basis Function, Support Vector Classifier

This model was set up similarly to the linear SVC and included the *C* and *tol* hyperparameters. The search space also included the *gamma* parameter, which defined the width or slope of the rbf function.

2.4.4c Model Iteration

The performance of each model was then estimated using a stratified three-fold cross-validation with 100 iterations. For each iteration, the data was split randomly into three

folds, with data trained on two of the folds and tested on the remaining third one. This was iterated 100 times to ensure different training and testing data subsets were used.

2.4.4d Model Evaluation

Based on all iterations across all folds, balanced accuracy score (median), confidence interval, interquartile range, recall score, precision score, and specificity score were calculated to evaluate the model. A balanced accuracy score is preferred when the groups are imbalanced, as was the case in this study. The importance of each channel was also determined (by calculating z-scores based on the *permutation_importance* Python function) for each feature and model to observe which channels the algorithms used most often for classification.

2.4.4e Group Classifications

(i) Healthy Control Participants and Patients

For the first classification, the three models described above were used to distinguish between all healthy controls (*n*=23) and patients (*n*=16). In this case, each fold was trained on 26 participants (15-16 healthy controls, 10-11 patients) and tested on 13 participants (7-8 healthy controls, 5-6 patients).

(ii) High and Low GOSE Scores (Patient Outcome)

For the second classification, the three models were used to distinguish between GOSE scores from patients only (*n*=14, since 2 patients did not have recorded GOSE scores). Patients that had a GOSE score of 1 (indicating death) were categorized as one group (10 patients, poor outcome group) and those with a score greater than 1 were another group (4 patients, good outcome group). This stratification was selected due to the small and already imbalanced sample size. In this case, each fold was trained on 9-10 patients (6-7 poor outcome, 2-3 good outcome) and tested on 4-5 patients (3-4 poor outcome, 1-2 good outcome).

(iii) High and Low GCS Scores (Patient Level of Consciousness)

For the third classification, the three models were used to distinguish between GCS scores in patients at the time of neuroimaging (*n*=16). Patients with a low GCS score between 3-5 were categorized as one group (9 patients) and those with a high GCS score

between 6-8 were another group (7 patients). This stratification was selected due to the small sample size of patients and differences in survival chances. A GCS score of 3-5 can present with high mortality and a lower chance of survival, whereas a GCS score of 6-8 shows more potential for survival if approached with aggressive treatment plans (Alves & Marshall, 2006). In this case, each fold was trained on 10-11 patients (6 with low GCS scores, 4-5 with high GCS scores) and tested on 5-6 patients (3 with low GCS scores, 2-3 high GCS scores).

2.4.4f Permutation Testing

The performance of the classification models (for all group classifications) was assessed using non-parametric permutation testing, which is ideal for estimating bias in uneven and small group sizes (Combrisson & Jerbi, 2015; Nichols & Holmes, 2002). This statistical analysis relies on generating a null distribution using permutations of the given data. The null distribution represents a spread of balanced accuracy scores that would occur if there was no real association between the labels and the data. The mean and variance of the null distribution are often influenced by idiosyncrasies in the data, such as outliers or unusual patterns (Combrisson & Jerbi, 2015). This distribution can then act as a reference point for evaluating the balanced accuracy scores against chance alone. To complete this permutation in this study, the labels of the data were randomly reassigned and the same classification models were rerun using the new shuffled data (Nichols & Holmes, 2002). The null hypothesis distribution was generated from 100 permutations of the randomly shuffled data and was compared to balanced accuracy scores generated from correctly labelled data. For there to be a statistically significant difference between groups, the median balanced accuracy score had to fall outside the upper 95% of the null distribution.

Chapter 3: Results

3.1 Whole-Brain Differences

The number of nodes were first compared between healthy controls and patients to see if there were any differences between participants. Nodes provide information about how many good channels patients have compared to healthy controls. Since the number of nodes were consistent across chromophores (HbO, HbR, and HbT), only results for HbO are shown below.

A Wilcoxon rank sum test for the number of nodes between the groups suggested that there is no significant difference between healthy controls and patients for any chromophores (*Figure 14*, $Z = -0.614$, $p = 0.540$).
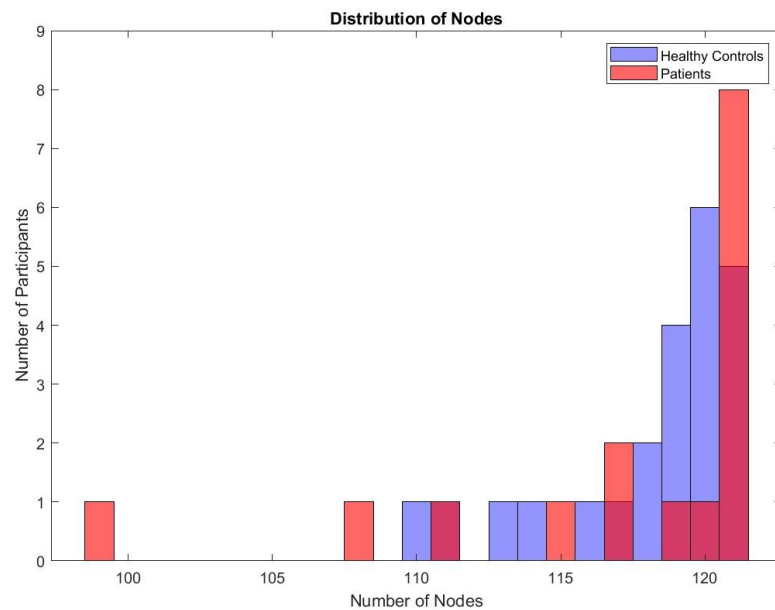
Figure 14. Number of nodes for healthy controls and patients.

Next, the number of edges between healthy controls and patients was compared for each chromophore. The number of edges provides insight into general connectivity differences since it directly corresponds to the number of total connections between nodes.

When comparing the number of edges between healthy controls and patients for HbO, there were no significant differences between the groups (*Figure 15, Z = 1.642, p = 0.101*).
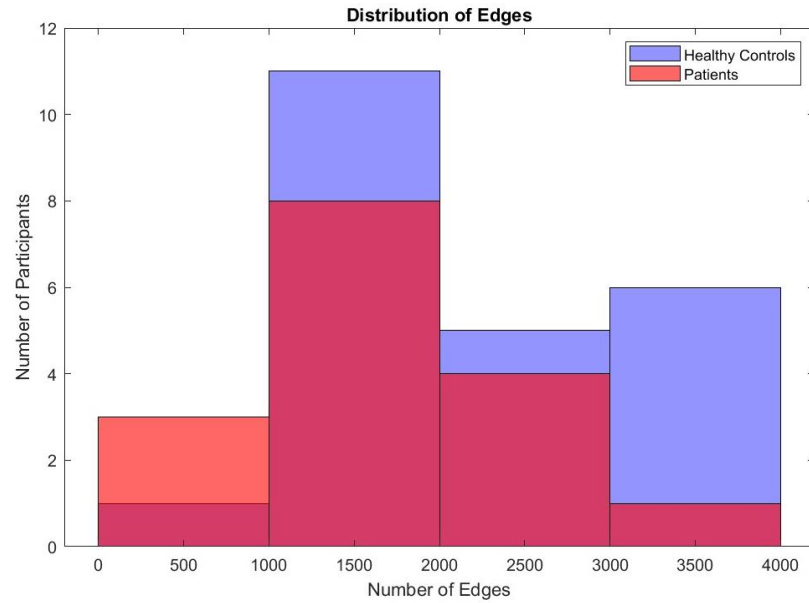
Figure 15. Distribution of edges for healthy controls and patients for HbO.

Comparing the number of edges between healthy controls and patients for HbR suggested no significant difference between the groups (*Figure 16, Z = 0.328, p = 0.743*).
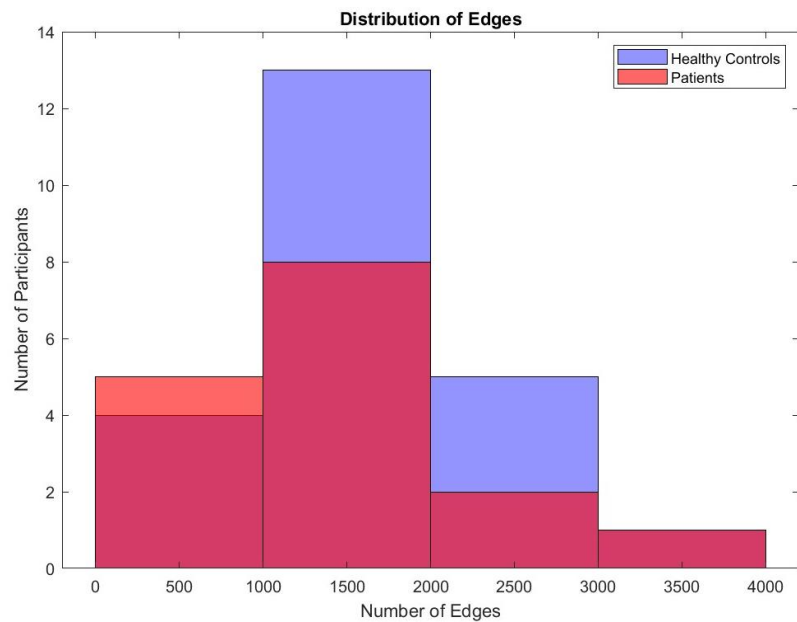
Figure 16. Distribution of edges for healthy controls and patients for HbR.

Lastly, there were no significant differences in the number of edges for HbT between healthy controls and patients (*Figure 17*, $Z = 0.671$, $p = 0.502$).
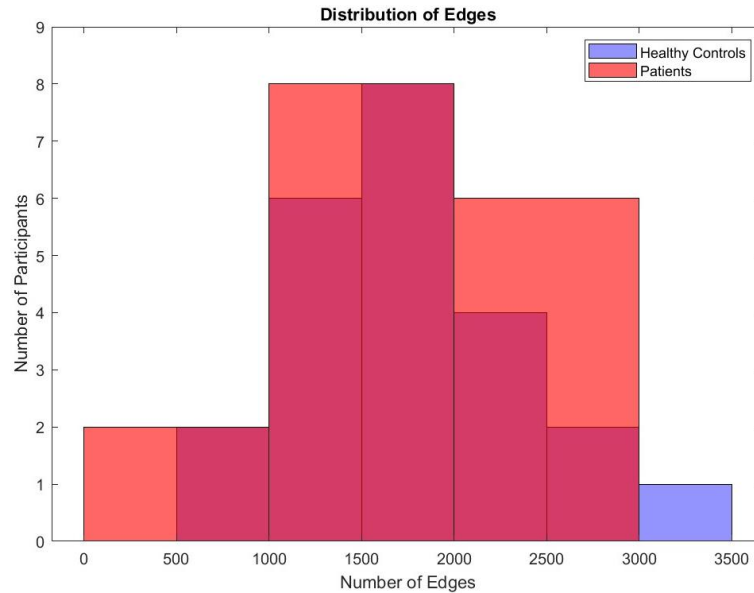
Figure 17. Distribution of edges for healthy controls and patients for HbT.

Although the number of nodes and edges did not differ significantly between groups for any chromophores, in principle, valuable information could still be derived from the graph metric values.

Thus, the whole-brain averages were computed for each healthy control and patient, for degree, clustering coefficient, and local efficiency, and for each chromophore to observe any significant global brain differences between groups. This computation was done by calculating the mean across all nodes in the brain to obtain a global brain value for the given metric. Significant differences were found for clustering coefficient between patients and healthy controls at the whole-brain level only for HbO.

Figures 18-20 show the global average degree, clustering coefficient, and local efficiency values, respectively, for each healthy control and patient for HbO, HbR, and HbT.
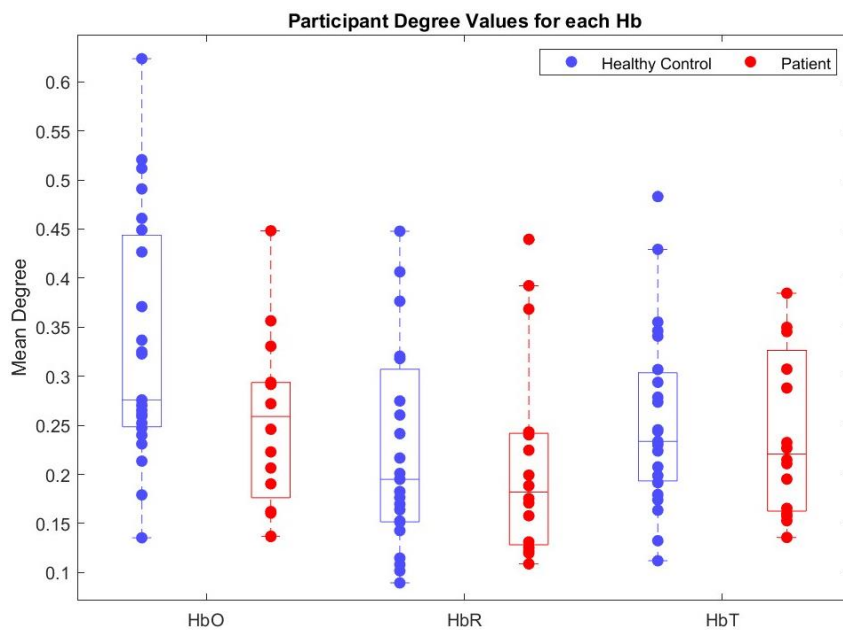
Figure 18. Whole-brain average degree values for healthy control and patient groups for all chromophores.
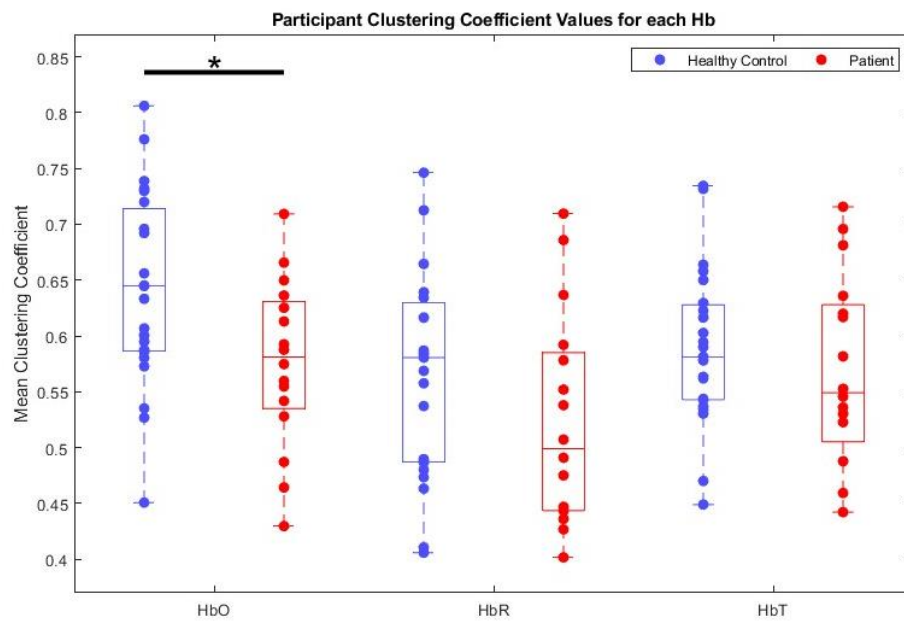
*Figure 19. Whole-brain average clustering coefficient values for healthy control and patient groups for all chromophores. *Black star indicates a statistical significance between groups.*

Figure 20. Whole-brain average local efficiency values for healthy control and patient groups for all chromophores.

Table 2 shows the Wilcoxon rank sum test *p*-values and *z*-values between groups for each metric and chromophore.

	HbO		HbR		HbT	
	p-value	*z*-value	*p*-value	*z*-value	*p*-value	*z*-value
Edges	0.101	1.642	0.743	0.328	0.502	0.671
Degree	0.074	1.785	0.764	0.328	0.578	0.557
Clustering Coefficient	0.031*	2.156	0.158	1.413	0.400	0.842
Local Efficiency	0.051	1.956	0.638	0.471	0.830	0.214

*Table 2. Whole-brain Wilcoxon rank sum test p-values and z-values between healthy controls and patients for HbO, HbR, and HbT. *Star indicates a significant difference between groups.*

Since HbO showed significant differences between groups for clustering coefficient, only HbO was explored further. The degree is one of the most basic graph metrics and is related to the number of edges. The distribution of degree values for each node was compared between healthy controls and patients for HbO (*Figure 21*). This comparison was done to eliminate any effects averaging the number of edges across the brain may have had. Therefore, all values of degree were compared, and results indicated a significant difference between groups ($Z = 13.534$, $p = 9.892e\text{-}42$). This analysis

suggested that important differences between healthy controls and patients are present but are being lost when averaging the number of edges across the brain.
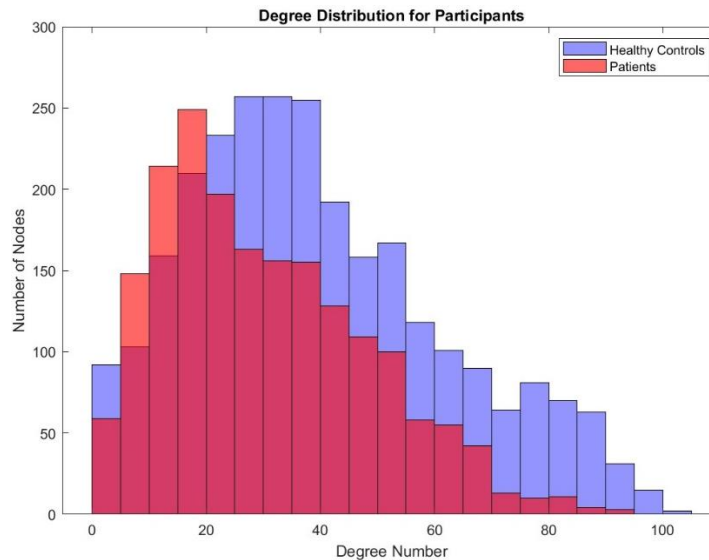
Figure 21. Degree distribution for healthy controls and patients.

3.2 Giant Component Differences

After further investigation, it was found that each participant had one giant component and several disconnected nodes (participants' isolated nodes comprised 0-18% of the total number of nodes). *Table 3* shows descriptive statistics for the size of the giant component for healthy controls and patients. As evident in *Table 3*, there was no difference between the average size of the giant component between groups.

	Mean	Median	Range	Minimum	Maximum
Healthy Controls	117	118	13	108	121
Patients	117	120	22	99	121

Table 3. Descriptive statistics for the size of the giant component for healthy controls and patients.

Although there was no difference in the mean size of the giant component between groups, the presence of isolated nodes still altered the values of metrics at the nodal level. When calculating graph metrics, isolated nodes compute a value of 0 since they do not have any edges connecting them to other nodes. Only the giant component was

investigated next to eliminate the effect these isolated nodes had on the metrics. Any nodes that were not part of the most connected network were removed. This changed the whole-brain metric values since all nodes that had values of 0 were removed when recalculating metrics. Thus, the giant component was extracted for each participant and each chromophore, and values for degree, clustering coefficient, and local efficiency were recalculated, as seen in *Figures 22-24*, respectively.

For the giant component analysis, only HbO showed significant group differences for clustering coefficient and local efficiency. This analysis suggested that significant differences exist between groups using graph metrics and further investigation is required to detect specific distinguishing features.
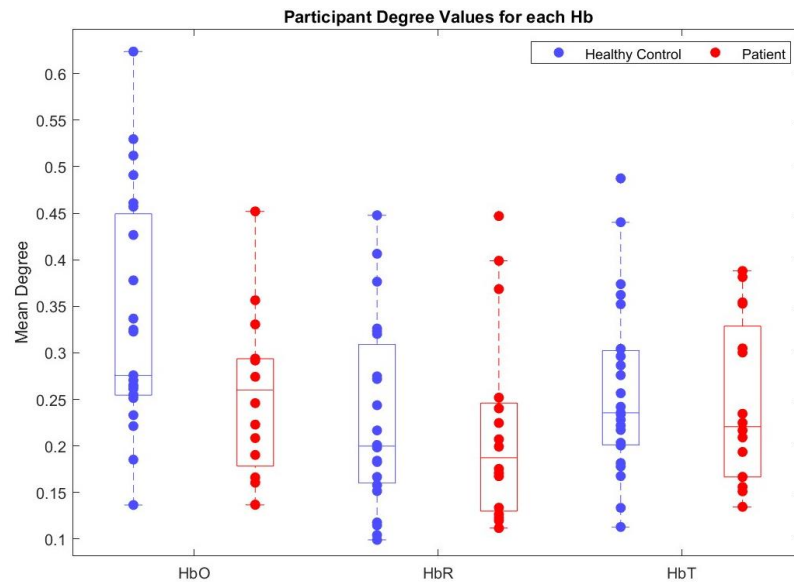
Figure 22. Giant component degree values for healthy control and patient groups for all chromophores.
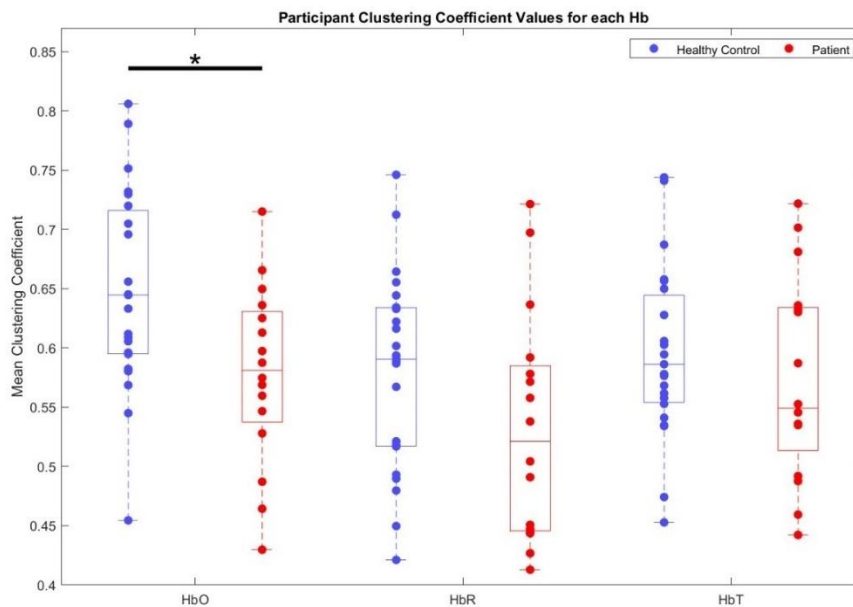
*Figure 23. Giant component clustering coefficient values for healthy control and patient groups for all chromophores. *Black star indicates a statistical significance between groups.*
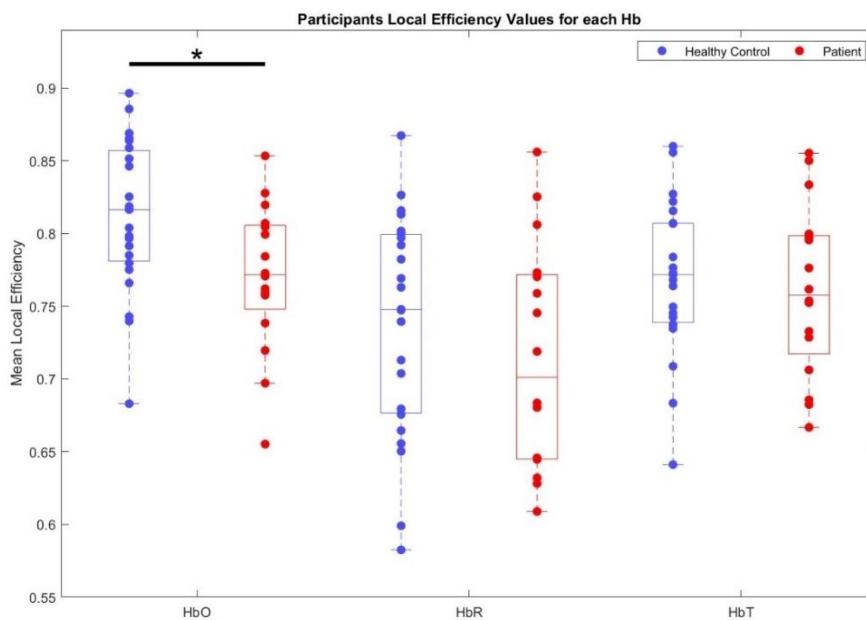
*Figure 24. Giant component local efficiency values for healthy control and patient groups for all chromophores. *Black star indicates a statistical significance between groups.*

Table 4 shows the Wilcoxon rank sum test *p*-values and *z*-values between groups for each metric and chromophore for the giant component.

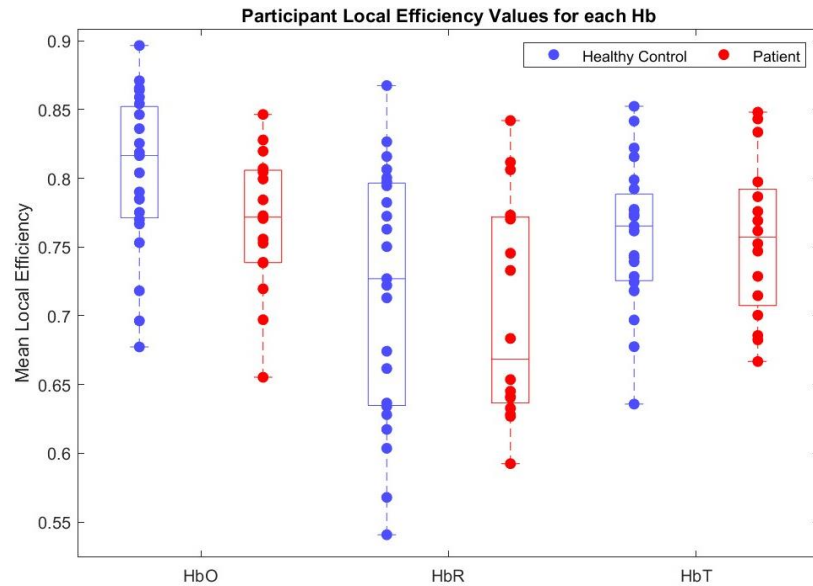|	HbO		HbR		HbT	
	p-value	*z*-value	*p*-value	*z*-value	*p*-value	*z*-value
Degree	0.070	1.813	0.743	0.328	0.558	0.585
Clustering Coefficient	0.020*	2.327	0.079	1.756	0.368	0.899
Local Efficiency	0.023*	2.270	0.297	1.042	0.578	0.557

*Table 4. Giant component Wilcoxon rank sum test p-values and z-values between healthy controls and patients for HbO, HbR, and HbT. *Star indicates a significant difference between groups.*

3.3 Betweenness Centrality Scores

Although a global analysis (for the whole-brain and giant component) showed some significant differences between healthy controls and patients using clustering coefficient and local efficiency, it could be that averaging across this subset of nodes in the brain still resulted in a loss of information and a regional analysis would be more suitable. Thus, the next step was to locate important nodes in the brain, which was achieved by looking at the betweenness centrality score for each node. The higher the betweenness centrality score, the more that node acted as a bridge between two other nodes and would be an important connector node in the brain. Exploring where important nodes (top 3) in the brain were located can provide a better understanding of potential regional differences between groups.

The betweenness centrality scores showed that for 23 healthy controls, 10 had their most important node in the frontal region, 10 in the parietal region, and 3 in the temporal region. Of the 16 patients, 10 had their most important node in the frontal region, 2 in the parietal region, 3 in the temporal region, and 1 in the occipital region. The second and third most important nodes (second and third highest betweenness centrality scores) were dispersed throughout the brain. *Table 5* shows the proportion of participants that had their top three most important nodes in the frontal, parietal, temporal, or occipital lobe.

	Frontal	Parietal	Temporal	Occipital
Healthy Controls	28/69 = 40.48%	24/69 = 34.78%	13/69 = 18.84%	4/69 = 5.80%
Patients	28/48 = 58.33%	6/48 = 12.5%	12/48 = 25%	2/48 = 4.17%

Table 5. Proportion of participants that have their top three most important nodes in the frontal, parietal, temporal, or occipital lobe.

A chi-squared test was run between healthy controls and patients to investigate differences in the location of the important nodes in the context of higher-order regions (frontal and parietal) and sensory regions (temporal and occipital). The chi-squared test revealed no significant differences between groups, X^2 (1, $N = 117$) = 0.30, $p = 0.59$. Regional analyses were too broad to locate differences between healthy controls and patients since there were no differences between where important nodes were located.

3.4 Local Channel Differences

Next, an even more localized analysis was used to probe findings from the giant component and regional analyses. This approach was more granular in that it examined the differences between groups without any averaging. In this analysis, the distribution of values for each channel was compared between healthy controls and patients using a Wilcoxon rank sum test and values were corrected for multiple comparisons (false discovery rate). This local analysis was completed for all graph metrics (i.e., degree, clustering coefficient, local efficiency, and betweenness centrality) and for all 121 channels. All bad channels and short channels were excluded from this analysis.

Findings from this approach showed significant differences between healthy controls and patients in 6 channels for degree, 80 channels for clustering coefficient, and 44 channels for local efficiency, as seen in *Figures 25-27*, respectively. All channels, for all metrics, had greater values for healthy controls compared to patients. Betweenness centrality showed no significant differences between groups for any channels.
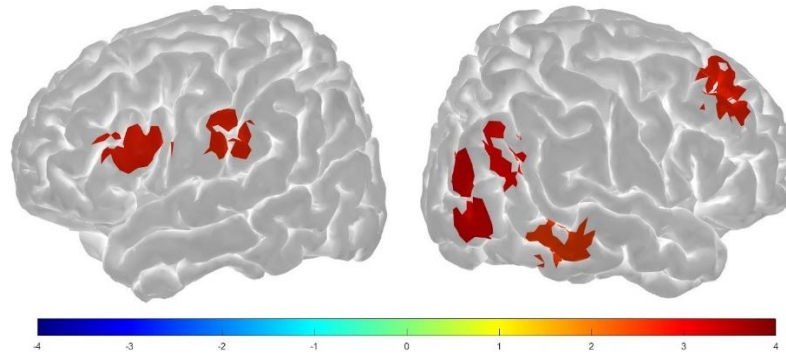
Figure 25. Significant channels (z-score) for degree projected onto the brain. Warm colours represent values that were greater for healthy controls compared to patients.
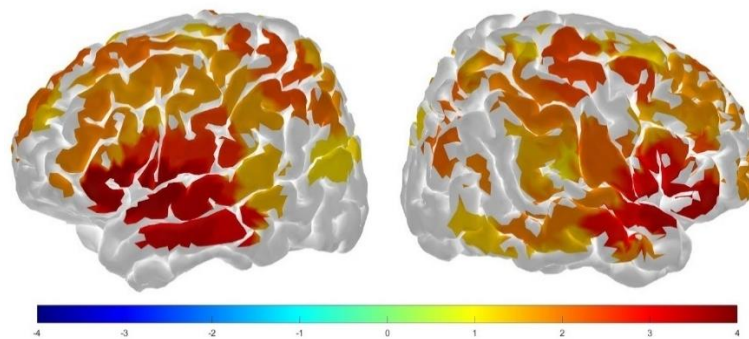
Figure 26. Significant channels (z-score) for clustering coefficient projected onto the brain. Warm colours represent values that were greater for healthy controls compared to patients.
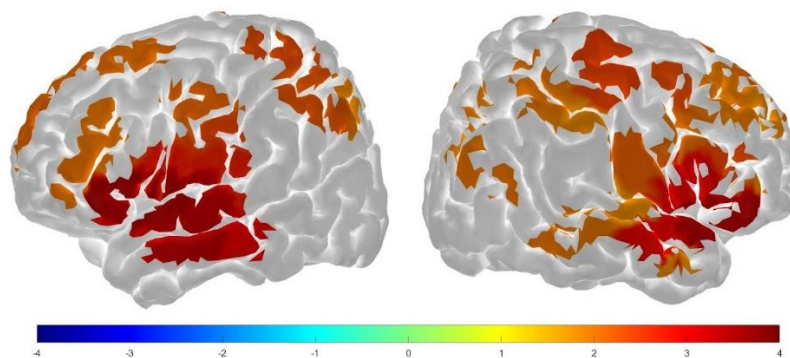
Figure 27. Significant channels (z-score) for local efficiency projected onto the brain. Warm colours represent values that were greater for healthy controls compared to patients.

Table 6 shows the graph metric *p*-values, and *z*-scores for each channel and its associated channel name in the brain, which showed a significant difference between groups.

Channel	Channel Name in the Brain	Degree		Clustering Coefficient		Local Efficiency	
		p-value	*z*-value	*p*-value	*z*-value	*p*-value	*z*-value
2	Frontal_Sup_Medial_L			0.021	2.091	0.038	2.121
5	Frontal_Sup_Medial_L			0.040	1.374		
10	Frontal_Inf_Tri_L			0.026	1.870	0.042	2.013
11	Cingulum_Mid_R			0.019	2.213	0.037	2.120
12	Frontal_Sup_L			0.031	1.699	0.047	1.899
14	Frontal_Sup_L			0.030	1.670		
15	Frontal_Mid_L			0.026	1.956	0.042	1.984
16	Frontal_Mid_L			0.031	1.672		
17	Frontal_Mid_L			0.046	1.214		
18	Frontal_Inf_Orb_L			0.010	2.744	0.012	2.872
19	Frontal_Inf_Tri_L			0.004	3.653	0.011	3.552
20	Frontal_Mid_L			0.021	2.084	0.042	2.042
21	Frontal_Mid_L			0.030	1.792		
22	Frontal_Mid_L			0.044	1.268		
23	Frontal_Inf_Tri_L	0.048	2.765	0.033	1.597		
24	Frontal_Inf_Oper_L			0.037	1.470		
25	Frontal_Inf_Oper_L			0.009	2.645	0.029	2.459
26	Frontal_Inf_Oper_L			0.010	2.658	0.013	2.807
27	Frontal_Inf_Oper_L			0.019	2.210	0.034	2.240
28	Postcentral_L			0.010	2.688	0.021	2.598
30	Precentral_L			0.047	1.195		
31	Precentral_L			0.032	1.676		
33	Parietal_Inf_L			0.033	1.583		
34	Precentral_L			0.031	1.670	0.037	2.156
35	Precentral_L			0.013	2.454	0.028	2.425
36	Postcentral_L	0.037	2.688				
38	Postcentral_L			0.032	1.628		
40	Temporal_Mid_L			0.006	3.178	0.010	3.208
41	Temporal_Mid_L			0.030	1.763		
42	Temporal_Sup_L			0.010	2.707	0.015	2.738
43	Temporal_Mid_L			0.032	1.626		
44	Temporal_Mid_L			0.006	3.001	0.014	2.942
45	Temporal_Mid_L			0.036	1.464		
46	Temporal_Mid_L			0.007	3.001	0.013	2.883
47	Temporal_Mid_L			0.014	2.479	0.028	2.389
48	Temporal_Sup_L			0.005	3.300	0.009	3.315
49	Postcentral_L			0.014	2.380	0.029	2.333
50	Parietal_Inf_L			0.014	2.356	0.033	2.270
51	Postcentral_L			0.035	1.508		
56	Temporal_Sup_L			0.035	1.499		
58	Temporal_Sup_L			0.038	1.413		
59	Parietal_Inf_L			0.021	2.120	0.032	2.240

60	Parietal_Inf_L			0.029	1.785	0.048	1.870
68	Occipital_Mid_L			0.047	1.191		
70	Occipital_Sup_L			0.044	1.250		
73	Frontal_Mid_R			0.030	1.756	0.048	1.813
76	Frontal_Sup_Orb_R			0.029	1.742		
78	Frontal_Sup_R	0.041	2.727	0.029	1.756	0.045	1.927
79	Frontal_Mid_R			0.033	1.562		
81	Frontal_Inf_Tri_R			0.024	2.006	0.047	1.829
82	Frontal_Inf_Orb_R			0.005	3.419	0.007	3.480
83	Frontal_Inf_Oper_R			0.007	3.042	0.012	2.932
84	Frontal_Sup_R			0.044	1.271		
85	Frontal_Mid_R			0.013	2.470	0.029	2.356
86	Frontal_Sup_R			0.042	1.314		
87	Frontal_Inf_Tri_R			0.013	2.429	0.029	2.398
88	Frontal_Inf_Oper_R			0.033	1.556	0.043	2.042
89	Rolandic_Oper_R			0.006	2.986	0.015	3.016
90	Rolandic_Oper_R			0.043	1.299		
91	Frontal_Inf_Oper_R			0.029	1.813	0.049	1.842
94	Precentral_R			0.013	2.413	0.029	2.441
96	Postcentral_R			0.024	2.013	0.048	1.842
98	Rolandic_Oper_R			0.021	2.144	0.037	2.173
101	SupraMarginal_R			0.030	1.727		
102	Insula_R			0.006	2.957	0.015	2.957
103	Temporal_Sup_R			0.042	1.328		
104	Temporal_Sup_R			0.025	1.927	0.047	1.842
106	Temporal_Mid_R			0.037	1.442		
107	Temporal_Mid_R			0.027	1.872	0.047	1.810
108	Temporal_Sup_R			0.041	1.348		
109	Postcentral_R			0.044	1.253		
110	Parietal_Inf_R			0.025	1.911	0.042	1.971
111	Parietal_Sup_R			0.035	1.523		
113	Temporal_Sup_R			0.049	1.156		
115	SupraMarginal_R			0.036	1.470		
116	Temporal_Mid_R			0.034	1.571		
120	Occipital_Mid_R	0.040	2.956				
121	Temporal_Mid_R			0.026	1.942	0.043	1.990
122	Temporal_Mid_R	0.049	2.527	0.042	1.328		
124	Temporal_Mid_R			0.041	1.375		
126	Parietal_Sup_R			0.021	2.135	0.046	1.897
127	Occipital_Mid_R			0.026	1.928	0.043	2.013
128	Occipital_Mid_R	0.030	3.241				

Table 6. List of channels, their associated channel name in the brain, p-values, and z-scores for degree, clustering coefficient, and local efficiency that were significantly different between groups.

3.5 Machine Learning

Once the local differences were detected, the data was inputted into machine learning models to determine if algorithms could classify between groups using the graph metrics. First, individual metrics (degree, clustering coefficient, local efficiency, betweenness centrality) for all 121 channels were inputted as features, and then all metrics were combined and inputted as one singular feature. Bad channels were removed for each metric, which included 0.04% of channels for degree, 1.61% for clustering coefficient, 2.03% for local efficiency, and 1.82% for betweenness centrality. The importance of a channel (for classifying groups) was only shown for statistically significant models that used clustering coefficient, if applicable. The statistical significance of median accuracy rates was based on non-parametric permutation testing.

3.5.1 Classification between Patients and Healthy Controls

Figure 28 shows the median accuracy rates for classification between healthy controls and patients for linear SVC, KNN, and rbf SVC models for individual and all metrics combined. Linear SVC and KNN models performed significantly well for individual and all metrics combined. The rbf SVC model performed slightly above significance for degree and all metrics combined.
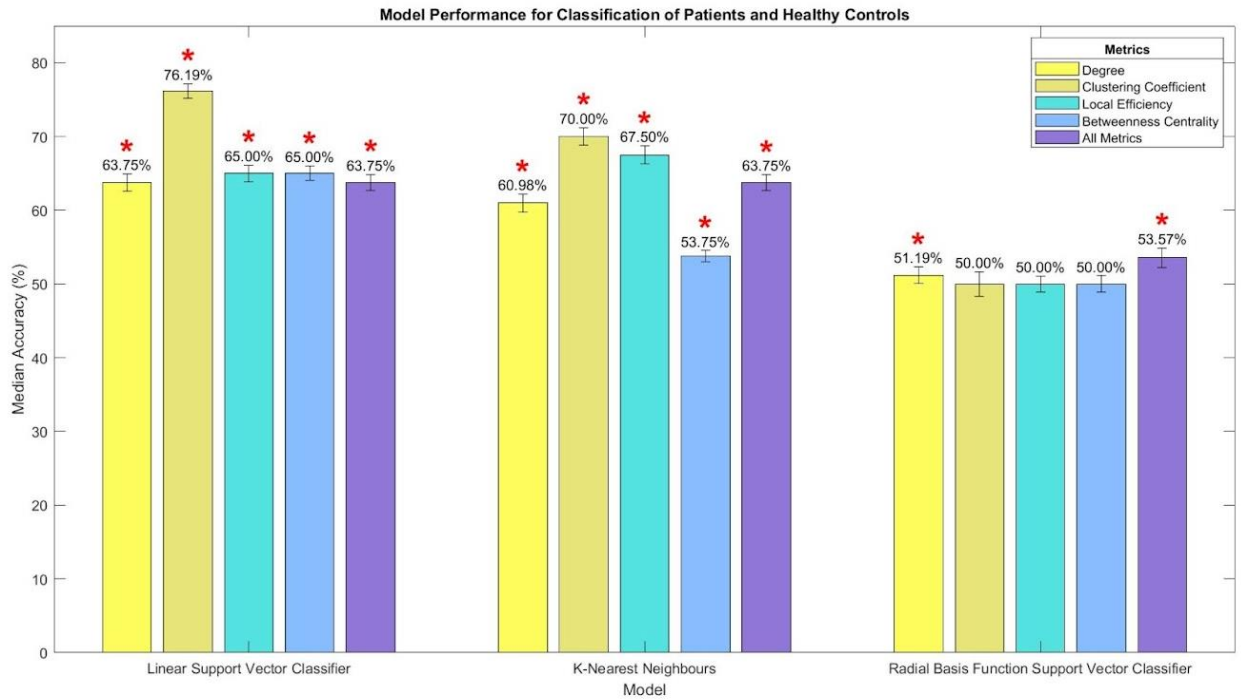
Figure 28. Median accuracy scores (with confidence interval as error bars) for classification between healthy controls and patients using three different models with various features (individual metrics and all metrics combined). Red stars represent statistical significance based on non-parametric permutation testing.

Table 7 shows the median accuracy, interquartile range, precision, recall, and specificity scores in percentages for classification between healthy controls and patients.

		Degree	Clustering Coefficient	Local Efficiency	Betweenness Centrality	All Metrics
Linear SVC	Median	63.75	76.19	65.00	65.00	63.75
	IQR	16.25	16.25	16.25	16.56	16.25
	Precision	69.50	79.77	71.98	72.45	71.44
	Recall	83.27	82.19	75.83	73.64	63.07
	Specificity	45.71	68.03	54.78	57.98	39.79
KNN	Median	60.98	70.00	67.50	53.75	63.75
	IQR	17.57	16.25	19.06	10.00	17.19
	Precision	67.06	76.42	73.38	62.29	70.34
	Recall	75.49	74.58	71.16	96.95	82.50
	Specificity	45.52	64.12	59.74	14.89	57.29
rbf SVC	Median	51.19	50.00	50.00	50.00	53.57
	IQR	13.75	20.24	13.75	11.25	18.08
	Precision	63.69	68.24	64.40	64.24	67.13
	Recall	90.06	91.29	89.17	90.27	79.50
	Specificity	23.08	31.28	24.17	22.38	8.82

Table 7. Median accuracy, interquartile range (IQR), precision, recall, and specificity scores (all in %) for classifying healthy controls and patients for all models and feature combinations.

Table 8 shows the confusion matrices for the models and features that achieved 70%+ performance accuracy for classification between healthy controls and patients.

	Clustering Coefficient
Linear SVC	
KNN	

Table 8. Confusion matrices for classification between healthy controls and patients for linear SVC clustering coefficient and KNN clustering coefficient. In each matrix, the top left and bottom right boxes represent the number of patients and healthy controls that were correctly classified, whereas the top right and bottom left boxes represent patients and healthy controls that were misclassified.

Figures 29-30 show the importance of each channel (*z*-scores) when using clustering coefficient values to distinguish between healthy controls and patients using a linear SVC and KNN model, respectively.
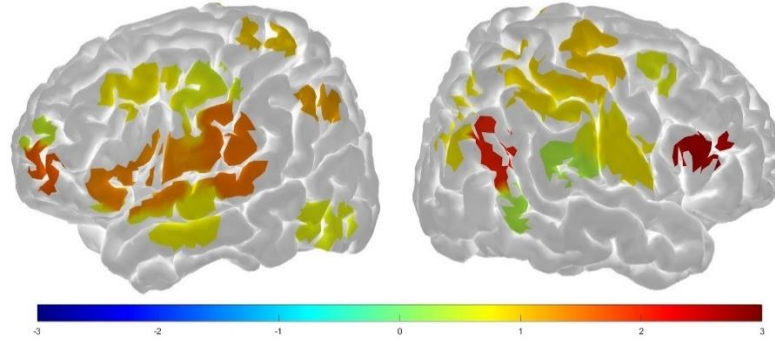
Figure 29. Importance of each channel (z-scores) when using clustering coefficient to distinguish between healthy controls and patients using a linear SVC.
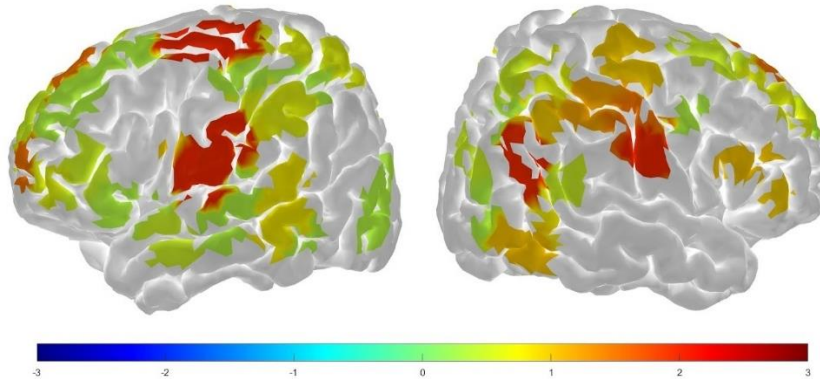
Figure 30. Importance of each channel (z-scores) when using clustering coefficient to distinguish between healthy controls and patients using a KNN model.

Linear SVC and KNN models performed well above chance when differentiating between healthy controls and patients using several metrics. Based on the importance scores, several channels were helpful for classifying between study groups using clustering coefficient. As expected, many of these channels overlapped with those that were significantly different between groups using statistical analyses (refer to section 3.4).

3.5.2 Classification between GOSE Scores

Figure 31 shows the median accuracy rates for classification between good outcomes
(i.e., GOSE score > 1) and poor outcomes (i.e., GOSE score = 1) for all three models and
features. Linear SVC and KNN models performed significantly well using degree,
clustering coefficient, and all metrics combined. Local efficiency and betweenness
centrality metrics for these models did not reach statistical significance. The rbf SVC
model performed at chance-levels for all features.
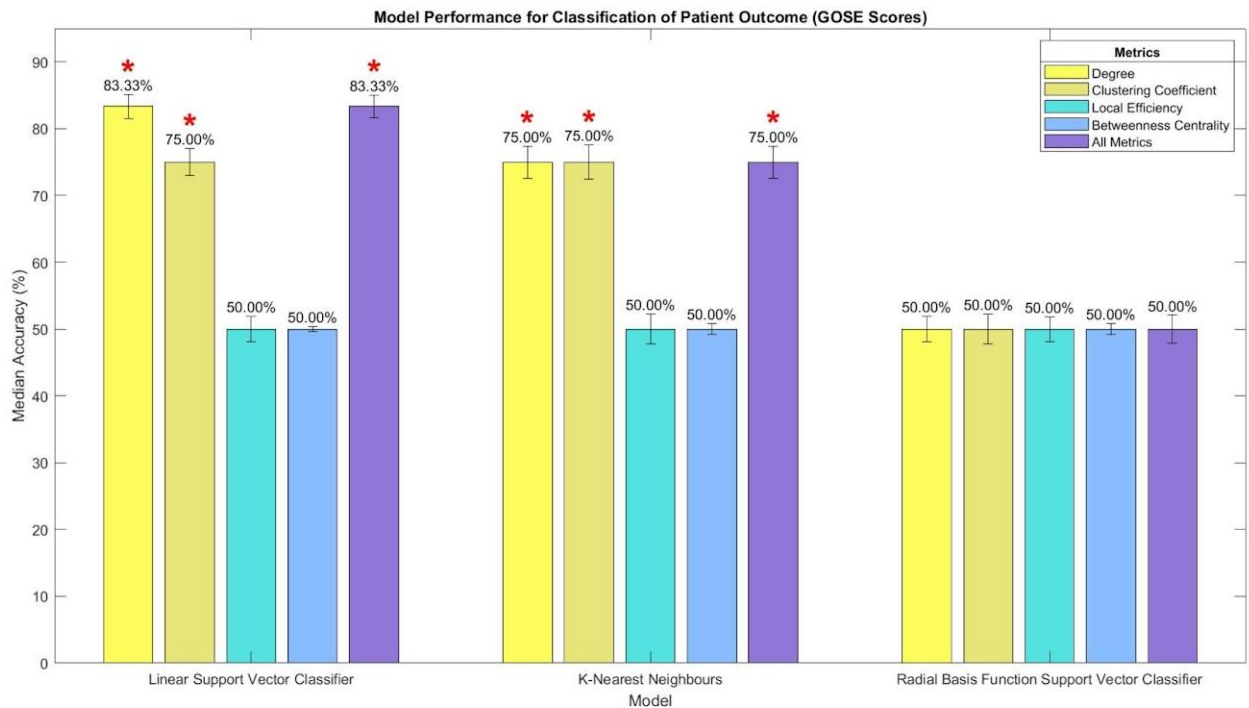
*Figure 31. Median accuracy scores (with confidence interval as error bars) for classification of
patient outcome using three different models with various features (individual metrics and all
metrics combined) for all models and feature combinations. Red stars represent statistical
significance based on non-parametric permutation testing.*

Table 9 shows the median accuracy, interquartile range, precision, recall, and specificity scores in percentages for classification between high and low GOSE scores.

		Degree	Clustering Coefficient	Local Efficiency	Betweenness Centrality	All Metrics
Linear SVC	Median	83.33	75.00	50.00	50.00	83.33
	IQR	41.67	50.00	50.00	0.00	43.75
	Precision	62.33	52.50	43.17	0.33	58.28
	Recall	67.50	50.50	46.67	0.33	67.00
	Specificity	87.19	98.89	97.44	99.33	97.81
KNN	Median	75.00	75.00	50.00	50.00	75.00
	IQR	37.50	50.00	40.62	0.00	50.00
	Precision	50.00	62.50	33.83	2.67	49.06
	Recall	65.83	55.33	29.67	2.17	48.33
	Specificity	83.17	99.19	99.83	98.56	99.00
rbf SVC	Median	50.00	50.00	50.00	50.00	50.00
	IQR	33.33	12.50	0.00	0.00	25.00
	Precision	31.28	22.61	15.00	3.11	23.39
	Recall	35.83	23.33	14.50	3.83	23.67
	Specificity	92.89	98.25	99.28	98.33	99.78

Table 9. Median accuracy, interquartile range (IQR), precision, recall, and specificity scores (all in %) for classifying patient outcomes for all models and feature combinations.

Table 10 shows the confusion matrices for the models and features that reached 70%+ accuracy for classification between high and low GOSE scores.

	Degree	Clustering Coefficient
Linear SVC		
KNN		

Table 10. Confusion matrices for classification of patient outcome for linear SVC degree and clustering coefficient, and KNN degree and clustering coefficient. In each matrix, the top left and bottom right boxes represent the number of patients with poor and good outcomes that were correctly classified, whereas the top right and bottom left boxes represent the number of patients with poor and good outcomes that were misclassified.

When distinguishing between high and low GOSE scores, linear SVC and KNN models performed well above chance when using degree, clustering coefficient, and all metrics combined.

3.5.3 Classification between GCS Scores

Figure 32 shows the median accuracy rates for classification between low (3-5) and high (6-8) GCS scores for all three models and all features. The linear SVC model performed significantly well for clustering coefficient and all metrics combined, and slightly above significance for degree. The KNN model performed significantly well for clustering coefficient, local efficiency, betweenness centrality, and all metrics combined. The rbf SVC model performed at chance-levels for all features.
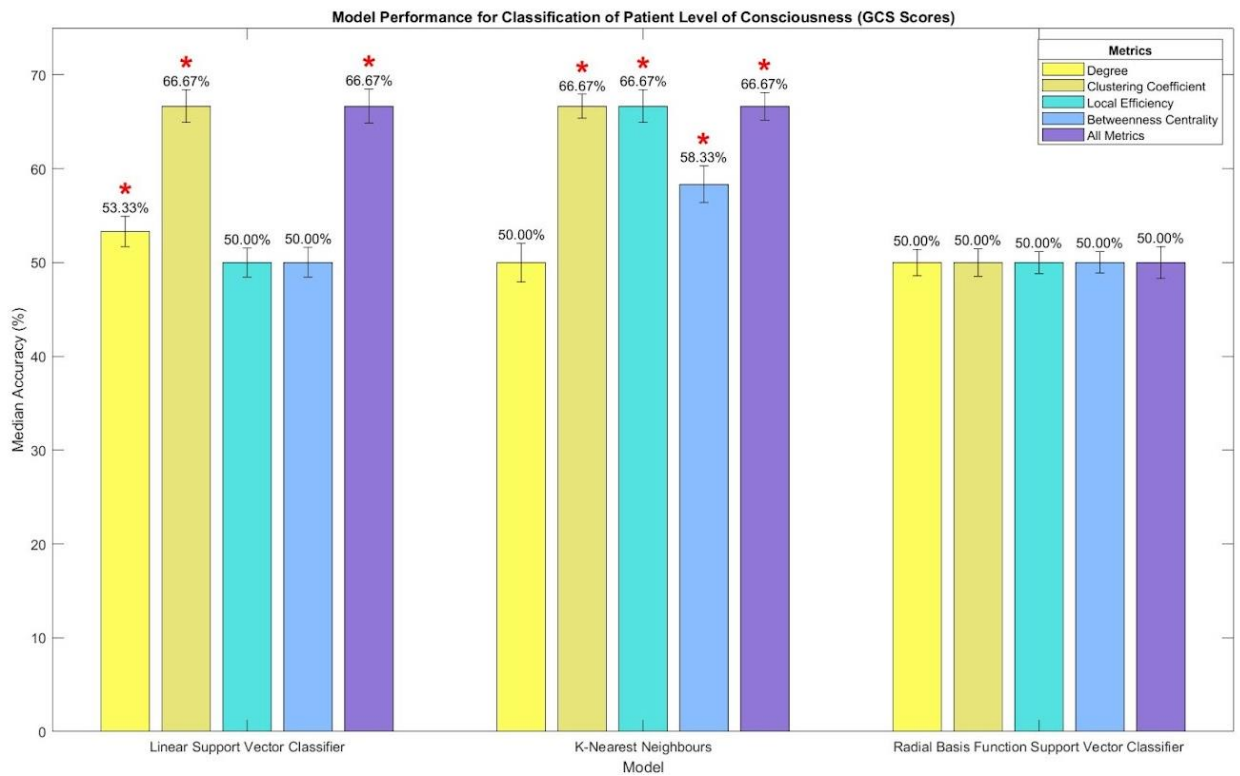
Figure 32. Median accuracy scores (with confidence interval as error bars) for classification of patient level of consciousness using three different models with various features (individual metrics and all metrics combined). Red stars represent statistical significance based on non-parametric permutation testing.

Table 11 shows the median accuracy, interquartile range, precision, recall, and specificity scores in percentages for classification between high and low GCS scores.

		Degree	Clustering Coefficient	Local Efficiency	Betweenness Centrality	All Metrics
Linear SVC	Median	58.33	66.67	50.00	50.00	66.67
	IQR	16.67	25.00	16.67	8.33	25.00
	Precision	44.58	57.83	33.29	27.11	54.12
	Recall	39.61	51.67	31.17	22.56	65.22
	Specificity	76.56	79.89	72.67	84.00	85.22
KNN	Median	50.00	66.67	66.67	58.33	66.67
	IQR	25.00	16.67	33.33	16.67	25.00
	Precision	42.63	63.12	53.41	46.57	57.18
	Recall	65.50	88.17	76.72	41.78	66.61
	Specificity	39.78	55.33	56.22	74.22	37.78
rbf SVC	Median	50.00	50.00	50.00	50.00	50.00
	IQR	8.33	16.67	0.00	0.00	16.67
	Precision	23.98	23.51	14.17	14.97	32.11
	Recall	22.83	21.67	14.00	12.28	35.67
	Specificity	84.22	92.00	89.56	91.33	98.11

Table 11. Median accuracy, interquartile range (IQR), precision, recall, and specificity scores (all in %) for classifying patient level of consciousness for all models and feature combinations.

Figure 33 shows the importance of each channel (*z*-scores) when using clustering coefficient values to distinguish between high and low GCS scores using a linear SVC model.
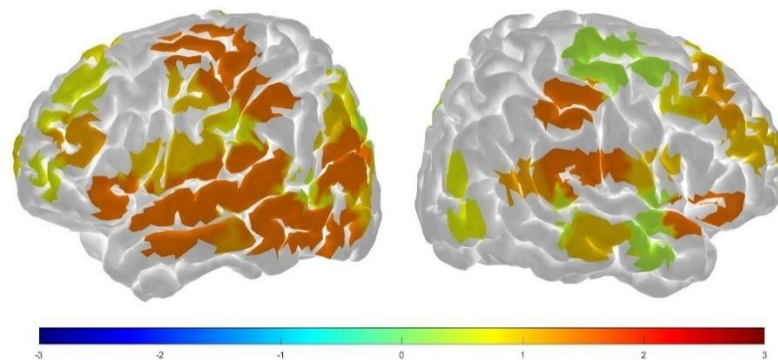
Figure 33. Importance of each channel (z-scores) when using the clustering coefficient to distinguish between patient level of consciousness using a linear SVC.

Classifying between high and low GCS scores was most accurate using linear SVC and KNN models and graph metrics of clustering coefficient, local efficiency, and all metrics combined were the most useful for this classification.

Chapter 4: Discussion

The present study investigated RSFC in 16 acutely brain-injured patients and 23 healthy controls using graph-theoretical analyses and machine learning algorithms. Whole-head neuroimaging data was collected using fNIRS, while behavioural assessments included measures of consciousness levels (i.e., GCS) and post-injury outcomes (i.e., GOSE).

Findings from this study indicated that whole-brain graph theory analyses could not distinguish between patients and healthy controls. However, local analyses identified differences in graph metrics, including degree, clustering coefficient, and local efficiency for multiple channels between groups. In particular, healthy controls had higher values for the three metrics than patients. These results were further investigated using three machine learning models. Of the three models used to assess these findings, the linear SVC and KNN algorithms performed above chance-levels when discriminating between two groups. Notably, clustering coefficient emerged as an important metric as the machine learning models were able to distinguish between healthy controls and patients with up to 76% accuracy using this metric. Furthermore, these algorithms discriminated between good and poor patient outcomes with up to 83% and 75% accuracy using degree and clustering coefficient, respectively. Lastly, using behavioral scores, machine learning models classified patients' level of consciousness with up to 66.67% accuracy using clustering coefficient and local efficiency.

4.1 Detecting Connectivity Differences using Graph Theory

Resting-state paradigms, which function as a 'baseline' measure of neural activity, can provide valuable information about network functionality, information integration and processing, and overall consciousness (Koculak & Wierzchoń, 2022). This paradigm captures the intrinsic connectivity in the brain and, therefore, can inform about any network disruptions that affect cognitive processing. According to studies on consciousness using resting-state paradigms, functional brain networks need to integrate and transfer information from a local to a global level for efficient conscious processing (Barttfeld et al., 2015; Heine et al., 2012). To achieve this, conscious processing requires complex interaction between multiple networks and the preserved ability to integrate

multisensory information (Crone et al., 2014; Demertzi et al., 2015; Di Perri et al., 2016; Han et al., 2016). When these functional networks within the brain are disrupted, information integration and communication are disturbed, which can result in altered states of consciousness.

4.1.1 Global and Local Connectivity Differences

The present study further explored how whole-brain RSFC differed in acutely brain-injured patients compared to healthy controls using graph theory. While previous studies have generally reported decreased functional connectivity across networks in critically brain-injured patients, this investigation aimed to provide a more comprehensive understanding of network connectivity, communication, and information processing in this population (Han et al., 2016; Hannawi et al., 2015; Koenig et al., 2014; Kondziella et al., 2016; Long et al., 2016; Norton et al., 2012; Snider & Edlow, 2020; Vanhaudenhuyse et al., 2010; Weng et al., 2017; X. Wu et al., 2015).

However, the analysis of RSFC data using graph metrics only revealed minimal differences between acutely brain-injured patients and healthy controls at the whole-brain level. This finding was unexpected, as it was hypothesized that patients would exhibit significant alterations in global network properties, given the severe disruption of consciousness and cognitive functions. The lack of significant differences at the whole-brain level suggests that acute brain injury may have resulted in minor localized changes in network connectivity, which did not substantially impact the overall functionality of the brain network (van der Horn et al., 2017). Nonetheless, the absence of whole-brain differences is consistent with previous studies that investigated connectivity in patients with mild TBI (Achard et al., 2012; Huang et al., 2024; van der Horn et al., 2017).

To further investigate this finding, targeted analyses were conducted to identify potential local, nodal connectivity differences. Compared to the control participants, acutely brain-injured patients showed reduced connectivity throughout the brain. The areas with reduced connectivity overlapped with resting-state networks, including the DMN and salience network, which have been consistently implicated in consciousness and cognitive processing (Crone et al., 2014; Demertzi et al., 2015). The DMN, in particular, has been associated with self-referential processing and autobiographical memory, both

of which are considered essential components of conscious experiences (Raichle, 2015). The salience network, in contrast, plays a crucial role in detecting and orienting attention toward stimuli, coordinating behavioural responses, and integrating cognitive, sensory, and emotional information (Uddin, 2015). The interplay between the DMN and salience network is thought to contribute to the emergence of consciousness due to their roles in the integration of internally generated and external information (Demertzi et al., 2015). These findings indicate that localized disruptions in the connectivity within resting-state networks, such as the DMN and salience networks, may underlie the alterations in consciousness and cognitive functioning of patients in the present study. The absence of global differences despite the presence of local disruptions could suggest that the brain may have developed compensatory mechanisms to maintain global functionality. Other resting-state networks or brain regions may compensate for the reduced connectivity in the default mode and salience networks, preserving the overall information integration and processing ability in the brain.

Alternatively, the absence of significant global differences between the graph metrics of the two groups could be explained by the small patient group size in this study. The sample size plays a crucial role in determining the power of a study to detect significant differences between groups. With a smaller sample size, higher within group variability, which is possible given the nature of the clinical population in this study, can reduce the ability to detect subtle but potentially meaningful differences between the groups. In this study, the small patient group size (n=16) may have resulted in insufficient statistical power to detect group differences in graph metrics at the whole-brain level. However, when specific channel-wise differences were assessed, variability was reduced and allowed for the detection of subtle and significant alterations in connectivity at the local level.

Given these findings, future research should aim to recruit larger samples for the patient group to ensure the presence of sufficient statistical power for detecting significant differences in the graph metrics at both global and local levels. Alternatively, longitudinal studies that follow patients from acute stages to the recovery or prolonged injury stages

can be utilized. This study design could provide insight into how local connectivity evolves and potentially influences whole-brain network functionality over time.

In line with previous research, the findings on connectivity at the nodal level demonstrated that critically brain-injured patients had lower metric values for degree, clustering coefficient, and local efficiency when compared to healthy controls (Achard et al., 2011; Chen et al., 2023; Crone et al., 2014; Han et al., 2016; Liu et al., 2023; Pandit et al., 2013; Weng et al., 2017). The brain is a complex system that relies on a balanced interplay between local processes and global integration (Heuvel & Sporns, 2013). When local processes are compromised, as indicated by the lower graph metric values of patients in this study, it can have widespread consequences on the overall network functionality and cognitive capacity. Particularly, local level network disruptions can lead to deficits in higher-order functioning (Han et al., 2016). For instance, disruptions in local connectivity within the DMN have been associated with impairments in self-referential processing and consciousness (Crone et al., 2013). This finding highlights the role of local network integrity in supporting higher-order cognitive processes.

In contrast to findings in the present study, previous studies have reported increased connectivity and higher values for degree, clustering coefficient, and local efficiency in patients with TBI (Caeyenberghs et al., 2012, 2017; Hillary, Rajtmajer, et al., 2014; Hillary, Román, et al., 2014; Imms et al., 2019; Nakamura et al., 2009; Yuan et al., 2017). These findings align with the hyperconnectivity hypothesis, which postulates that damage to a neural system can result in increased connections as a compensatory mechanism. Such compensation entails the recruitment of supplementary neural resources during network disruptions to enhance connectivity density, which could lead to high metabolic costs throughout the brain (Hillary, Román, et al., 2014).

The results from the present study do not align with the hyperconnectivity hypothesis. Differences in the findings reported in this study and those conducted in the past could be attributed to differences in pathophysiological mechanisms that may be involved in patients with hypoxic-ischemic brain injury (i.e., focus of the current study) versus patients with TBIs (i.e., samples from existing literature). TBIs include a physical injury to the brain, typically by a violent blow to the head, that results in damaged brain tissue

and altered brain function (Menon et al., 2010). Since hypoxic-ischemic brain injuries are caused by another underlying medical condition and not physical damage to brain tissue, they may not trigger the same hyperconnectivity response as TBIs but may lead to more localized disruptions in neural networks, as indicated by the decreased graph metric values in this study (Busl & Greer, 2010).

Other than nature of brain injuries, inconsistencies between connectivity and graph metric findings between the current study and previous research could be due to methodological differences, such as testing patients in different phases (e.g., post-acute or chronic injury phases), employment of different neuroimaging paradigms (e.g., passive or active paradigms), or utilization of different types of graphs (e.g., weighted or directed graphs). To elaborate, investigating patients months or even years post-injury, for example, can result in hyperconnectivity, which as mentioned above acts as a functional compensatory mechanism (Caeyenberghs et al., 2012). Hyperconnectivity may occur in the chronic or prolonged phases as patients have had more time to reconstruct and transform network connectivity in response to their injuries. Alternatively, the graph theory approach employed can also yield different results across studies. For example, using weighted graphs can provide insight into both the presence and strength of connectivity, whereas binary graphs only examine the presence or absence of a connection (Hillary, Rajtmajer, et al., 2014). These, albeit subtle, differences in data collection and analysis can potentially drive the variability in results acquired in this field. Nonetheless, the current study builds on previous literature with the findings that connectivity and graph metric values are decreased in acutely brain-injured patients (Pandit et al., 2013).

Overall, the absence of global connectivity differences and the presence of local connectivity differences, have important implications for understanding consciousness and brain functionality in acutely brain-injured patients. While localized disruptions in multiple resting-state networks, such as the DMN and salience network, may contribute to altered states of consciousness, the brain's ability to maintain overall network functionality suggests some magnitude of resilience and adaptability. This highlights the complexity of brain connectivity and the need to consider both global and local network properties in critically brain-injured patients when assessing brain function.

4.1.2 Graph Metrics and Network Functionality

The degree, clustering coefficient, and local efficiency describe the functionality of the resting brain and how network connectivity, information processing, and communication may be altered post-injury. The degree of a node indicates the number of connections each channel has and, therefore, how connected the brain as a whole may be. A higher degree indicates that the channel functionally interacts with many other channels (Bullmore & Sporns, 2012; Rubinov & Sporns, 2010).

Results from the present study demonstrate that certain nodes across patients had a significantly lower number of connections, which indicates decreased interactions from those nodes. Nodes with a reduced number of connections were primarily located in the frontal and postcentral gyri, and the middle temporal and middle occipital gyri. These findings have important implications for the altered states of consciousness observed in the patient group. Self-reflective and somatosensory processes, mediated by the frontal and postcentral gyri, are crucial components of conscious experience (Morin & Michaud, 2007; Weilnhammer et al., 2021; G.-R. Wu et al., 2019). These processes contribute to introspective thought, self-awareness, and bodily self-consciousness (Blanke, 2012; Northoff et al., 2006). Furthermore, the middle temporal and middle occipital gyri, which are associated with attentional and memory processes, play a role in the content and maintenance of conscious states by selecting relevant information that can provide for a continuous conscious experience (Baddeley, 2003; Boly et al., 2013; Hannawi et al., 2015; Koch et al., 2016; Tu et al., 2013; G.-R. Wu et al., 2019).

Since conscious experiences arise from the complex interplay of self-reflective, somatosensory, attentional, and memory processes, a decrease in the degree of nodes in these regions support a disruption in these processes, and by extension, consciousness (Giacino et al., 2014). Decreases in connectivity, observed in these specific nodes, could potentially lead to widespread changes throughout the brain, affecting overall network dynamics. Moreover, the nodes with a lower degree in the present study are considered part of the DMN and frontoparietal network. In the consciousness literature, both of these networks are considered central for integrating information across brain regions and supporting conscious experiences (Demertzi et al., 2013; Raichle, 2015). Studies have

reported impairments in these networks in patients with DoC, which further indicates that disruptions in the connectivity of these resting-state networks may be resulting in deficits in widescale information integration and processing, and ultimately producing a fragmented conscious experience.

The clustering coefficient measures the interconnectivity in local neighbourhoods. A higher clustering coefficient indicates increased connections between neighbouring nodes and represents the ability to functionally segregate local information processing (Bullmore & Sporns, 2012; Caeyenberghs et al., 2017). This ability to divide processes allows for faster and more efficient processing. However, if clustering is low, local neighbourhoods may not be as connected and information processing can be disrupted.

Findings from this study reported that 66% of channels in patients had lower clustering coefficient values compared to healthy controls, which is indicative of deficits in local information processing. Although the clustering coefficient values represent a local deficit, numerous channels showed disruptions in clustering ability, which suggests that deficits in clustering ability may contribute to whole network disturbances. In addition, channels that showed clustering disruptions were highly dispersed throughout the brain, and therefore, multiple networks were possibly affected. These findings are in line with previous studies that have shown disruptions in multiple resting-state networks, including the default mode, frontoparietal, visual, executive control, somatomotor, salience, and auditory networks in patients with DoC (Crone et al., 2014; Han et al., 2016; Hannawi et al., 2015; Heine et al., 2012; Kazazian et al., 2020; X. Wu et al., 2015).

Reduced clustering in functional networks has significant implications for the emergence and maintenance of conscious states. For instance, the DMN is involved in processes that support consciousness, including self-referential processing, autobiographical memory, and higher-order cognition (Raichle, 2015). Therefore, disruptions in the local connectivity of the DMN may lead to impairments in multiple processes critical for consciousness, such as self-awareness and integration of personal experiences, ultimately affecting consciousness as well (Demertzi et al., 2013). Similarly, the frontoparietal network has been implicated in attentional control, working memory, and conscious perception (Bor & Seth, 2012). Decreased clustering in the frontoparietal network,

therefore, may impair the ability to perceive and attend to internal and external stimuli, which can further prompt changes in the conscious experience of those stimuli (Boly et al., 2013). Furthermore, disruptions in the sensory networks, including the visual, somatomotor, and auditory networks, can also impact consciousness. These networks provide the raw materials required for the perception and construction of conscious experiences (Dehaene & Changeux, 2011). Impairments in sensory networks can distort the integration and processing of sensory information, and lead to distortions in conscious experiences of the stimuli. Overall, decreases in clustering coefficient across multiple networks may have a global impact, which can disrupt the brain's ability to support conscious processing.

Local efficiency measures the brain's ability to communicate and transfer information at the local level and assesses the capacity to distribute and integrate information (Bullmore & Sporns, 2012; Chen et al., 2023). Inefficient integration of information at the local level could result in far-reaching effects, where information is not being transferred, leading to disrupted communication throughout the brain.

In the present study, compared to healthy controls, 36% of channels in patients had lower values for local efficiency. Analogous to previous findings, the regions with lower local efficiency scores in this study included the auditory, default mode, salience, executive control, and frontoparietal networks (Achard et al., 2011; Liu et al., 2023; Weng et al., 2017). As discussed above, these networks play a crucial role in supporting different aspects of conscious processing. For example, the auditory and salience networks are involved in detecting and integrating relevant sensory stimuli, whereas the default mode, executive control, and frontoparietal networks are associated with higher-order cognition (Bor & Seth, 2012; Raichle, 2015; Seeley et al., 2007). Decreased local efficiency in these networks can compromise the processing and integration of sensory information, which can disrupt the generation of a unified conscious experience. The dispersion of channels with reduced local efficiency throughout multiple resting-state networks suggests a negative impact on the overall connectivity and functionality of each network. This disruption across networks can result in a breakdown of the brain's local organization, leading to difficulties in maintaining consciousness.

The results from patients discussed in this study indicate a disruption in RSFC in multiple regions of the brain. Specifically, patients demonstrated decreased connectivity and an imbalance between functional segregation and integration of information (Bullmore & Sporns, 2012; Chen et al., 2023; Oujamaa et al., 2023; Weng et al., 2017). Such disturbances in processing across neural networks could potentially be driving deficits in higher-order cognitive functioning and conscious processing in critically brain-injured patients (Pandit et al., 2013; Weng et al., 2017). Altogether, these results highlight the importance of specialized local processes and global distribution processes for overall network functionality.

The application of graph theory in this study provides a quantitative and objective approach for understanding the neural mechanisms underlying critically brain-injured patients in the ICU. While the findings here are correlational, they offer valuable insights into the relationship between graph metrics and consciousness-related processes that may be affected in the brain. In this study, the decreases noted in degree, clustering coefficient, and local efficiency suggest that disruptions in local connectivity, information processing, and communication may alter overall network functionality. These findings highlight the importance of considering the brain as an integrated system of multiple networks that interact in complex ways to allow for consciousness. By identifying disturbances in specific networks and processes, this study provides a more comprehensive understanding of the neural correlates underlying impairments in consciousness in patients with critical brain injuries. Future work can build on these findings by exploring additional graph metrics to determine differences, especially between patients with various brain injuries, in network connectivity and functionality.

4.1.3 Classification of Healthy Controls and Patients

Following the assessment of local connectivity, machine learning classifiers were employed to investigate the distinguishability of graph metrics between patients and control participants. The linear SVC model demonstrated the highest accuracy of up to 76%, which indicates that this classifier was able to find an optimal linear boundary that effectively separated the two study groups. This finding suggests that differences in graph metrics between patients and control participants are linearly separable. In addition to

accuracy scores, other performance measures can reveal details about the model's ability to correctly identify healthy controls and patients. The recall score describes the model's ability to identify most of the patients, whereas the precision score describes how correctly the model can predict a patient. The high recall and precision scores indicate that this algorithm correctly identified most of the patients in the dataset. Additionally, the specificity score describes the model's ability to correctly identify the healthy controls. In this classification, the low specificity scores indicate that the algorithm had some difficulty discerning all the control participants.

The KNN model, which relies on proximity between data point values, achieved an accuracy rate of up to 70% for differentiating between graph metrics of patients and healthy controls. This accuracy score suggests that graph metrics, especially clustering coefficient, form relatively distinct clusters in the feature space, allowing the classifier to identify new data points accurately. Furthermore, the recall, precision, and specificity scores, indicate that the KNN algorithm correctly identified a large proportion of patients. However, analogous to the linear SVC model, this machine learning algorithm also had issues when identifying all healthy controls.

Lastly, the rbf SVC model performed at or around 50% for all graph metrics, indicating that determining a non-linear decision boundary between the two groups was difficult. Despite the low accuracy score, this model was highly effective at identifying most patients in the dataset, as indicated by the high recall scores. This finding suggests that the algorithm rarely missed identifying a patient. However, the low precision scores imply that the model frequently misclassified healthy controls as patients. In other words, while the model was able to correctly identify a large proportion of the patients, it also incorrectly labeled many healthy controls as patients, leading to a high number of false positives. The low specificity scores further supported that the model struggled to identify healthy controls correctly.

Overall, the performance accuracies for the machine learning classifiers investigated in this study imply that simple algorithms, such as linear SVC and KNN, may be sufficient for distinguishing between critically brain-injured patients and healthy controls. This finding is expected due to the significant differences in levels of consciousness and

cognitive processing between the patient and healthy control groups. It could be that the machine learning models are able to identify patterns that can easily binarize the graph metrics based on the presence or absence of impairments in consciousness. Furthermore, the model's ability to identify and classify patients with high sensitivity suggests that the patient group must have unique or consistent graph metric features that distinguish them from the control participants. In contrast, the inconsistency in the identification and classification of the healthy controls implies that there may be more variability in the features of the controls (i.e., more heterogeneity), which makes them difficult to categorize. Therefore, these models demonstrate the ability to identify patients successfully but require further refinements for accurately classifying healthy controls.

Although high accuracy scores were noted in the machine learning classifiers implemented in this study, 100% accuracy was not accomplished due to the sample size and neurobiological heterogeneity within the patient group. The sample size in this study is relatively small, which can reduce the models' ability to learn and generalize the algorithms effectively. A larger and more representative dataset could improve the classification accuracy and reliability. Alternatively, the heterogeneity within the patient group and any overlap in graph metrics between groups could lead to challenges in accurate classification. Indeed, the patient group in this study presented with diverse etiologies, including differences in the severity and location of the brain injury, which could have led to variability in their graph metrics. Furthermore, patients with less severe brain injuries and impairments may have had graph metrics that were more similar to those of healthy controls, making it difficult for the models to establish clear boundaries between the two groups with 100% accuracy.

Despite these limitations, the linear SVC and KNN models were able to achieve relatively high-performance accuracy scores, suggesting that there are indeed identifiable pattens and meaningful differences between the graph metrics of patients and healthy controls.

4.2 Clinical Assessment of Acutely Brain-Injured Patients

4.2.1 Prognosis using Graph Metrics and Machine Learning

Although several clinical tools exist to help inform the prognostic process, tools that can predict good functional recovery after severe brain injury are scarce (Fins & Bernat, 2018; Fischer et al., 2022). Given this, neuroimaging can become an objective substitute for or complement to behavioural assessments for predicting good or poor patient outcomes (Fernández-Espejo & Owen, 2013; Owen, 2022; Young & Edlow, 2021; Young & Peterson, 2022). Many studies have used functional neuroimaging, primarily fMRI, for neuroprognostication in patients (Arbabshirani et al., 2017; Edlow et al., 2021; Huang et al., 2024; Koenig et al., 2014; Kolisnyk et al., 2023; Moreira da Silva et al., 2020; Nakamura et al., 2009; Oujamaa et al., 2023; Owen, 2022; Wagner et al., 2020; X. Wu et al., 2015). Moreover, minimal research has been conducted using fNIRS and graph theory for prognosticating acutely brain-injured patients. Studies that have used this approach investigated recovery from DoC rather than acute outcome prediction (Shu et al., 2023). Thus, the present study is among the first to lay the groundwork for using fNIRS, along with graph theory and machine learning, for early neuroprognostication of functional recovery in acute ICU patients.

Early-stage neuroprognostication in critically brain-injured patients is crucial for making decisions regarding life-sustaining measures and general patient care. Neuroprognostication in the ICU is an ongoing process in which decisions are re-evaluated as more information is uncovered (Young & Peterson, 2022). Decisions regarding WLSM are based on physician prognosis and the patients' level of consciousness in real-time, which is influenced by GCS scores and severity of the injury (McCredie et al., 2016; van Veen et al., 2020; Williamson et al., 2020; Young & Edlow, 2021). While important, these subjective measures are not reliable. Indeed, physicians often do not have enough information to determine patient prognosis in the acute phase of injury accurately. Up to 65% of physicians have reported that an accurate prognosis would be more helpful within the first 7 days of admission and greatly influence patient care decisions (Turgeon et al., 2013; Williamson et al., 2020). Studies have also shown that up to 26% of out-of-hospital cardiac arrest patients who had early WLSM may not

only have survived if they remained on life-support, but possibly, 64% of them may have had favourable functional outcomes (Elmer et al., 2016). This finding exemplifies that poor prognosis can lead to biases that ultimately impact patient care and lead to the self-fulfilling prophecy (Becker et al., 2001; Bernat, 2016). Since a critical aspect of patient care and decisions regarding life-sustaining measures is identifying the presence of covert consciousness, investing all possible efforts in detecting covert consciousness in acutely brain-injured patients is a moral responsibility (Fernández-Espejo & Owen, 2013). Therefore, to provide additional information during early-stage prognosis, functional neuroimaging can be implemented to aid physicians and family members when making important decisions regarding patient care and life-sustaining measures.

The present study employed neuroimaging in conjunction with graph theory and machine learning algorithms to prognosticate critically brain-injured patients. Indeed, the machine learning models implemented in this study classified good and poor patient outcomes with up to 83% accuracy using degree, clustering coefficient, and a combination of all graph metrics combined. Analogous to results for between group differentiation, the linear SVC model had the highest performance accuracy for distinguishing between good and poor outcomes. Furthermore, the KNN model performed well when differentiating between outcomes, which indicates local similarity between data points of the same class. In contrast, the chance-level performance of the rbf SVC algorithm suggests that the graph metrics used in this study may not be well-suited for a non-linear boundary. Overall, the performances of these models once again suggest that simple algorithms may be sufficient for classifying patient outcomes using graph metrics.

To comprehensively assess the models, the classifier's performance measures were further investigated. First, specificity scores were used to measure the proportion of patients with poor outcomes that the model correctly identified. A high specificity score indicates that the model effectively identified patients with poor outcomes. A machine learning model's specificity can aid in early identification of patients who are more likely to have a poor outcome, which is essential for ensuring appropriate treatment planning and resource allocation. In contrast, recall scores measure the model's ability to correctly identify all patients with good outcomes, which minimizes the risk of patients being

misclassified as having poor outcomes. Finally, precision scores measure the model's ability to ensure that patients predicted to have a good outcome truly have a good outcome, which minimizes the erroneous misclassification of patients with poor outcomes as those with good outcomes. A high recall score can reduce undertreatment ensuring that all patients receive the appropriate care they require, whereas a high precision score can reduce overtreatment. The findings from this study suggest that all three models had high specificity and a high capacity for correctly identifying patients with poor outcomes. The linear SVC model presented with the highest recall and precision scores, suggesting that it was most effective and accurate at identifying patients with good outcomes.

Although promising, these findings are limited by the small and uneven sample size in this study (10 patients had poor outcomes while only 4 had good outcomes). While efforts were made to mitigate the effect of the imbalanced sample size, such as calculating balanced accuracy scores and implementing three-fold cross-validation techniques over multiple iterations, the results should be interpreted with caution. Furthermore, the small sample size in this study may lead to overfitting, where a model learns to fit the noise along with the underlying patterns in the dataset, and therefore, fails to generalize to new data (Vabalas et al., 2019). As a result, the accuracy scores observed in this study may be optimistic, and the model's performance on new, unseen data could be lower. Future studies should recruit larger and more balanced patient cohorts to validate findings, such as those in this study, and further assess the performance of the machine learning models. Even with the small sample size and variability in the etiologies of the patient group, the machine learning analysis conducted in this study was able to accurately distinguish between good and poor patient outcomes. This finding indicates that graph theory and machine learning methods may be generalizable across different types of brain injuries. Future research should follow-up on these findings by identifying graph metrics specific to different brain injuries (e.g., structural vs metabolic injuries) and investigating the precision of single-subject level neuroprognostication.

Another important point to note about the sample is that out of the 10 patients who passed away (i.e., the poor outcome group), 6 underwent WLSM. This observation raises the

question of whether the graph theory and machine learning approach used in this study would have been able to determine patient survival had they remained on life-sustaining measures. What if the patients misclassified as good outcome would have indeed survived if they remained on life-support measures? If some of these patients had the potential for recovery, their graph metrics may have been more similar to those of the good outcome group, which could have also affected the classifier's performance, potentially leading to lower accuracy in distinguishing between the two outcome groups. Given this, future investigations should explore the effect WLSM has on graph metrics and whether graph metric values change post-injury, potentially acting as an indicator of recovery. Despite WLSM in the poor patient outcome group, the high-performance rates of linear SVC and KNN models on graph metrics obtained using fNIRS is a promising starting point. The results from our study suggest that these analyses warrant further investigation for predicting good and poor patient outcomes. Future studies with larger sample sizes and more balanced outcome groups could help validate these findings and address the effects of WLSM on graph metrics in the poor outcome group.

4.2.2 Diagnosis using Graph Metrics and Machine Learning

In this study, graph metrics were also used to distinguish patients' level of consciousness, as assessed by the GCS. Patients were classified based on whether they received a low (3-5) or high (6-8) GCS score. Machine learning models were able to classify GCS scores with up to 66% accuracy, using clustering coefficient, local efficiency, and all metrics combined.

Again, the interpretation and generalizability of these findings is limited by the small sample size in this study. An accuracy score of 66% means that approximately 10-11 patients were correctly classified, which is only 2-3 more patients than those classified at the chance-level of 8 correct classifications. This marginal improvement raises questions about the practical utility of this machine learning model for this specific classification, given that the accuracy rates obtained in this study are similar to behavioural assessments. The remaining 33% of misclassified patients warrant further discussion. As mentioned earlier, behavioural measures can be inaccurate, leading to high misdiagnoses rates. Hence, there is a possibility that some patients in this study may have had higher

levels of consciousness than that indicated by the low GCS scores, however, the classifier could not accurately identify them. Suppose the GCS scores were indeed inaccurate in assessing the level of consciousness in some of the misclassified patients. In that case, graph metrics may have captured aspects of consciousness that were not reflected in behavioural scores, thereby classifying patients as a higher level of consciousness and resulting in a lower accuracy score.

An example of this limitation is the case of the Guillain-Barré Syndrome (GBS) patient in this study. GBS is a neurological disorder in which the immune system attacks the peripheral nervous system. In severe cases, this disorder can lead to muscle weakness that results in full-body neuromuscular paralysis (Willison et al., 2016). Although these patients cannot communicate or move, they may be fully conscious and aware of their surroundings (Norton et al., 2023). In the present study, the GBS patient received a GCS score of 3, indicating the lowest possible level of consciousness at the time of testing. However, this patient went on to make a full neurological recovery. If the machine learning models had correctly identified a higher level of consciousness in this patient compared to the GCS score, then the classifier's performance would be lower. In addition to misclassification of higher consciousness levels, it is important to consider the possibility that some of the misclassified patients had lower levels of consciousness than what was indicated by their GCS scores. In such cases, the classifiers' performance would once again be lower due to the inaccurate and inflated GCS scores.

Thus, it is crucial to recognize that the graph metrics were used to predict the patients' behavioural scores (i.e., GCS scores) rather than their actual level of consciousness. The inaccuracies in behavioural assessments imply that a significant portion of the graph metric classification could be based on inaccurate GCS scores, potentially leading to misclassifications and incorrect conclusions about levels of consciousness. Despite these limitations, the findings in this study may still provide some insight into the relationship between graph metrics and behavioural measures of consciousness. Specifically, the findings in this study suggest that the relationship between graph metrics and behavioural measures can be classified more effectively using a linear SVC and KNN model rather than the complex rbf SVC model.

Future studies should address the limitations discussed above to understand the diagnostic potential of graph metrics further. Next steps in this specific area involve recruitment of a larger patient group and comparison between the performance of graph metric classifiers and more established diagnostic tools. While it may seem promising that classification of patients' GCS scores reached up to 66% accuracy using graph theory, it is important to interpret these findings with caution. Overall, the results from this study highlight the potential for graph metrics to provide insight into consciousness beyond that acquired from behavioural assessments, all the while emphasizing the need for more accurate and comprehensive assessments of consciousness.

4.3 Feasibility of fNIRS in the ICU

Findings from the present study demonstrate the feasibility of using fNIRS to test acutely brain-injured patients. ICU patients typically present with unstable medical conditions that require frequent surveillance, and therefore, can not be transported to different areas of the hospital for fMRI scans without significant risks (Fanara et al., 2010). fNIRS allows for non-invasive bedside testing, which ensures continuous monitoring of patients, eliminating potential complications that might arise during relocation. In addition to portability, fNIRS offers inexpensive and high-quality measurement of neural activity. Indeed, previous studies have demonstrated that HbO rs-fNIRS signals highly correlate with observations made using fMRI (Duan et al., 2012; Sasai et al., 2012; Scarapicchia et al., 2017).

Over the course of the present study, several disadvantages associated with using fNIRS for testing brain-injured patients emerged. Primarily, patients with critical brain injuries may have structural damages that can affect the position of the optodes on the scalp. Improper positioning of optodes can reduce the signal quality and introduce motion artifacts (Abdalmalak et al., 2021). Furthermore, certain intracranial injuries, such as subdural or superficial lobar hematomas, may interfere with the signal quality, making data collection impractical. Brain injuries and surgeries, such as open-head wounds or craniotomies, altogether prevent the use of fNIRS in a large subset of brain-injured ICU patients. While these limitations reduce the generalizability of this modality, fNIRS nevertheless allows for accessible and early-stage neuroimaging in many ICU patients,

which remains a largely understudied clinical population. Another limitation of fNIRS includes the difficulties associated with setting up the cap, such that all regions of interest are adequately captured. For instance, unresponsive patients are typically lying on their backs, which makes attaching probes for the occipital lobe and other areas at the back of the head difficult. Future studies should design and test montages that can narrow the scope of regions and probes to those of the highest importance in this clinical population.

Overall, this study provided valuable insights into the practical application of fNIRS in the ICU setting. Particularly, it emphasized that careful consideration of patient positioning, probe placement, and signal quality is essential for obtaining reliable data. Despite challenges encountered, such as the optode placements in occipital regions, fNIRS data was successfully collected from a large cohort of critically brain-injured patients (n=16). While fNIRS may not be suitable for all brain-injured patients, this study demonstrates its potential as a valuable tool for assessing acute brain function in the ICU setting.

4.3.1 Hemoglobin Differences in fNIRS Data

One unexpected yet interesting finding from this study was the lack of differences for all chromophores between patients and healthy controls. While HbO showed some differences at the whole-brain and giant component level, HbR and HbT did not show any differences at any level. Previous studies have shown that an increase or decrease in HbO should be expected with a respective decrease or increase in HbR (Kinder et al., 2022; Luke et al., 2021; Pinti et al., 2020). Although the present study detected changes in HbO, there were no significant changes in HbR between groups.

The absence of HbR differences in the present study could be due to the fact that HbO is more sensitive to changes in cerebral blood flow, which is why it is reported more frequently in fNIRS literature compared to HbR or HbT (Hoshi et al., 2001; Suzuki et al., 2004). The discrepancy in HbO and HbR findings may be attributed to their distinct roles in neurovascular coupling (i.e., local neural activity and subsequent changes in cerebral blood flow). Typically, the amount of oxygen delivered to active brain regions exceeds the amount used by those regions. This results in a significant increase in HbO, and only a slight decrease in HbR (Ferrari & Quaresima, 2012; Kim et al., 2017). The relatively

higher increases in oxygenated blood suggests that HbO may be a more sensitive indicator of neuronal activity, whereas changes in HbR may be too small to capture significant group differences (Buxton et al., 2004). Indeed, this was observed in the present study as changes in HbO, but not HbR, were detected between patients and healthy controls. This finding indicates that for resting-state paradigms, where spontaneous neuronal activity is measured, HbO may be more suitable for detecting changes in neural activity.

Although HbO may be a more sensitive measure for assessing neural activity, reporting findings from all chromophores is essential. A recent review revealed that fNIRS literature does not have standardized practices for choosing which chromophore to report (Kinder et al., 2022). Most studies only report HbO without providing any justification as to why other chromophores were excluded. This is problematic since numerous studies have shown that when only one chromophore is reported, results trend toward significance. When both HbO and HbR (or HbT) are reported, findings are less likely to trend towards significance, which can mitigate the issue of falsely positive results (Botvinik-Nezer et al., 2020; Hocke et al., 2018). With consideration of these reports and recommendations from relatively more standardized fNIRS protocols, the present study reported findings for HbO, HbR, and HbT, which provided a comprehensive profile of the results (Kinder et al., 2022). Therefore, even though there were significant differences for HbO between patients and control participants at the local level in this study, these differences should be carefully considered alongside the non-significant findings for HbR and HbT.

4.4 Conclusion

The present study explored the acute phase of critical brain injury in 16 patients and 23 healthy controls using fNIRS-based RSFC. Resting-state data was analyzed using graph theory and machine learning to find quantifiable differences in the functional connectivity of patients and healthy controls. Although whole-brain differences between groups were minimal, graph theory analysis was able to detect significant local channel-level differences for three metrics, including degree, clustering coefficient, and local efficiency. These graph metrics were significantly lower for patients than healthy controls across all

channels that showed a difference. Furthermore, machine learning models, particularly linear SVC and KNN algorithms, were able to distinguish between patients and healthy controls with up to 76% accuracy. These same models were also able to predict good and poor outcomes with up to 83% accuracy and differentiate between high and low behavioural assessment scores with up to 66% accuracy.

The findings from this study have several implications. First, this study validated the use of rs-fNIRS in the ICU, a setting where behavioural assessments are insufficient when assessing consciousness and traditional fMRI is not feasible. Second, quantifiable differences between critically brain-injured patients and healthy controls were detected through the use of graph theory. These differences led to a better understanding of brain processes and functionality, including changes in network connectivity, communication, and information transmission in altered states of consciousness. Third, the machine learning algorithms developed in this study reached high accuracy scores when differentiating between study groups and predicting patient outcomes. These findings provide a gateway to continue exploring rs-fNIRS, graph theory, and machine learning for patient diagnosis and prognosis.

Overall, this study provided a better understanding of network functionality in altered states of consciousness, robust tools for diagnosis and prognosis in acutely brain-injured patients, and, most importantly, the hope to improve patient care and treatment.

References

Abdalmalak, A., Milej, D., Norton, L., Debicki, D. B., Owen, A. M., & Lawrence, K. St. (2021). The Potential Role of fNIRS in Evaluating Levels of Consciousness. *Frontiers in Human Neuroscience*, *15*. https://www.frontiersin.org/articles/10.3389/fnhum.2021.703405

Abdalmalak, A., Novi, S. L., Kazazian, K., Norton, L., Benaglia, T., Slessarev, M., Debicki, D. B., Lawrence, K. St., Mesquita, R. C., & Owen, A. M. (2022). Effects of Systemic Physiology on Mapping Resting-State Networks Using Functional Near-Infrared Spectroscopy. *Frontiers in Neuroscience*, *16*. https://www.frontiersin.org/articles/10.3389/fnins.2022.803297

Achard, S., Delon-Martin, C., Vértes, P. E., Renard, F., Schenck, M., Schneider, F., Heinrich, C., Kremer, S., & Bullmore, E. T. (2012). Hubs of brain functional networks are radically reorganized in comatose patients. *Proceedings of the National Academy of Sciences*, *109*(50), 20608–20613. https://doi.org/10.1073/pnas.1208933109

Achard, S., Kremer, S., Schenck, M., Renard, F., Ong-Nicolas, C., Namer, J. I., Mutschler, V., Schneider, F., & Delon-Martin, C. (2011). Global Functional Disconnections in Post-anoxic Coma Patient. *The Neuroradiology Journal*, *24*(2), 311–315. https://doi.org/10.1177/197140091102400222

Alves, W. M., & Marshall, L. F. (2006). CHAPTER 4—Traumatic Brain Injury. In W. M. Alves & B. E. Skolnick (Eds.), *Handbook of Neuroemergency Clinical Trials* (pp. 61–79). Academic Press. https://doi.org/10.1016/B978-012648082-5/50007-1

Amiri, M., Fisher, P. M., Raimondo, F., Sidaros, A., Cacic Hribljan, M., Othman, M. H., Zibrandtsen, I., Albrechtsen, S. S., Bergdal, O., Hansen, A. E., Hassager, C., Højgaard, J. L. S., Jakobsen, E. W., Jensen, H. R., Møller, J., Nersesjan, V., Nikolic, M., Olsen, M. H., Sigurdsson, S. T., … Kondziella, D. (2023). Multimodal prediction of residual consciousness in the intensive care unit: The CONNECT-ME study. *Brain*, *146*(1), 50–64. https://doi.org/10.1093/brain/awac335

Arbabshirani, M. R., Plis, S., Sui, J., & Calhoun, V. D. (2017). Single subject prediction of brain disorders in neuroimaging: Promises and pitfalls. *NeuroImage*, *145*, 137–165. https://doi.org/10.1016/j.neuroimage.2016.02.079

Baddeley, A. (2003). Working memory: Looking back and looking forward. *Nature Reviews Neuroscience*, *4*(10), 829–839. https://doi.org/10.1038/nrn1201

Barabási, A.-L. (2014). *Network Science*. http://networksciencebook.com/

Barttfeld, P., Uhrig, L., Sitt, J. D., Sigman, M., Jarraya, B., & Dehaene, S. (2015). Signature of consciousness in the dynamics of resting-state brain activity.

Proceedings of the National Academy of Sciences, *112*(3), 887–892.
https://doi.org/10.1073/pnas.1418031112

Becker, K. J., Baxter, A. B., Cohen, W. A., Bybee, H. M., Tirschwell, D. L., Newell, D.
W., Winn, H. R., & Longstreth, W. T. (2001). Withdrawal of support in
intracerebral hemorrhage may lead to self-fulfilling prophecies. *Neurology, 56*(6),
766–772. https://doi.org/10.1212/WNL.56.6.766

Bergstra, J., Yamins, D., & Cox, D. D. (2013). *Making a Science of Model Search:
Hyperparameter Optimization in Hundreds of Dimensions for Vision
Architectures*. https://dash.harvard.edu/handle/1/12561000

Berlingeri, M., Magnani, F. G., Salvato, G., Rosanova, M., & Bottini, G. (2019).
Neuroimaging Studies on Disorders of Consciousness: A Meta-Analytic
Evaluation. *Journal of Clinical Medicine*, *8*(4), 516.
https://doi.org/10.3390/jcm8040516

Bernat, J. L. (2016). Prognostic Limitations of Syndromic Diagnosis in Disorders of
Consciousness. *AJOB Neuroscience*, *7*(1), 46–48.
https://doi.org/10.1080/21507740.2016.1146367

Bhavsar, H., & Panchal, M. H. (2012). *A Review on Support Vector Machine for Data
Classification*. *1*(10).

Blanco, B., Molnar, M., & Caballero-Gaudes, C. (2018). Effect of prewhitening in
resting-state functional near-infrared spectroscopy data. *Neurophotonics*, *5*(4),
040401. https://doi.org/10.1117/1.NPh.5.4.040401

Blanke, O. (2012). Multisensory brain mechanisms of bodily self-consciousness. *Nature
Reviews Neuroscience*, *13*(8), 556–571. https://doi.org/10.1038/nrn3292

Boas, D. A., Elwell, C. E., Ferrari, M., & Taga, G. (2014). Twenty years of functional
near-infrared spectroscopy: Introduction for the special issue. *NeuroImage*, *85 Pt
1*, 1–5. https://doi.org/10.1016/j.neuroimage.2013.11.033

Boly, M., Seth, A. K., Wilke, M., Ingmundson, P., Baars, B., Laureys, S., Edelman, D., &
Tsuchiya, N. (2013). Consciousness in humans and non-human animals: Recent
advances and future directions. *Frontiers in Psychology*, *4*.
https://doi.org/10.3389/fpsyg.2013.00625

Bonilauri, A., Pirastru, A., Sangiuliano Intra, F., Isernia, S., Cazzoli, M., Blasi, V., Baselli,
G., & Baglio, F. (2023). Surface-based integration approach for fNIRS-fMRI
reliability assessment. *Journal of Neuroscience Methods*, *398*, 109952.
https://doi.org/10.1016/j.jneumeth.2023.109952

Bor, D., & Seth, A. K. (2012). Consciousness and the Prefrontal Parietal Network:
Insights from Attention, Working Memory, and Chunking. *Frontiers in
Psychology*, *3*. https://doi.org/10.3389/fpsyg.2012.00063

Botvinik-Nezer, R., Holzmeister, F., Camerer, C. F., Dreber, A., Huber, J., Johannesson, M., Kirchler, M., Iwanir, R., Mumford, J. A., Adcock, R. A., Avesani, P., Baczkowski, B. M., Bajracharya, A., Bakst, L., Ball, S., Barilari, M., Bault, N., Beaton, D., Beitner, J., … Schonberg, T. (2020). Variability in the analysis of a single neuroimaging dataset by many teams. *Nature*, *582*(7810), 84–88. https://doi.org/10.1038/s41586-020-2314-9

Bullmore, E., & Sporns, O. (2012). The economy of brain network organization. *Nature Reviews Neuroscience*, *13*(5), 336–349. https://doi.org/10.1038/nrn3214

Busl, K. M., & Greer, D. M. (2010). Hypoxic-ischemic brain injury: Pathophysiology, neuropathology and mechanisms. *NeuroRehabilitation*, *26*(1), 5–13. https://doi.org/10.3233/NRE-2010-0531

Butterworth, R. F. (1999). Metabolic Encephalopathies. In *Basic Neurochemistry: Molecular, Cellular and Medical Aspects. 6th edition*. Lippincott-Raven. https://www.ncbi.nlm.nih.gov/books/NBK20383/

Buxton, R. B., Uludağ, K., Dubowitz, D. J., & Liu, T. T. (2004). Modeling the hemodynamic response to brain activation. *NeuroImage*, *23*, S220–S233. https://doi.org/10.1016/j.neuroimage.2004.07.013

Caeyenberghs, K., Leemans, A., Heitger, M. H., Leunissen, I., Dhollander, T., Sunaert, S., Dupont, P., & Swinnen, S. P. (2012). Graph analysis of functional brain networks for cognitive control of action in traumatic brain injury. *Brain*, *135*(4), 1293–1307. https://doi.org/10.1093/brain/aws048

Caeyenberghs, K., Verhelst, H., Clemente, A., & Wilson, P. H. (2017). Mapping the functional connectome in traumatic brain injury: What can graph metrics tell us? *NeuroImage*, *160*, 113–123. https://doi.org/10.1016/j.neuroimage.2016.12.003

Chen, H., Miao, G., Wang, S., Zheng, J., Zhang, X., Lin, J., Hao, C., Huang, H., Jiang, T., Gong, Y., & Liao, W. (2023). Disturbed functional connectivity and topological properties of the frontal lobe in minimally conscious state based on resting-state fNIRS. *Frontiers in Neuroscience*, *17*. https://www.frontiersin.org/articles/10.3389/fnins.2023.1118395

Combrisson, E., & Jerbi, K. (2015). Exceeding chance level by chance: The caveat of theoretical chance levels in brain signal classification and statistical assessment of decoding accuracy. *Journal of Neuroscience Methods*, *250*, 126–136. https://doi.org/10.1016/j.jneumeth.2015.01.010

Crone, J. S., Höller, Y., Bergmann, J., Golaszewski, S., Trinka, E., & Kronbichler, M. (2013). Self-Related Processing and Deactivation of Cortical Midline Regions in Disorders of Consciousness. *Frontiers in Human Neuroscience*, *7*, 504. https://doi.org/10.3389/fnhum.2013.00504

Crone, J. S., Soddu, A., Höller, Y., Vanhaudenhuyse, A., Schurz, M., Bergmann, J., Schmid, E., Trinka, E., Laureys, S., & Kronbichler, M. (2014). Altered network properties of the fronto-parietal network and the thalamus in impaired consciousness. *NeuroImage: Clinical*, *4*, 240–248. https://doi.org/10.1016/j.nicl.2013.12.005

Dehaene, S., & Changeux, J.-P. (2011). Experimental and Theoretical Approaches to Conscious Processing. *Neuron*, *70*(2), 200–227. https://doi.org/10.1016/j.neuron.2011.03.018

Demertzi, A., Antonopoulos, G., Heine, L., Voss, H. U., Crone, J. S., de Los Angeles, C., Bahri, M. A., Di Perri, C., Vanhaudenhuyse, A., Charland-Verville, V., Kronbichler, M., Trinka, E., Phillips, C., Gomez, F., Tshibanda, L., Soddu, A., Schiff, N. D., Whitfield-Gabrieli, S., & Laureys, S. (2015). Intrinsic functional connectivity differentiates minimally conscious from unresponsive patients. *Brain*, *138*(9), 2619–2631. https://doi.org/10.1093/brain/awv169

Demertzi, A., Soddu, A., & Laureys, S. (2013). Consciousness supporting networks. *Current Opinion in Neurobiology*, *23*(2), 239–244. https://doi.org/10.1016/j.conb.2012.12.003

Di Perri, C., Bahri, M. A., Amico, E., Thibaut, A., Heine, L., Antonopoulos, G., Charland-Verville, V., Wannez, S., Gomez, F., Hustinx, R., Tshibanda, L., Demertzi, A., Soddu, A., & Laureys, S. (2016). Neural correlates of consciousness in patients who have emerged from a minimally conscious state: A cross-sectional multimodal imaging study. *The Lancet Neurology*, *15*(8), 830–842. https://doi.org/10.1016/S1474-4422(16)00111-3

Duan, L., Zhang, Y.-J., & Zhu, C.-Z. (2012). Quantitative comparison of resting-state functional connectivity derived from fNIRS and fMRI: A simultaneous recording study. *NeuroImage*, *60*(4), 2008–2018. https://doi.org/10.1016/j.neuroimage.2012.02.014

Edlow, B. L., Chatelle, C., Spencer, C. A., Chu, C. J., Bodien, Y. G., O'Connor, K. L., Hirschberg, R. E., Hochberg, L. R., Giacino, J. T., Rosenthal, E. S., & Wu, O. (2017). Early detection of consciousness in patients with acute severe traumatic brain injury. *Brain*, *140*(9), 2399–2414. https://doi.org/10.1093/brain/awx176

Edlow, B. L., Claassen, J., Schiff, N. D., & Greer, D. M. (2021). Recovery from disorders of consciousness: Mechanisms, prognosis and emerging therapies. *Nature Reviews Neurology*, *17*(3), Article 3. https://doi.org/10.1038/s41582-020-00428-x

Egawa, S., Ader, J., Shen, Q., Nakagawa, S., Fujimoto, Y., Fujii, S., Masuda, K., Shirota, A., Ota, M., Yoshino, Y., Amai, H., Miyao, S., Nakamoto, H., Kuroda, Y., Doyle, K., Grobois, L., Vrosgou, A., Carmona, J. C., Velazquez, A., … Claassen, J. (2023). Long-Term Outcomes of Patients with Stroke Predicted by Clinicians to

have no Chance of Meaningful Recovery: A Japanese Cohort Study. *Neurocritical Care*, *38*(3), 733–740. https://doi.org/10.1007/s12028-022-01644-7

Elmer, J., Torres, C., Aufderheide, T. P., Austin, M. A., Callaway, C. W., Golan, E., Herren, H., Jasti, J., Kudenchuk, P. J., Scales, D. C., Stub, D., Richardson, D. K., & Zive, D. M. (2016). Association of early withdrawal of life-sustaining therapy for perceived neurological prognosis with mortality after cardiac arrest. *Resuscitation*, *102*, 127–135. https://doi.org/10.1016/j.resuscitation.2016.01.016

Erickson, B. J., Korfiatis, P., Akkus, Z., & Kline, T. L. (2017). Machine Learning for Medical Imaging. *RadioGraphics*, *37*(2), 505–515. https://doi.org/10.1148/rg.2017160130

Fernández-Espejo, D., & Owen, A. M. (2013). Detecting awareness after severe brain injury. *Nature Reviews Neuroscience*, *14*(11), 801–809. https://doi.org/10.1038/nrn3608

Ferrari, M., & Quaresima, V. (2012). A brief review on the history of human functional near-infrared spectroscopy (fNIRS) development and fields of application. *NeuroImage*, *63*(2), 921–935. https://doi.org/10.1016/j.neuroimage.2012.03.049

Fins, J. J., & Bernat, J. L. (2018). Ethical, palliative, and policy considerations in disorders of consciousness. *Neurology*, *91*(10), 471–475. https://doi.org/10.1212/WNL.0000000000005927

Fischer, D., Edlow, B. L., Giacino, J. T., & Greer, D. M. (2022). Neuroprognostication: A conceptual framework. *Nature Reviews Neurology*, *18*(7), 419–427. https://doi.org/10.1038/s41582-022-00644-7

Fornito, A., Zalesky, A., & Bullmore, E. T. (2016). *Fundamentals of Brain Network Analysis*. Academic Press. https://doi.org/10.1016/B978-0-12-407908-3.09999-4

Giacino, J. T., Fins, J. J., Laureys, S., & Schiff, N. D. (2014). Disorders of consciousness after acquired brain injury: The state of the science. *Nature Reviews Neurology*, *10*(2), 99–114. https://doi.org/10.1038/nrneurol.2013.279

Giacino, J. T., Katz, D. I., Schiff, N. D., Whyte, J., Ashman, E. J., Ashwal, S., Barbano, R., Hammond, F. M., Laureys, S., Ling, G. S. F., Nakase-Richardson, R., Seel, R. T., Yablon, S., Getchius, T. S. D., Gronseth, G. S., & Armstrong, M. J. (2018). Practice Guideline Update Recommendations Summary: Disorders of Consciousness: Report of the Guideline Development, Dissemination, and Implementation Subcommittee of the American Academy of Neurology; the American Congress of Rehabilitation Medicine; and the National Institute on Disability, Independent Living, and Rehabilitation Research. *Archives of Physical Medicine and Rehabilitation*, *99*(9), 1699–1709. https://doi.org/10.1016/j.apmr.2018.07.001

Gill-Thwaites, H. (2006). Lotteries, loopholes and luck: Misdiagnosis in the vegetative state patient. *Brain Injury*, *20*(13–14), 1321–1328. https://doi.org/10.1080/02699050601081802

Gomez, L. A., Shen, Q., Doyle, K., Vrosgou, A., Velazquez, A., Megjhani, M., Ghoshal, S., Roh, D., Agarwal, S., Park, S., Claassen, J., & Kleinberg, S. (2023). Classification of Level of Consciousness in a Neurological ICU Using Physiological Data. *Neurocritical Care*, *38*(1), 118–128. https://doi.org/10.1007/s12028-022-01586-0

Greicius, M. D., Krasnow, B., Reiss, A. L., & Menon, V. (2003). Functional connectivity in the resting brain: A network analysis of the default mode hypothesis. *Proceedings of the National Academy of Sciences*, *100*(1), 253–258. https://doi.org/10.1073/pnas.0135058100

Han, K., Chapman, S. B., & Krawczyk, D. C. (2016). Disrupted Intrinsic Connectivity among Default, Dorsal Attention, and Frontoparietal Control Networks in Individuals with Chronic Traumatic Brain Injury. *Journal of the International Neuropsychological Society*, *22*(2), 263–279. https://doi.org/10.1017/S1355617715001393

Hannawi, Y., Lindquist, M. A., Caffo, B. S., Sair, H. I., & Stevens, R. D. (2015). Resting brain activity in disorders of consciousness. *Neurology*, *84*(12), 1272–1280. https://doi.org/10.1212/WNL.0000000000001404

He, Y., & Evans, A. (2010). Graph theoretical modeling of brain connectivity. *Current Opinion in Neurology*, *23*(4), 341. https://doi.org/10.1097/WCO.0b013e32833aa567

Heine, L., Soddu, A., Gómez, F., Vanhaudenhuyse, A., Tshibanda, L., Thonnard, M., Charland-Verville, V., Kirsch, M., Laureys, S., & Demertzi, A. (2012). Resting State Networks and Consciousness. *Frontiers in Psychology*, *3*, 295. https://doi.org/10.3389/fpsyg.2012.00295

Heuvel, M. P. van den, & Sporns, O. (2013). Network hubs in the human brain. *Trends in Cognitive Sciences*, *17*(12), 683–696. https://doi.org/10.1016/j.tics.2013.09.012

Hillary, F. G., Rajtmajer, S. M., Roman, C. A., Medaglia, J. D., Slocomb-Dluzen, J. E., Calhoun, V. D., Good, D. C., & Wylie, G. R. (2014). The Rich Get Richer: Brain Injury Elicits Hyperconnectivity in Core Subnetworks. *PLOS ONE*, *9*(8), e104021. https://doi.org/10.1371/journal.pone.0104021

Hillary, F. G., Román, C., Venkatesan, U., Rajtmajer, S., Bajo, R., & Castellanos, N. (2014). Hyperconnectivity is a Fundamental Response to Neurological Disruption. *Neuropsychology*, *29*. https://doi.org/10.1037/neu0000110

Hocke, L. M., Oni, I. K., Duszynski, C. C., Corrigan, A. V., Frederick, B. D., & Dunn, J. F. (2018). Automated Processing of fNIRS Data—A Visual Guide to the Pitfalls

and Consequences. *Algorithms*, *11*(5), Article 5. https://doi.org/10.3390/a11050067

Homan, R. W., Herman, J., & Purdy, P. (1987). Cerebral location of international 10–20 system electrode placement. *Electroencephalography and Clinical Neurophysiology*, *66*(4), 376–382. https://doi.org/10.1016/0013-4694(87)90206-9

Hoshi, Y., Kobayashi, N., & Tamura, M. (2001). Interpretation of near-infrared spectroscopy signals: A study with a newly developed perfused rat brain model. *Journal of Applied Physiology*, *90*(5), 1657–1662. https://doi.org/10.1152/jappl.2001.90.5.1657

Huang, S., Han, J., Zheng, H., Li, M., Huang, C., Kui, X., & Liu, J. (2024). Structural and functional connectivity of the whole brain and subnetworks in individuals with mild traumatic brain injury: Predictors of patient prognosis. *Neural Regeneration Research*, *19*(7), 1553. https://doi.org/10.4103/1673-5374.387971

Huff, J. S., & Tadi, P. (2024). Coma. In *StatPearls*. StatPearls Publishing. http://www.ncbi.nlm.nih.gov/books/NBK430722/

Huppert, T. J., Diamond, S. G., Franceschini, M. A., & Boas, D. A. (2009). HomER: A review of time-series analysis methods for near-infrared spectroscopy of the brain. *Applied Optics*, *48*(10), D280–D298.

Huppert, T. J., Hoge, R. D., Diamond, S. G., Franceschini, M. A., & Boas, D. A. (2006). A temporal comparison of BOLD, ASL, and NIRS hemodynamic responses to motor stimuli in adult humans. *NeuroImage*, *29*(2), 368–382. https://doi.org/10.1016/j.neuroimage.2005.08.065

Imms, P., Clemente, A., Cook, M., D'Souza, W., Wilson, P. H., Jones, D. K., & Caeyenberghs, K. (2019). The structural connectome in traumatic brain injury: A meta-analysis of graph metrics. *Neuroscience & Biobehavioral Reviews*, *99*, 128–137. https://doi.org/10.1016/j.neubiorev.2019.01.002

Izzy, S., Compton, R., Carandang, R., Hall, W., & Muehlschlegel, S. (2013). Self-Fulfilling Prophecies Through Withdrawal of Care: Do They Exist in Traumatic Brain Injury, Too? *Neurocritical Care*, *19*(3), 347–363. https://doi.org/10.1007/s12028-013-9925-z

Jain, R., & Ramakrishnan, A. G. (2020). Electrophysiological and Neuroimaging Studies – During Resting State and Sensory Stimulation in Disorders of Consciousness: A Review. *Frontiers in Neuroscience*, *14*. https://www.frontiersin.org/articles/10.3389/fnins.2020.555093

Jain, S., & Iverson, L. M. (2024). Glasgow Coma Scale. In *StatPearls*. StatPearls Publishing. http://www.ncbi.nlm.nih.gov/books/NBK513298/

Kazazian, K., Norton, L., Gofton, T. E., Debicki, D., & Owen, A. M. (2020). Cortical Function in Acute Severe Traumatic Brain Injury and at Recovery: A Longitudinal fMRI Case Study. *Brain Sciences*, *10*(9), 604. https://doi.org/10.3390/brainsci10090604

Kazazian, K., Norton, L., Laforge, G., Abdalmalak, A., Gofton, T. E., Debicki, D., Slessarev, M., Hollywood, S., Lawrence, K. St., & Owen, A. M. (2021). Improving Diagnosis and Prognosis in Acute Severe Brain Injury: A Multimodal Imaging Protocol. *Frontiers in Neurology*, *12*. https://www.frontiersin.org/articles/10.3389/fneur.2021.757219

Kim, H. Y., Seo, K., Jeon, H. J., Lee, U., & Lee, H. (2017). Application of Functional Near-Infrared Spectroscopy to the Study of Brain Function in Humans and Animal Models. *Molecules and Cells*, *40*(8), 523–532. https://doi.org/10.14348/molcells.2017.0153

Kinder, K. T., Heim, H. L. R., Parker, J., Lowery, K., McCraw, A., Eddings, R. N., Defenderfer, J., Sullivan, J., & Buss, A. T. (2022). Systematic review of fNIRS studies reveals inconsistent chromophore data reporting practices. *Neurophotonics*, *9*(4), 040601. https://doi.org/10.1117/1.NPh.9.4.040601

Koch, C., Massimini, M., Boly, M., & Tononi, G. (2016). Neural correlates of consciousness: Progress and problems. *Nature Reviews Neuroscience*, *17*(5), 307–321. https://doi.org/10.1038/nrn.2016.22

Koculak, M., & Wierzchoń, M. (2022). Consciousness Science Needs Some Rest: How to Use Resting-State Paradigm to Improve Theories and Measures of Consciousness. *Frontiers in Neuroscience*, *16*. https://doi.org/10.3389/fnins.2022.836758

Koenig, M. A., Holt, J. L., Ernst, T., Buchthal, S. D., Nakagawa, K., Stenger, V. A., & Chang, L. (2014). MRI Default Mode Network Connectivity is Associated with Functional Outcome after Cardiopulmonary Arrest. *Neurocritical Care*, *20*(3), 348–357. https://doi.org/10.1007/s12028-014-9953-3

Kolisnyk, M., Kazazian, K., Rego, K., Novi, S. L., Wild, C. J., Gofton, T. E., Debicki, D. B., Owen, A. M., & Norton, L. (2023). Predicting neurologic recovery after severe acute brain injury using resting-state networks. *Journal of Neurology*, *270*(12), 6071–6080. https://doi.org/10.1007/s00415-023-11941-6

Kondziella, D., Fisher, P. M., Larsen, V. A., Hauerberg, J., Fabricius, M., Møller, K., & Knudsen, G. M. (2017). Functional MRI for Assessment of the Default Mode Network in Acute Brain Injury. *Neurocritical Care*, *27*(3), 401–406. https://doi.org/10.1007/s12028-017-0407-6

Kondziella, D., Friberg, C. K., Frokjaer, V. G., Fabricius, M., & Møller, K. (2016). Preserved consciousness in vegetative and minimal conscious states: Systematic

review and meta-analysis. *Journal of Neurology, Neurosurgery & Psychiatry*, *87*(5), 485–492. https://doi.org/10.1136/jnnp-2015-310958

Koutrouli, M., Karatzas, E., Paez-Espino, D., & Pavlopoulos, G. A. (2020). A Guide to Conquer the Biological Network Era Using Graph Theory. *Frontiers in Bioengineering and Biotechnology*, *8*. https://www.frontiersin.org/articles/10.3389/fbioe.2020.00034

Laaksonen, J., & Oja, E. (1996). Classification with learning k-nearest neighbors. *Proceedings of International Conference on Neural Networks (ICNN'96)*, *3*, 1480–1483. https://doi.org/10.1109/ICNN.1996.549118

Lacerte, M., Hays Shapshak, A., & Mesfin, F. B. (2024). Hypoxic Brain Injury. In *StatPearls*. StatPearls Publishing. http://www.ncbi.nlm.nih.gov/books/NBK537310/

Laird, A. R., Fox, P. M., Eickhoff, S. B., Turner, J. A., Ray, K. L., McKay, D. R., Glahn, D. C., Beckmann, C. F., Smith, S. M., & Fox, P. T. (2011). Behavioral Interpretations of Intrinsic Connectivity Networks. *Journal of Cognitive Neuroscience*, *23*(12), 4022–4037. https://doi.org/10.1162/jocn_a_00077

Lanka, P., Rangaprakash, D., Dretsch, M. N., Katz, J. S., Denney, T. S., & Deshpande, G. (2020). Supervised machine learning for diagnostic classification from large-scale neuroimaging datasets. *Brain Imaging and Behavior*, *14*(6), 2378–2416. https://doi.org/10.1007/s11682-019-00191-8

Latora, V., & Marchiori, M. (2001). Efficient Behavior of Small-World Networks. *Physical Review Letters*, *87*(19), 198701. https://doi.org/10.1103/PhysRevLett.87.198701

Laureys, S., Celesia, G. G., Cohadon, F., Lavrijsen, J., León-Carrión, J., Sannita, W. G., Sazbon, L., Schmutzhard, E., von Wild, K. R., Zeman, A., Dolce, G., & the European Task Force on Disorders of Consciousness. (2010). Unresponsive wakefulness syndrome: A new name for the vegetative state or apallic syndrome. *BMC Medicine*, *8*(1), 68. https://doi.org/10.1186/1741-7015-8-68

Li, M., Yang, Y., Zhang, Y., Gao, Y., Jing, R., Dang, Y., Chen, X., He, J., & Si, J. (2021). Detecting Residual Awareness in Patients With Prolonged Disorders of Consciousness: An fNIRS Study. *Frontiers in Neurology*, *12*, 618055. https://doi.org/10.3389/fneur.2021.618055

Li, M.-T., Sun, J.-W., Zhan, L.-L., Antwi, C. O., Lv, Y.-T., Jia, X.-Z., & Ren, J. (2023). The effect of seed location on functional connectivity: Evidence from an image-based meta-analysis. *Frontiers in Neuroscience*, *17*. https://www.frontiersin.org/articles/10.3389/fnins.2023.1120741

Liu, Y., Kang, X., Chen, B., Song, C., Liu, Y., Hao, J., Yuan, F., & Jiang, W. (2023). Detecting residual brain networks in disorders of consciousness: A resting-state

fNIRS study. *Brain Research*, *1798*, 148162.
https://doi.org/10.1016/j.brainres.2022.148162

Long, J., Xie, Q., Ma, Q., Urbin, M. A., Liu, L., Weng, L., Huang, X., Yu, R., Li, Y., &
Huang, R. (2016). Distinct Interactions between Fronto-Parietal and Default
Mode Networks in Impaired Consciousness. *Scientific Reports*, *6*(1), 38866.
https://doi.org/10.1038/srep38866

Luke, R., Shader, M. J., Gramfort, A., Larson, E., Lee, A. K., & McAlpine, D. (2021).
*Oxygenated hemoglobin signal provides greater predictive performance of
experimental condition than de-oxygenated* (p. 2021.11.19.469225). bioRxiv.
https://doi.org/10.1101/2021.11.19.469225

Lv, H., Wang, Z., Tong, E., Williams, L. M., Zaharchuk, G., Zeineh, M., Goldstein-
Piekarski, A. N., Ball, T. M., Liao, C., & Wintermark, M. (2018). Resting-State
Functional MRI: Everything That Nonexperts Have Always Wanted to Know.
AJNR: American Journal of Neuroradiology, *39*(8), 1390–1399.
https://doi.org/10.3174/ajnr.A5527

Magnin, B., Mesrob, L., Kinkingnéhun, S., Pélégrini-Issac, M., Colliot, O., Sarazin, M.,
Dubois, B., Lehéricy, S., & Benali, H. (2009). Support vector machine-based
classification of Alzheimer's disease from whole-brain anatomical MRI.
Neuroradiology, *51*(2), 73–83. https://doi.org/10.1007/s00234-008-0463-x

Mat, B., Sanz, L. R. D., Arzi, A., Boly, M., Laureys, S., & Gosseries, O. (2022). New
Behavioral Signs of Consciousness in Patients with Severe Brain Injuries.
Seminars in Neurology, *42*(3), 259–272. https://doi.org/10.1055/a-1883-0861

McCredie, V. A., Alali, A. S., Xiong, W., Rubenfeld, G. D., Cuthbertson, B. H., Scales, D.
C., & Nathens, A. B. (2016). Timing of withdrawal of life-sustaining therapies in
severe traumatic brain injury: Impact on overall mortality. *Journal of Trauma and
Acute Care Surgery*, *80*(3), 484. https://doi.org/10.1097/TA.0000000000000922

Medina, J. P., Nigri, A., Stanziano, M., D'Incerti, L., Sattin, D., Ferraro, S., Rossi
Sebastiano, D., Pinardi, C., Marotta, G., Leonardi, M., Bruzzone, M. G., &
Rosazza, C. (2022). Resting-State fMRI in Chronic Patients with Disorders of
Consciousness: The Role of Lower-Order Networks for Clinical Assessment.
Brain Sciences, *12*(3), 355. https://doi.org/10.3390/brainsci12030355

Menon, D. K., Schwab, K., Wright, D. W., & Maas, A. I. (2010). Position Statement:
Definition of Traumatic Brain Injury. *Archives of Physical Medicine and
Rehabilitation*, *91*(11), 1637–1640. https://doi.org/10.1016/j.apmr.2010.05.017

Mesquita, R. C., Franceschini, M. A., & Boas, D. A. (2010). Resting state functional
connectivity of the whole head with near-infrared spectroscopy. *Biomedical
Optics Express*, *1*(1), 324–336. https://doi.org/10.1364/BOE.1.000324

Messina, Z., Hays Shapshak, A., & Mills, R. (2024). Anoxic Encephalopathy. In *StatPearls*. StatPearls Publishing. http://www.ncbi.nlm.nih.gov/books/NBK539833/

Monti, M. M., Vanhaudenhuyse, A., Coleman, M. R., Boly, M., Pickard, J. D., Tshibanda, L., Owen, A. M., & Laureys, S. (2010). Willful Modulation of Brain Activity in Disorders of Consciousness. *New England Journal of Medicine*, *362*(7), 579–589. https://doi.org/10.1056/NEJMoa0905370

Moreira da Silva, N., Cowie, C. J. A., Blamire, A. M., Forsyth, R., & Taylor, P. N. (2020). Investigating Brain Network Changes and Their Association With Cognitive Recovery After Traumatic Brain Injury: A Longitudinal Analysis. *Frontiers in Neurology*, *11*. https://doi.org/10.3389/fneur.2020.00369

Morin, A., & Michaud, J. (2007). Self-awareness and the left inferior frontal gyrus: Inner speech use during self-related processing. *Brain Research Bulletin*, *74*(6), 387–396. https://doi.org/10.1016/j.brainresbull.2007.06.013

Multi-Society Task Force on PVS. (1994). Medical aspects of the persistent vegetative state (1). *The New England Journal of Medicine*, *330*(21), 1499–1508. https://doi.org/10.1056/NEJM199405263302107

Nakamura, T., Hillary, F. G., & Biswal, B. B. (2009). Resting Network Plasticity Following Brain Injury. *PLOS ONE*, *4*(12), e8220. https://doi.org/10.1371/journal.pone.0008220

Newman, M. E. J. (2016). *Networks: An introduction* (Reprinted). Oxford University Press.

Nichols, T. E., & Holmes, A. P. (2002). Nonparametric permutation tests for functional neuroimaging: A primer with examples. *Human Brain Mapping*, *15*(1), 1–25. https://doi.org/10.1002/hbm.1058

Nielsen, A. N., Barch, D. M., Petersen, S. E., Schlaggar, B. L., & Greene, D. J. (2020). Machine Learning With Neuroimaging: Evaluating Its Applications in Psychiatry. *Biological Psychiatry: Cognitive Neuroscience and Neuroimaging*, *5*(8), 791–798. https://doi.org/10.1016/j.bpsc.2019.11.007

Niu, H., Li, Z., Liao, X., Wang, J., Zhao, T., Shu, N., Zhao, X., & He, Y. (2013). Test-Retest Reliability of Graph Metrics in Functional Brain Networks: A Resting-State fNIRS Study. *PLOS ONE*, *8*(9), e72425. https://doi.org/10.1371/journal.pone.0072425

Northoff, G., Heinzel, A., de Greck, M., Bermpohl, F., Dobrowolny, H., & Panksepp, J. (2006). Self-referential processing in our brain—A meta-analysis of imaging studies on the self. *NeuroImage*, *31*(1), 440–457. https://doi.org/10.1016/j.neuroimage.2005.12.002

Norton, L., Graham, M., Kazazian, K., Gofton, T., Weijer, C., Debicki, D., Fernandez-Espejo, D., Thenayan, E. A., & Owen, A. M. (2023). Use of functional magnetic resonance imaging to assess cognition and consciousness in severe Guillain-Barré syndrome. *International Journal of Clinical and Health Psychology*, *23*(2), 100347. https://doi.org/10.1016/j.ijchp.2022.100347

Norton, L., Hutchison, R. M., Young, G. B., Lee, D. H., Sharpe, M. D., & Mirsattari, S. M. (2012). Disruptions of functional connectivity in the default mode network of comatose patients. *Neurology*, *78*(3), 175–181. https://doi.org/10.1212/WNL.0b013e31823fcd61

Novi, S. L., Rodrigues, R. B. M. L., & Mesquita, R. C. (2016). Resting state connectivity patterns with near-infrared spectroscopy data of the whole head. *Biomedical Optics Express*, *7*(7), 2524–2537. https://doi.org/10.1364/BOE.7.002524

Othman, M. H., Bhattacharya, M., Møller, K., Kjeldsen, S., Grand, J., Kjaergaard, J., Dutta, A., & Kondziella, D. (2021). Resting-State NIRS–EEG in Unresponsive Patients with Acute Brain Injury: A Proof-of-Concept Study. *Neurocritical Care*, *34*(1), 31–44. https://doi.org/10.1007/s12028-020-00971-x

Oujamaa, L., Delon-Martin, C., Jaroszynski, C., Termenon, M., Silva, S., Payen, J.-F., & Achard, S. (2023). Functional hub disruption emphasizes consciousness recovery in severe traumatic brain injury. *Brain Communications*, *5*(6), fcad319. https://doi.org/10.1093/braincomms/fcad319

Owen, A. M. (2019). The Search for Consciousness. *Neuron*, *102*(3), 526–528. https://doi.org/10.1016/j.neuron.2019.03.024

Owen, A. M. (2022). Improving prognostication after severe brain injury. *The Lancet Neurology*, *21*(8), 673–674. https://doi.org/10.1016/S1474-4422(22)00262-9

Owen, A. M., Coleman, M. R., Boly, M., Davis, M. H., Laureys, S., & Pickard, J. D. (2006). Detecting Awareness in the Vegetative State. *Science*, *313*(5792), 1402–1402. https://doi.org/10.1126/science.1130197

Pandit, A. S., Expert, P., Lambiotte, R., Bonnelle, V., Leech, R., Turkheimer, F. E., & Sharp, D. J. (2013). Traumatic brain injury impairs small-world topology. *Neurology*, *80*(20), 1826–1833. https://doi.org/10.1212/WNL.0b013e3182929f38

Pedregosa, F., Varoquaux, G., Gramfort, A., Michel, V., Thirion, B., Grisel, O., Blondel, M., Prettenhofer, P., Weiss, R., Dubourg, V., Vanderplas, J., Passos, A., Cournapeau, D., Brucher, M., Perrot, M., & Duchesnay, É. (2011). Scikit-learn: Machine Learning in Python. *Journal of Machine Learning Research*, *12*(85), 2825–2830.

Pereira, F., Mitchell, T., & Botvinick, M. (2009). Machine learning classifiers and fMRI: A tutorial overview. *NeuroImage*, *45*(1, Supplement 1), S199–S209. https://doi.org/10.1016/j.neuroimage.2008.11.007

Pinti, P., Tachtsidis, I., Hamilton, A., Hirsch, J., Aichelburg, C., Gilbert, S., & Burgess, P. W. (2020). The present and future use of functional near-infrared spectroscopy (fNIRS) for cognitive neuroscience. *Annals of the New York Academy of Sciences*, *1464*(1), 5–29. https://doi.org/10.1111/nyas.13948

Porcaro, C., Nemirovsky, I. E., Riganello, F., Mansour, Z., Cerasa, A., Tonin, P., Stojanoski, B., & Soddu, A. (2022). Diagnostic Developments in Differentiating Unresponsive Wakefulness Syndrome and the Minimally Conscious State. *Frontiers in Neurology*, *12*. https://www.frontiersin.org/articles/10.3389/fneur.2021.778951

Posner, J. B., Saper, C. B., Schiff, N. D., & Claassen, J. (2019). *Plum and Posner's Diagnosis and Treatment of Stupor and Coma*. Oxford University Press. https://doi.org/10.1093/med/9780190208875.001.0001

Qin, P., Wu, X., Huang, Z., Duncan, N. W., Tang, W., Wolff, A., Hu, J., Gao, L., Jin, Y., Wu, X., Zhang, J., Lu, L., Wu, C., Qu, X., Mao, Y., Weng, X., Zhang, J., & Northoff, G. (2015). How are different neural networks related to consciousness? *Annals of Neurology*, *78*(4), 594–605. https://doi.org/10.1002/ana.24479

Quaresima, V., & Ferrari, M. (2019). A Mini-Review on Functional Near-Infrared Spectroscopy (fNIRS): Where Do We Stand, and Where Should We Go? *Photonics*, *6*(3), Article 3. https://doi.org/10.3390/photonics6030087

Raichle, M. E. (2015). The brain's default mode network. *Annual Review of Neuroscience*, *38*, 433–447. https://doi.org/10.1146/annurev-neuro-071013-014030

Raichle, M. E., MacLeod, A. M., Snyder, A. Z., Powers, W. J., Gusnard, D. A., & Shulman, G. L. (2001). A default mode of brain function. *Proceedings of the National Academy of Sciences*, *98*(2), 676–682. https://doi.org/10.1073/pnas.98.2.676

Rohaut, B., Eliseyev, A., & Claassen, J. (2019). Uncovering Consciousness in Unresponsive ICU Patients: Technical, Medical and Ethical Considerations. *Critical Care*, *23*, 78. https://doi.org/10.1186/s13054-019-2370-4

Rubinov, M., & Sporns, O. (2010). Complex network measures of brain connectivity: Uses and interpretations. *NeuroImage*, *52*(3), 1059–1069. https://doi.org/10.1016/j.neuroimage.2009.10.003

Rupawala, M., Dehghani, H., Lucas, S. J. E., Tino, P., & Cruse, D. (2018). Shining a Light on Awareness: A Review of Functional Near-Infrared Spectroscopy for Prolonged Disorders of Consciousness. *Frontiers in Neurology*, *9*. https://doi.org/10.3389/fneur.2018.00350

Sarracanie, M., & Salameh, N. (2020). Low-Field MRI: How Low Can We Go? A Fresh View on an Old Debate. *Frontiers in Physics*, *8*. https://doi.org/10.3389/fphy.2020.00172

Sasai, S., Homae, F., Watanabe, H., Sasaki, A. T., Tanabe, H. C., Sadato, N., & Taga, G. (2012). A NIRS–fMRI study of resting state network. *NeuroImage*, *63*(1), 179–193. https://doi.org/10.1016/j.neuroimage.2012.06.011

Scarapicchia, V., Brown, C., Mayo, C., & Gawryluk, J. R. (2017). Functional Magnetic Resonance Imaging and Functional Near-Infrared Spectroscopy: Insights from Combined Recording Studies. *Frontiers in Human Neuroscience*, *11*, 419. https://doi.org/10.3389/fnhum.2017.00419

Schnakers, C., Vanhaudenhuyse, A., Giacino, J., Ventura, M., Boly, M., Majerus, S., Moonen, G., & Laureys, S. (2009). Diagnostic accuracy of the vegetative and minimally conscious state: Clinical consensus versus standardized neurobehavioral assessment. *BMC Neurology*, *9*(1), 35. https://doi.org/10.1186/1471-2377-9-35

Scholkmann, F., Kleiser, S., Metz, A. J., Zimmermann, R., Mata Pavia, J., Wolf, U., & Wolf, M. (2014). A review on continuous wave functional near-infrared spectroscopy and imaging instrumentation and methodology. *NeuroImage*, *85 Pt 1*, 6–27. https://doi.org/10.1016/j.neuroimage.2013.05.004

Seeley, W. W., Menon, V., Schatzberg, A. F., Keller, J., Glover, G. H., Kenna, H., Reiss, A. L., & Greicius, M. D. (2007). Dissociable Intrinsic Connectivity Networks for Salience Processing and Executive Control. *Journal of Neuroscience*, *27*(9), 2349–2356. https://doi.org/10.1523/JNEUROSCI.5587-06.2007

Senders, J. T., Staples, P. C., Karhade, A. V., Zaki, M. M., Gormley, W. B., Broekman, M. L. D., Smith, T. R., & Arnaout, O. (2018). Machine Learning and Neurosurgical Outcome Prediction: A Systematic Review. *World Neurosurgery*, *109*, 476-486.e1. https://doi.org/10.1016/j.wneu.2017.09.149

Shamout, F., Zhu, T., & Clifton, D. A. (2021). Machine Learning for Clinical Outcome Prediction. *IEEE Reviews in Biomedical Engineering*, *14*, 116–126. https://doi.org/10.1109/RBME.2020.3007816

Shu, Z., Wu, J., Li, H., Liu, J., Lu, J., Lin, J., Liang, S., Wu, J., Han, J., & Yu, N. (2023). fNIRS-based functional connectivity signifies recovery in patients with disorders of consciousness after DBS treatment. *Clinical Neurophysiology*, *147*, 60–68. https://doi.org/10.1016/j.clinph.2022.12.011

Smitha, K., Akhil Raja, K., Arun, K., Rajesh, P., Thomas, B., Kapilamoorthy, T., & Kesavadas, C. (2017). Resting state fMRI: A review on methods in resting state connectivity analysis and resting state networks. *The Neuroradiology Journal*, *30*(4), 305–317. https://doi.org/10.1177/1971400917697342

Snider, S. B., & Edlow, B. L. (2020). Magnetic Resonance Imaging in Disorders of Consciousness. *Current Opinion in Neurology*, *33*(6), 676–683. https://doi.org/10.1097/WCO.0000000000000873

Song, M., Yang, Y., He, J., Yang, Z., Yu, S., Xie, Q., Xia, X., Dang, Y., Zhang, Q., Wu, X., Cui, Y., Hou, B., Yu, R., Xu, R., & Jiang, T. (2018). Prognostication of chronic disorders of consciousness using brain functional networks and clinical characteristics. *eLife*, *7*. https://doi.org/10.7554/eLife.36173

Suzuki, M., Miyai, I., Ono, T., Oda, I., Konishi, I., Kochiyama, T., & Kubota, K. (2004). Prefrontal and premotor cortices are involved in adapting walking and running speed on the treadmill: An optical imaging study. *NeuroImage*, *23*(3), 1020–1026. https://doi.org/10.1016/j.neuroimage.2004.07.002

Teasdale, G., & Jennett, B. (1974). ASSESSMENT OF COMA AND IMPAIRED CONSCIOUSNESS: A Practical Scale. *The Lancet*, *304*(7872), 81–84. https://doi.org/10.1016/S0140-6736(74)91639-0

Threlkeld, Z. D., Bodien, Y. G., Rosenthal, E. S., Giacino, J. T., Nieto-Castanon, A., Wu, O., Whitfield-Gabrieli, S., & Edlow, B. L. (2018). Functional networks reemerge during recovery of consciousness after acute severe traumatic brain injury. *Cortex; a Journal Devoted to the Study of the Nervous System and Behavior*, *106*, 299–308. https://doi.org/10.1016/j.cortex.2018.05.004

Tu, S., Qiu, J., Martens, U., & Zhang, Q. (2013). Category-selective attention modulates unconscious processes in the middle occipital gyrus. *Consciousness and Cognition*, *22*(2), 479–485. https://doi.org/10.1016/j.concog.2013.02.007

Tulay, E. E., Metin, B., Tarhan, N., & Arıkan, M. K. (2019). Multimodal Neuroimaging: Basic Concepts and Classification of Neuropsychiatric Diseases. *Clinical EEG and Neuroscience*, *50*(1), 20–33. https://doi.org/10.1177/1550059418782093

Turgeon, A. F., Lauzier, F., Burns, K. E. A., Meade, M. O., Scales, D. C., Zarychanski, R., Moore, L., Zygun, D. A., McIntyre, L. A., Kanji, S., Hébert, P. C., Murat, V., Pagliarello, G., Fergusson, D. A., & Group, for the C. C. C. T. (2013). Determination of Neurologic Prognosis and Clinical Decision Making in Adult Patients With Severe Traumatic Brain Injury: A Survey of Canadian Intensivists, Neurosurgeons, and Neurologists*. *Critical Care Medicine*, *41*(4), 1086. https://doi.org/10.1097/CCM.0b013e318275d046

Turgeon, A. F., Lauzier, F., Simard, J.-F., Scales, D. C., Burns, K. E. A., Moore, L., Zygun, D. A., Bernard, F., Meade, M. O., Dung, T. C., Ratnapalan, M., Todd, S., Harlock, J., & Fergusson, D. A. (2011). Mortality associated with withdrawal of life-sustaining therapy for patients with severe traumatic brain injury: A Canadian multicentre cohort study. *CMAJ*, *183*(14), 1581–1588. https://doi.org/10.1503/cmaj.101786

Uddin, L. Q. (2015). Salience processing and insular cortical function and dysfunction. *Nature Reviews Neuroscience*, *16*(1), 55–61. https://doi.org/10.1038/nrn3857

Vabalas, A., Gowen, E., Poliakoff, E., & Casson, A. J. (2019). Machine learning algorithm validation with a limited sample size. *PLOS ONE*, *14*(11), e0224365. https://doi.org/10.1371/journal.pone.0224365

van den Heuvel, M. P., & Hulshoff Pol, H. E. (2010). Exploring the brain network: A review on resting-state fMRI functional connectivity. *European Neuropsychopharmacology*, *20*(8), 519–534. https://doi.org/10.1016/j.euroneuro.2010.03.008

van der Horn, H. J., Kok, J. G., de Koning, M. E., Scheenen, M. E., Leemans, A., Spikman, J. M., & van der Naalt, J. (2017). Altered Wiring of the Human Structural Connectome in Adults with Mild Traumatic Brain Injury. *Journal of Neurotrauma*, *34*(5), 1035–1044. https://doi.org/10.1089/neu.2016.4659

van Veen, E., van der Jagt, M., Citerio, G., Stocchetti, N., Epker, J. L., Gommers, D., Burdorf, L., Menon, D. K., Maas, A. I. R., Lingsma, H. F., & Kompanje, E. J. O. (2020). End-of-life practices in traumatic brain injury patients: Report of a questionnaire from the CENTER-TBI study. *Journal of Critical Care*, *58*, 78–88. https://doi.org/10.1016/j.jcrc.2020.04.001

Vanhaudenhuyse, A., Noirhomme, Q., Tshibanda, L. J.-F., Bruno, M.-A., Boveroux, P., Schnakers, C., Soddu, A., Perlbag, V., Ledoux, D., Brichant, J.-F., Moonen, G., Maquet, P., Greicius, M. D., Laureys, S., & Boly, M. (2010). Default network connectivity reflects the level of consciousness in non-communicative brain-damaged patients. *Brain*, *133*(1), 161–171. https://doi.org/10.1093/brain/awp313

Vincent, J. L., Patel, G. H., Fox, M. D., Snyder, A. Z., Baker, J. T., Van Essen, D. C., Zempel, J. M., Snyder, L. H., Corbetta, M., & Raichle, M. E. (2007). Intrinsic functional architecture in the anaesthetized monkey brain. *Nature*, *447*(7140), 83–86. https://doi.org/10.1038/nature05758

Wagner, F., Hänggi, M., Weck, A., Pastore-Wapp, M., Wiest, R., & Kiefer, C. (2020). Outcome prediction with resting-state functional connectivity after cardiac arrest. *Scientific Reports*, *10*(1), Article 1. https://doi.org/10.1038/s41598-020-68683-y

Wang, J., Gao, X., Xiang, Z., Sun, F., & Yang, Y. (2023). Evaluation of consciousness rehabilitation via neuroimaging methods. *Frontiers in Human Neuroscience*, *17*. https://www.frontiersin.org/articles/10.3389/fnhum.2023.1233499

Wang, J., Zuo, X., & He, Y. (2010). Graph-based network analysis of resting-state functional MRI. *Frontiers in Systems Neuroscience*, *4*. https://www.frontiersin.org/articles/10.3389/fnsys.2010.00016

Watts, D. J., & Strogatz, S. H. (1998). Collective dynamics of 'small-world' networks. *Nature*, *393*(6684), 440–442. https://doi.org/10.1038/30918

Weilnhammer, V., Fritsch, M., Chikermane, M., Eckert, A.-L., Kanthak, K., Stuke, H., Kaminski, J., & Sterzer, P. (2021). *Evidence for an Active Role of Inferior Frontal Cortex in Conscious Experience* (p. 2020.05.28.114645). bioRxiv. https://doi.org/10.1101/2020.05.28.114645

Weng, L., Xie, Q., Zhao, L., Zhang, R., Ma, Q., Wang, J., Jiang, W., He, Y., Chen, Y., Li, C., Ni, X., Xu, Q., Yu, R., & Huang, R. (2017). Abnormal structural connectivity between the basal ganglia, thalamus, and frontal cortex in patients with disorders of consciousness. *Cortex*, *90*, 71–87. https://doi.org/10.1016/j.cortex.2017.02.011

Wernick, M. N., Yang, Y., Brankov, J. G., Yourganov, G., & Strother, S. C. (2010). Machine Learning in Medical Imaging. *IEEE Signal Processing Magazine*, *27*(4), 25–38. https://doi.org/10.1109/MSP.2010.936730

Williamson, T., Ryser, M. D., Ubel, P. A., Abdelgadir, J., Spears, C. A., Liu, B., Komisarow, J., Lemmon, M. E., Elsamadicy, A., & Lad, S. P. (2020). Withdrawal of Life-supporting Treatment in Severe Traumatic Brain Injury. *JAMA Surgery*, *155*(8), 723–731. https://doi.org/10.1001/jamasurg.2020.1790

Willison, H. J., Jacobs, B. C., & Doorn, P. A. van. (2016). Guillain-Barré syndrome. *The Lancet*, *388*(10045), 717–727. https://doi.org/10.1016/S0140-6736(16)00339-1

Wilson, L., Boase, K., Nelson, L. D., Temkin, N. R., Giacino, J. T., Markowitz, A. J., Maas, A., Menon, D. K., Teasdale, G., & Manley, G. T. (2021). A Manual for the Glasgow Outcome Scale-Extended Interview. *Journal of Neurotrauma*, *38*(17), 2435–2446. https://doi.org/10.1089/neu.2020.7527

Wilson, L., PETTIGREW, L., & Teasdale, G. (1998). Structured Interviews for the Glasgow Outcome Scale and the Extended Glasgow Outcome Scale: Guidelines for Their Use. *Journal of Neurotrauma*, *15*, 573–585. https://doi.org/10.1089/neu.1998.15.573

Wright, L., De Marco, M., & Venneri, A. (2021). A Graph Theory Approach to Clarifying Aging and Disease Related Changes in Cognitive Networks. *Frontiers in Aging Neuroscience*, *13*, 676618. https://doi.org/10.3389/fnagi.2021.676618

Wu, G.-R., Di Perri, C., Charland-Verville, V., Martial, C., Carrière, M., Vanhaudenhuyse, A., Laureys, S., & Marinazzo, D. (2019). Modulation of the spontaneous hemodynamic response function across levels of consciousness. *NeuroImage*, *200*, 450–459. https://doi.org/10.1016/j.neuroimage.2019.07.011

Wu, X., Zou, Q., Hu, J., Tang, W., Mao, Y., Gao, L., Zhu, J., Jin, Y., Wu, X., Lu, L., Zhang, Y., Zhang, Y., Dai, Z., Gao, J.-H., Weng, X., Zhou, L., Northoff, G., Giacino, J. T., He, Y., & Yang, Y. (2015). Intrinsic Functional Connectivity Patterns Predict Consciousness Level and Recovery Outcome in Acquired Brain Injury. *Journal of Neuroscience*, *35*(37), 12932–12946. https://doi.org/10.1523/JNEUROSCI.0415-15.2015

Yeo, B. T., Krienen, F. M., Sepulcre, J., Sabuncu, M. R., Lashkari, D., Hollinshead, M., Roffman, J. L., Smoller, J. W., Zöllei, L., Polimeni, J. R., Fischl, B., Liu, H., & Buckner, R. L. (2011). The organization of the human cerebral cortex estimated by intrinsic functional connectivity. *Journal of Neurophysiology*, *106*(3), 1125–1165. https://doi.org/10.1152/jn.00338.2011

Young, M. J., & Edlow, B. L. (2021). The Quest for Covert Consciousness. *Neurology*, *96*(19), 893–896. https://doi.org/10.1212/WNL.0000000000011734

Young, M. J., & Peterson, A. (2022). Neuroethics across the Disorders of Consciousness Care Continuum. *Seminars in Neurology*, *42*(3), 375–392. https://doi.org/10.1055/a-1883-0701

Yuan, W., Treble-Barna, A., Sohlberg, M. M., Harn, B., & Wade, S. L. (2017). Changes in Structural Connectivity Following a Cognitive Intervention in Children With Traumatic Brain Injury: A Pilot Study. *Neurorehabilitation and Neural Repair*, *31*(2), 190–201. https://doi.org/10.1177/1545968316675430

Zebari, R., Mohsin Abdulazeez, A., Zeebaree, D., Zebari, D., & Saeed, J. (2020). A Comprehensive Review of Dimensionality Reduction Techniques for Feature Selection and Feature Extraction. *Journal of Applied Science and Technology Trends*, *1*, 56–70. https://doi.org/10.38094/jastt1224

Appendices

Appendix A: Western Ethics Approval

Date: 5 February 2024

To: Dr. Adrian M. Owen

Project ID: 114967

Review Reference: 2024-114967-88867

Study Title: Improving Diagnosis and Prognosis in Acute Brain Injury: A Multimodal Imaging Approach (MIMIC Study - Multimodal IMaging in Intensive Care)

Application Type: Continuing Ethics Review (CER) Form

Review Type: Delegated

Date Approval Issued: 05/Feb/2024 14:44

REB Approval Expiry Date: 07/Feb/2025

_____

Dear Dr. Adrian M. Owen,

The Western University Research Ethics Board has reviewed the application. This study, including all currently approved documents, has been re-approved until the expiry date noted above.

REB members involved in the research project do not participate in the review, discussion or decision.

Western University REB operates in compliance with, and is constituted in accordance with, the requirements of the Tri-Council Policy Statement: Ethical Conduct for Research Involving Humans (TCPS 2); the International Conference on Harmonisation Good Clinical Practice Consolidated Guideline (ICH GCP); Part C, Division 5 of the Food and Drug Regulations; Part 4 of the Natural Health Products Regulations; Part 3 of the Medical Devices Regulations and the provisions of the Ontario Personal Health Information Protection Act (PHIPA 2004) and its applicable regulations. The REB is registered with the U.S. Department of Health & Human Services under the IRB registration number IRB 00000940.

Please do not hesitate to contact us if you have any questions.

Electronically signed by:

Mr. Joshua Hatherley, Ethics Coordinator on behalf of Dr. N. Poonai, HSREB Chair 05/Feb/2024 14:44

Reason: I am approving this document

Note: This correspondence includes an electronic signature (validation and approval via an online system that is compliant with all regulations).

Appendix B: Letter of Information and Consent - Healthy Control Volunteers

Letter of Information and Consent – Healthy Control Volunteers

Study Title: Improving Diagnosis and Prognosis in Acute Brain Injury: A Multimodal Imaging Approach

Principal Investigator
Dr. Adrian Owen, Ph.D., Professor of Cognitive Neuroscience and Imaging
Department of Physiology and Pharmacology, Western University

Funder: Canadian Institute of Health Research Foundation Grant

Conflict of Interest: There are no conflicts of interest to declare related to this study.

Introduction: You are invited to take part in a voluntary research study. Before you make a decision, it is important that you are aware of why the research is being done and what it will involve. The goal of the study is to determine whether certain brain images are useful for the diagnosis of coma (whether or not a patient is conscious) and the prognosis following brain injury (whether or not a patient will have a good outcome). We plan to recruit both patient participants who have sustained a severe brain injury and healthy participants who will be the control group. By comparing a group age-matched healthy participants to unconscious patients, we hope to learn more about how the brain operates to give rise to consciousness and if we can use tests to predict outcomes for patients admitted to the hospital. This letter is for healthy control participants. There is a separate letter for patients.

Why is this study being done?
Advances in life-saving medical technology have increased survival rates for patients after a serious brain injury. The recovery and continued care of these people often require long stays in intensive care units (ICUs), where important treatment decisions are made to increase the chances of regaining awareness and recovering thinking-related ability. The decisions made by the ICU healthcare teams have can affect patients' survival and outcomes. The ability to determine a patient's level of awareness and whether or not a patient will have a good outcome are challenging and treatment decisions are usually based on a patient's behavioral responses which can be unreliable.

In this study we plan to determine if new tools that look at brain images (called fMRI), brain function (fNIRS), and brain wave activity (called EEG) can identify awareness and predict good outcomes in unconscious patients.

How many people will take part in this study?
There will be a total of 700 people enrolled in the study over 7 years. We will recruit 350 participants to our study group who are unconscious and currently in the intensive care units at

London Health Sciences Centre and 350 healthy conscious participants from the London community who will be in the control group.

As a healthy control participant, it is expected that study procedures will take approximately 3-4 hrs in total. If you are interested and would prefer to do the tests on two separate days that is possible.

What will happen during this study?
This study will use three different imaging methods (fMRI, fNIRS, EEG) to assess brain activity. You may be eligible for some or all of the imaging methods. FNIRS and EEG testing will occur at the Brain and Mind Institute at Western University while fMRI scanning will occur at Robarts Research Institute or at University or Victoria Hospital.

EEG Recording:
You will be seated a comfortable position while fitted with an electrode cap, which containing 128 electrodes, placed on your head. Fitting the cap will take approximately 20 minutes. After the fitting of the cap, some sounds will be presented over earphones. We will make sure before testing starts that that the volume of the sounds are at a comfortable level. The sounds you will hear will be everyday things like beeps, sentences, songs, and movie clips. Most of the sounds will be benign and are not expected to cause an emotional response. However, some of the movie clips may be suspenseful or tense in nature. In adults who are part of the study, a somatosensory evoked potential task may be completed, where the nerve at your wrist will be electrical stimulated causing a small twitch in your thumb, and we will record the corresponding electrophysiological response. The total time of the testing will be approximately 60 min.

FNIRS Recording:
FNIRS is a portable imaging tool that measures the way brain activity changes when you perform different tasks by using sensors that record the way that light is absorbed in the brain. An fNIRS cap will be placed on your head and will sit gently on the head surface. You may take part in 6 tasks during the testing time where you will hear different sounds presented to you over earphones. The sounds you will hear will be everyday things like beeps, sentences, songs, and movie clips. Most of the sounds will be benign and are not expected to cause an emotional response. However, some of the movie clips may be suspenseful or tense in nature. In some tasks we may also ask you to try to follow an instruction given to you. In adults who are part of the study, a somatosensory evoked potential task will be completed, where the nerve at your wrist will be electrical stimulated causing a small twitch in your thumb. The total time of the testing will be approximately 60 min.

FMRI Recording:
Eligible participants will also undergo a research fMRI scan, which is a specialized MRI scan that is a noninvasive test that uses a strong magnetic field and radio waves to look at blood flow in the brain to detect areas of activity. These changes in blood flow, which are captured on a computer, help us understand more about how the brain works. The scan allows us to understand the activity in areas of the brain in response to various stimuli (for example, the brain's response to hearing sounds). In adults who are part of the study, a somatosensory evoked potential task will be completed, where the nerve at your wrist will be electrical stimulated causing a small twitch in your thumb. You will be comfortably positioned inside the MRI scanner and the same stimuli presented to you in the fNIRS recordings will be used in the fMRI imaging. The total time of this test will be approximately 60 min.

These are images of the equipment being used in this study.
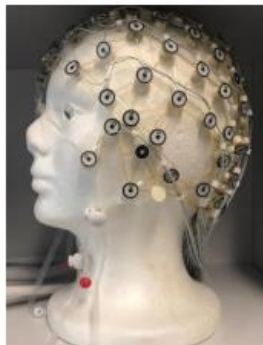
| EEG Cap Machine | fNIRS Cap | fMRI Machine |

What are the risks and harms of participating in this study?

FMRI: There are no known biological risks associated with MR imaging. Some people cannot have an MRI because they have some type of metal in their body. For instance, if you have a heart pacemaker, artificial heart valves, metal implants such as metal ear implants, bullet pieces, chemotherapy or insulin pumps or any other metal such as metal clips or rings, they cannot have an MRI. During this test, you will lie in a small closed area inside a large magnetic tube. Some people may get scared or anxious in small places (claustrophobic). An MRI may also cause possible anxiety for people due to the loud banging made by the machine and the confined space of the testing area. You will be given specially designed headphones to help reduce the noise.

EEG: The risks associated with having EEG electrodes placed on the head are minimal and include the potential for slight irritation of the scalp. This irritation will resolve on its own. EEG equipment does not penetrate or abrade the skin. The electrodes are housed in a net which stretches across the head. The correct sized electrode net will be chosen based upon the circumference of the participants head, making it more comfortable for them.

FNIRS: The amount of light that goes into the brain with fNIRS is about the same as the amount of light that goes into the brain when walking outside on a sunny day. The NIRS procedure is non-invasive, painless, and safe. The NIRS system uses a class 1 laser, which is safe for eye and skin exposure. The laser will not emit enough heat to cause any burning or discomfort. The experimenter may need to part small areas of hair using a swab in order for the fNIRS probes to have good contact with participants skin. This may cause mild discomfort, but this will be minimized by using trained experimenters.

What are the benefits?

There will be no direct benefits to you for participating in this study. However, research ultimately derived from this study may be used in establishing new diagnostic and prognostic guidelines for comatose patients after brain injury.

Voluntary Participation

Your participation in this study is voluntary. You may decide not to be in this study, or to be in the study now and then change your mind later. You may leave the study at any time without affecting your care. This form and your permission will never expire unless you change your mind and withdraw it.

What are the rights of participants?

You do not waive any legal right by signing this consent form. If you are harmed as a direct result of taking part in this study, all necessary medical treatment will be made available to you at no cost.

What are the costs to participants? Are participants paid to be in this study?

You will be reimbursed approximately $20 per hour for your participation in this study. This is intended to include your travel costs, parking, all miscellaneous expenses you have from participation. You will not be charged for any tests conducted for this study, including the MRI scan.

Can participants choose to leave the study?

If you decide to withdraw or are withdrawn from the study, the data already collected as part of the study will nonetheless be preserved, analyzed or used to ensure the completeness of the study. You may withdraw your permission by telling the study staff. If you choose to withdraw from the study, no further information will be collected.

How will participant's information be kept confidential?

While you take part in this study, the principal investigator and study staff will collect information about you that is necessary to answer the scientific objectives of the study. The information will be kept in your study file. Any identifying information (for example, your contact and demographic information), will be stored in a secure, password-protected database. Only the local researchers involved in this study at Western University and London Health Sciences Centre will have access to this information.

Personal identifiers collected in this study include full name, age, date of birth, sex, and contact information. All the information collected about you during the study will remain confidential. You will be identified by a numbered code. The key to this code will be kept by the principal investigator, in a locked space. The paper documents will be kept in a locked filing cabinet and the electronic files will be kept on a computer locked with a password and linked to a secure network. The investigators will preserve the data collected during this study indefinitely. The nominative data and codes linking them to you will be preserved for 25 years, and then destroyed. Contact and demographic information (name, sex/gender, age) will be securely stored on the password protected Ripple platform, which is an online platform managed by Western University's BrainsCAN program. Only the researchers of this study and the BrainsCAN coordinator(s), who administers the database system, will have access to your identifiable information as stated above. The study data could be published in specialized medical journals or shared with others during scientific meetings, but it will be impossible to identify you. If research results are published, your name and other personal information will not be given. .

Qualified representatives of the following organizations may look at your medical/clinical study records at the site where these records are held, for quality assurance (to check that the

information collected for the study is correct and follows proper laws and guidelines).
- Representatives of Lawson Quality Assurance Education Program
- Representatives of the Western University's Health Sciences Research Ethics Board that oversees the ethical conduct of this study.

Open Source Data Statement
Deidentified data may be accessible by the study investigators as well as the broader scientific community in a public repository. This shared data may be viewed and analyzed by other researchers. The shared data will not contain any information that can identify you. All identifiable information will be deleted from the dataset collected so that your anonymity will be protected.

Will I know the results of my study tests?
Your individual study results will not be provided to you. If requested you can be sent any publications resulting from the study – in such a case, you will need to provide a mailing address. If study staff note any incidental findings, they will alert your medical care team, to examine the data and treat the findings as is medically necessary.

Whom do participants contact for questions?
If you have any questions about your rights as a research participant or the conduct of this study, you may contact the Patient Experience Office at LHSC at (519) 685-8500 ext. 52036.

If you have any questions about your rights as a research participant or the conduct of this study, you may contact The Office of Human Research Ethics (519) 661-3036, 1-844-720-9816, email: ethics@uwo.ca. The REB is a group of people who oversee the ethical conduct of research studies. The HSREB is not part of the study team. Everything that you discuss will be kept confidential.

Title of research project*:* Improving Diagnosis and Prognosis in Acute Brain Injury: A Multimodal Imaging Approach

Consent Form – Healthy Controls

Eligible Testing Procedures:

The study team has assessed the participant's eligibility and these tests can be completed:

- ❑ fMRI
- ❑ fNIRS
- ❑ EEG

_____   _____   _____
Print Name of Research Staff   Signature   Date

Participant Consent

This study has been explained to me and any questions I had have been answered.

I know that I may leave the study at any time. I agree to take part in this study.

You agree to the following imaging tests to be completed:

- ❑ fMRI
- ❑ fNIRS
- ❑ EEG

_____   _____   _____
Print Name of Participant   Signature   Date

Person Obtaining Consent:

My signature means that I have explained the study to the individual named above. I have answered all questions.

_____   _____   _____
Print Name of Person   Signature   Date
Obtaining Consent

Appendix C: Letter of Information and Consent - Patient Volunteers

Letter of Information and Consent - Patient Volunteers

Study Title: Improving Diagnosis and Prognosis in Acute Brain Injury: A Multimodal Imaging Approach

Principal Investigator
Dr. Adrian Owen, Ph.D., Professor of Cognitive Neuroscience and Imaging
Department of Physiology and Pharmacology, Western University
London, Ontario, Canada, Telephone:

Funder: Canadian Institute of Health Research Foundation Grant

Conflict of Interest: There are no conflicts of interest to declare related to this study.

Introduction:
NOTE: In this Consent document, "you" always refers to the study participants. If you are a substitute decision maker (SDM) (i.e. someone who makes the decision of participation on behalf of a participant), please remember that "you" refers to the study patient. As the SDM, you will be asked to review and sign this consent form on behalf of the participant. If the participant regains consciousness, they will be asked to sign this consent form.

You are invited to take part in a voluntary research study. Before you make a decision, it is important that you are aware of why the research is being done and what it will involve. The goal of the study is to determine whether certain brain images are useful for the diagnosis of coma (whether or not a patient is conscious) and the prognosis following brain injury (whether or not a patient will have a good outcome).

Why is this study being done?
Advances in life-saving medical technology have increased survival rates for patients after a serious brain injury. The recovery and continued care of these people often require long stays in intensive care units (ICUs), where important treatment decisions are made to increase the chances of regaining awareness and recovering thinking-related ability. The decisions made by the ICU healthcare teams can affect patients' survival and outcomes. The ability to determine a patient's level of awareness and whether or not a patient will have a good outcome are challenging and treatment decisions are usually based on a patient's behavioral responses which can be unreliable.

In this study we plan to determine if new tools that look at brain images (called fMRI), brain function (fNIRS), and brain wave activity (called EEG) can identify consciousness and predict favorable outcomes in unconscious patients.

How many people will take part in this study?

This study is taking place at the London Health Sciences Centre within the Intensive Care Unit at University Hospital and the Critical Care Trauma Centre at Victoria Hospital. There will be a total of 700 people enrolled in the study over 7 years. We will recruit 350 participants to our study group who are unconscious and 350 healthy conscious participants who will be in the control group. A healthy control group is needed to determine difference between brain activity in people with normal levels of wakefulness compared to the brain activity of unconscious participants.

It is expected that you will be in the study for 1 year.

What will happen during this study?

This study will use three different imaging methods (fMRI, fNIRS, EEG) to assess brain activity and level of consciousness. You may be eligible for some or all of the imaging methods.

EEG Recordings (performed as close as possible to days 3, 5, and 7 of admission to ICU): Testing will occur at your bedside and you will remain in their bed in a comfortable position while fitted with an electrode cap, which containing 128 electrodes, placed on your head. Fitting the cap will take approximately 20 minutes. After the fitting of the cap, some sounds will be presented over earphones. We will make sure before testing starts that that the volume of the sounds are at a comfortable level. The sounds you will hear will be everyday things like beeps, sentences, songs, and movie clips. Most of the sounds will be benign and are not expected to cause an emotional response. However, some of the movie clips may be suspenseful or tense in nature. We will measure your brain waves in response to these sounds. The total time of the testing will be approximately 60 min. In adult patients, you may also have a somatosensory evoked potential test during the recording, where the nerve at your wrist will be electrical stimulated causing a small twitch in your thumb to understand how your brain processes sensations. We will measure the changes in your brain activity to the stimulation.

FNIRS Recordings (performed as close as possible to days 3, 5, and 7 of admission to ICU): FNIRS is a portable imaging tool that will be used at your bedside that measures the way brain activity changes when you perform different tasks by using sensors that record the way that light is absorbed in the brain. An fNIRS cap will be placed on your head and will sit gently on the head surface. You may take part in 6 tasks during a 60 minute testing time. You will hear different sounds presented to you over earphones. The sounds you will hear will be everyday things like beeps, sentences, songs, and movie clips. Most of the sounds will be benign and are not expected to cause an emotional response. However, some of the movie clips may be suspenseful or tense in nature. In some tasks we may also ask you to try to follow an instruction given to you. In adult patients, you will also have a somatosensory

evoked potential test during the recording, where the nerve at your wrist will be electrical stimulated causing a small twitch in your thumb to understand how your brain processes sensations. We will measure the changes in your brain activity to the stimulation.

<u>FMRI Recordings (performed as close as possible to day 5 of admission to ICU):</u>
Eligible participants will undergo a research fMRI scan, which is a specialized MRI scan that is a noninvasive test that uses a strong magnetic field and radio waves to look at blood flow in the brain to detect areas of activity. These changes in blood flow, which are captured on a computer, help us understand more about how the brain works. The scan allows us to understand the activity in areas of the brain in response to various stimuli (for example, the brain's response to hearing sounds). When possible, the fMRI scans will be combined with any other MRI imaging your doctor requests for your care. You will be accompanied by a nurse and respiratory technologist during the MRI scanning and you will be comfortably positioned inside the MRI scanner. In adult patients, you will also have a somatosensory evoked potential test during the recording, where the nerve at your wrist will be electrical stimulated causing a small twitch in your thumb to understand how your brain processes sensations. The total time of the study will be approximately 60 min. The same stimuli presented to you in the fNIRS recordings will be used in the fMRI imaging.

Below, are images of the equipment being used in this study.
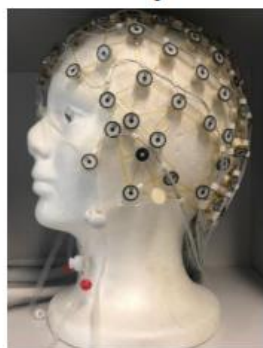
EEG Cap	fNIRS Cap	fMRI Machine

<u>Follow-up Testing</u>
During your hospital stay, once you are able to do so, we will ask you to complete computerized tests that assess your cognitive ability, called Creyos (formerly Cambridge Brain Sciences) (creyos.com). This battery of six short tests assesses your memory, attention and language. It will take approximately 20 minutes to complete. A member of the study team will come to your room, with a tablet or laptop, to have you complete the tests. After discharge from the hospital, you will be sent an email invitation to complete the cognitive tests online from home at 3, 6, and 12 months. If you do not have access to a

computer with the internet after discharge, you will be invited to the Western Interdisciplinary Research Building at Western University to complete the online cognitive testing or a member of the research team will make arrangements to visit you.

At 3, 6, and 12 months from the time injury, you will receive a phone call from a member of the study team. This phone call will last no more than 10 minutes, and its purpose is to assess your level of recovery. If eligible, we may invite you to come back to the hospital at 12 months to repeat the imaging tests you took part in while you were in ICU.

You may be eligible to enroll in another study, titled "ESTABLISH: **E**arly **S**evere illness **TrA**nslational **B**io**L**ogy **I**nformatic**S** in **H**umans". If eligible, a separate letter of information will be presented to you. If you choose to enrol in that study, which also includes the Creyos assessments, you will only complete the testing once per time point and the data will then be shared with the ESTABLISH study.

You may also be eligible to enroll in a complementary study, titled "Brain protein microparticles in critical illness" where blood samples will be collected, and the level of proteins found in the blood will be compared to the extent of patient recovery. If eligible, and second letter of information will be presented to you. If and only if you choose to also enroll and consent to the MIMIC study and the microparticles study, we will collect a blood sample on the day of functional MRI imaging.

Summary of Tests and Procedures

	Enrolment	In-hospital testing (days from ICU admission or medically suitable)				Months post injury		
		Day 2-3	Day 4-6	Day7-10	Regain awareness	3	6	12
ENROL:								
Eligibility Screen	X							
Informed Consent	X							
TESTING:								
EEG*		x	x	x				x
fNIRS*		x	x	x				x
fMRI*			x					x
ASSESSMENT:								
Cognitive Tests					x	x	x	x
Phone Interview						x	x	x

* if eligible and willing to participate

What are the risks and harms of participating in this study?

<u>FMRI:</u> There are no known biological risks associated with MR imaging. Some people cannot have an MRI because they have some type of metal in their body. For instance, if you have a heart pacemaker, artificial heart valves, metal implants such as metal ear implants, bullet pieces, chemotherapy or insulin pumps or any other metal such as metal clips or rings, they cannot have an MRI. During this test, you will lie in a small closed area inside a large magnetic tube. Some people may get scared or anxious in small places (claustrophobic). An

MRI may also cause possible anxiety for people due to the loud banging made by the machine and the confined space of the testing area. You will be given specially designed headphones to help reduce the noise. There are rare risks associated with moving outside of the ICU for procedures like MRI imaging. To reduce these risks a physician associated with the study will assess you to make sure you are medical stable for the scan. When possible, the research images will be taken at the same time as the medically required images so you do not need to travel twice to the MRI scanner. A bedside nurse and a respiratory therapist will always travel with you and will monitor you throughout the duration of scanning.

EEG: The risks associated with having EEG electrodes placed on the head are very little and include the possibility of small irritation of the scalp. This irritation will resolve on its own. EEG equipment does not penetrate or scrape the skin. The electrodes are housed in a net which stretches across the head. The correct sized electrode net will be chosen based upon the size of your head, making it more comfortable for you.

FNIRS: The amount of light that goes into the brain with fNIRS is about the same as the amount of light that goes into the brain when walking outside on a sunny day. The NIRS procedure is non-invasive, painless, and safe. The NIRS system uses a class 1 laser, which is safe for eye and skin exposure. The laser will not give off enough heat to cause any burning or discomfort. The experimenter may need to part small areas of hair using a swab in order for the fNIRS probes to have good contact with your skin. This may cause very mild discomfort.

Cognitive Testing: Creyos will record your internet protocol (IP) addresses when you complete the thinking-related testing online. Storage of your IP address runs the risk of privacy breaches that is associated with your IP address for example your network, device or service. Your IP address also provides information on the following areas, online services for which an individual has registered; personal interests, based on websites visited; and organizational associations.

What are the benefits?
This study may help determine your level of consciousness. Usually, doctors measure your level of consciousness on how you respond to them at the bedside, but this method may not be able to identify some patients who have an injury to their motor system that causes them to be unable to respond to external stimulation, but are aware. Both fMRI and EEG tests that will be used in this study, have shown that 15%-20% of patients in a vegetative state are misdiagnosed and they are more aware than the doctors can tell with the tools they have at the bedside. It is currently unknown if patients in a coma with a recent injury could have this type of awareness that can't otherwise be detected. This study may be able to find awareness in some brain injured patients and it could help doctors make a proper finding about your level of consciousness. Additionally, some patients who are aware may be able to use the imaging tasks to communicate their thoughts and needs through using their brain activity.

There will be no direct benefit to patients in terms of prognostication, as the predictive value of the study tests has not been established.

Can participation in this study end early?

You may be taken off the study early if the study doctor no longer feels this is the best option for you, or the Regulatory Authorities research ethics board withdraw permission for this study to continue. If you are removed from this study, the study team will discuss the reasons with you. Your medical care will not change.

Voluntary Participation

Your participation in this study is voluntary. You may decide not to be in this study, or to be in the study now and then change your mind later. You may leave the study at any time without affecting your care. This form and your permission will never expire unless you change your mind and withdraw it.

What are the costs to participants? Are participants paid to be in this study?

If you come back for follow up testing at 12 months, you will be reimbursed for your travel costs, parking, and all miscellaneous expenses you have from participation.

What other choices are there?

An alternative to the procedures described above is not to participate in the study and continue on just as you do now.

What are the rights of participants?

You do not waive any legal right by signing this consent form. If you are harmed as a direct result of taking part in this study, all necessary medical treatment will be made available to you at no cost.

What are the costs to participants? Are participants paid to be in this study?

You will not incur any out-of-pocket expenses while you are in hospital and no compensation will be provided to you while in hospital. If you are eligible, you may return for imaging at 12 months following your injury. At that time you will be compensated for your out-of-pocket expenses (e.g. travel and parking).

Can participants choose to leave the study?

If you decide to withdraw or are withdrawn from the study, the data already collected as part of the study will nonetheless be preserved, analyzed or used to ensure the completeness of the study. If you choose to withdraw from the study, no further information will be collected. You may withdraw your permission by telling the study staff.

How will participant's information be kept confidential?

While you take part in this study, the principal investigator and study staff will collect information about you that is necessary to answer the scientific objectives of the study. The information will be kept in your study file. This information may comprise the details

contained in your medical file regarding your past and present medical history, your lifestyle habits and results from exams and procedures, which will be carried out. Any identifying information (for example, your contact and demographic information), will be stored in a secure, password-protected database. Only the local researchers involved in this study at Western University and London Health Sciences Centre will have access to this information.

Personal identifiers collected in this study include full name, hospital number, age, date of birth, sex, and contact information.
All the information collected about you during the study will remain confidential. You will be identified by a numbered code. The key to this code will be stored in a secure, password-protected database. The paper documents will be kept in a locked filing cabinet and the electronic files will be kept on a computer locked with a password and linked to a secure network. The investigators will preserve the data collected during this study indefinitely. The nominative data and codes linking them to you will be preserved for 25 years, and then destroyed. Contact and demographic information (name, telephone number, email, date of birth, date of death, sex/gender, age) will be securely stored on the password protected Ripple platform, which is an online platform managed by Western University's BrainsCAN program. Only the researchers of this study and the BrainsCAN coordinator(s), who administers the database system, will have access to your identifiable information as stated above.

The study data could be published in specialized medical journals or shared with others during scientific meetings, but it will be impossible to identify you. If research results are published, your name and other personal information will not be given.
Qualified representatives of the following organizations may look at your medical/clinical study records at the site where these records are held, for quality assurance (to check that the information collected for the study is correct and follows proper laws and guidelines).
- Representatives of Lawson Quality Assurance Education Program
- Representatives of the Western University's Health Sciences Research Ethics Board that oversees the ethical conduct of this study.

Open Source Data Statement
Deidentified data may be accessible by the study investigators as well as the broader scientific community in a public repository. This shared data may be viewed and analyzed by other researchers. The shared data will not contain any information that can identify you. All identifiable information will be deleted from the dataset collected so that your anonymity will be protected.

Will I know the results of my study tests?
Study findings that are relevant to patient care will be given to your doctors. A doctor who understands the study procedures and methods and limitations of the study will interpret the findings and discuss these with you or your family. The test results may either be in alignment with other clinical test results or they could be inconclusive. If requested, you or

your family can be sent any publications resulting from the study – in such a case, you will need to provide a mailing address. If study staff note any incidental findings, they will alert your medical care team, to examine the data and treat the findings as is medically necessary.

Whom do participants contact for questions?
If you have any questions about your rights as a research participant or the conduct of this study, you may contact the Patient Relations Office at LHSC at (519) 685-8500 ext. 52036. If you have any questions about your rights as a research participant or the conduct of this study, you may contact The Office of Human Research Ethics (519) 661-3036, 1-844-720-9816, email: ethics@uwo.ca. The REB is a group of people who oversee the ethical conduct of research studies. The HSREB is not part of the study team. Everything that you discuss will be kept confidential.

Title of research project: Improving Diagnosis and Prognosis in Acute Brain Injury: A Multimodal Imaging Approach

Consent Form

Eligible Testing Procedures:

The study team has assessed the participant's eligibility and these tests can be completed:

- ❑ fMRI
- ❑ fNIRS
- ❑ EEG

_____   _____   _____

Print Name of Research Staff   Signature   Date

Substitute Decision Maker Consent

Your signature on this form indicates that you are acting as a substitute decision maker(s) for the participant and the study has been explained to you and all your questions have been answered to your satisfaction. You agree to allow the person you represent to take part in the study. You know that the person you represent can leave the study at any time. You agree to the following imaging tests to be completed:

- ❑ fMRI
- ❑ fNIRS
- ❑ EEG

_____   _____   _____

Print Name of Substitute   Signature   Date
Decision Maker

_____

Relationship to Participant

Person Obtaining Consent:

My signature means that I have explained the study to the individual named above. I have answered all questions.

_____   _____   _____

Print Name of Person   Signature   Date
Obtaining Consent

If applicable (Substitute Decision Maker who cannot read English):

If obtaining verbal consent:

_____   _____

Name of Substitute   Date of Participant Verbal
Decision Maker   Consent

_____   _____   _____

Name of person obtaining   Signature of person obtaining   Date
consent   consent

Was the participant assisted during the consent process?
- ❑ Yes
- ❑ No

If YES, please check the relevant box and complete the signature space below:

- ❑ The person signing below acted as a translator for the participant during the consent process and attests that the study as set out in this form was accurately translated and has had any questions answered.

_____   _____   _____

Print Name of Translator   Signature   Date (DD-MM-YYYY)

_____

Language

Title of research project:	Improving Diagnosis and Prognosis in Acute Brain Injury: A Multimodal Imaging Approach

Re-Consent of Participant

At the time of enrollment into the study, you were unable to provide consent for the study and your substitute decision maker consented to your participation. You have now regained the capacity to consent and to decide whether to continue to participate in the research study.

This study has been explained to me and any questions I had have been answered.
I know that I may leave the study at any time. I agree to take part in this study.

Participant Consent:

_____   _____   _____

Print Name of Participant   Signature   Date

Person Obtaining Consent:
My signature means that I have explained the study to the participant named above. I have answered all questions.

_____   _____   _____

Print Name of Person
Obtaining Consent   Signature   Date

If applicable (Participant who cannot read English):
Was the participant assisted during the consent process?
- ❏ Yes
- ❏ No

If YES, please check the relevant box and complete the signature space below:

- ❏ The person signing below acted as a translator for the participant during the consent process and attests that the study as set out in this form was accurately translated and has had any questions answered.

_____   _____ _____

Print Name of Translator   Signature   Date (DD-MM-YYYY)

_____
Language

Curriculum Vitae

Name: Ira Gupta

Post-secondary Masters in Science, Specialization in Neuroscience
Education and   The University of Western Ontario
Degrees: London, ON, Canada
       2022-2024

       Bachelors in Science, Specialization in Neuroscience
       The University of Western Ontario
       London, ON, Canada
       2018-2022

Honours and   Dean's Research Scholarship
Awards: 2023-2024

       Southern Ontario Neuroscience Association
       Poster Presentation Winner
       2023

       Western Graduate Research Scholarship
       2022-2024

       Continuing Entrance Scholarship
       2018-2022

Related Work   Research Assistant
Experience: The University of Western Ontario
       2023-2024

Publications

Wilkey, E. D., **Gupta, I.**, Peiris, A., & Ansari, D. (2023). The mathematical brain at rest. Current Opinion in Behavioral Sciences, 49, 101246. https://doi.org/10.1016/j.cobeha.2022.101246

Gupta, I. (2021). Task-Based and Resting-State Functional Connectivity in Children with Dyscalculia. Undergraduate Student Research Internships Conference. https://ir.lib.uwo.ca/usri/usri2021/researchoutputshowcase/171

Peiris, A., **Gupta, I.**, Peters, L., & Wilkey, E. (2021). Intergenerational Transmission of Functional Connectivity Profiles in Isolated Reading and Math Networks: A Scoping Review and Study Proposal. Undergraduate Student Research Internships Conference. https://ir.lib.uwo.ca/usri/usri2021/researchoutputshowcase/180

Oral Presentations

Gupta, I. May 2023. Clinical Neurological Sciences Research Day. London, ON, Canada.

Poster Presentations

Gupta, I. April 2024. Cognitive Neuroscience Society. Toronto, ON, Canada.

Gupta, I. October 2023. WestNIRS Workshop and Conference. London, ON, Canada.

Gupta, I. September 2023. BrainsCAN Research Impact Day. London, ON, Canada.

Gupta, I. June 2023. London Health Research Day. London, ON, Canada.

Gupta, I. May 2023. Southern Ontario Neuroscience Association. Scarborough, ON, Canada.

Gupta, I. February 2023. Lake Ontario Visionary Establishment. Niagara Falls, ON, Canada.